Polymer 103 (2016) 124–131

Contents lists available at ScienceDirect

Polymer

journal homepage: www.elsevier.com/locate/polymer

Short communication

Describing mixture permeation across polymeric membranes by a combination of Maxwell-Stefan and Flory-Huggins models

Rajamani Krishna

Van 't Hoff Institute for Molecular Sciences, University of Amsterdam, Science Park 904, 1098 XH, Amsterdam, The Netherlands

ARTICLE INFO

Article history:
Received 7 August 2016
Received in revised form
15 September 2016
Accepted 17 September 2016
Available online 18 September 2016

Keywords:
Flory huggins thermodynamics
Membrane permeation
Maxwell-Stefan diffusion
Thermodynamic correction factors
Fick diffusivity matrix

ABSTRACT

The primary objective of this article is to develop an analytic procedure for calculating the permeation fluxes of mixtures of penetrant molecules across polymeric membranes. The developed approach combines (1) the Flory-Huggins (F-H) description of phase equilibrium thermodynamics, and (2) the Maxwell-Stefan (M-S) diffusion formulation. For compatibility reasons, the M-S equations are re-formulated in terms of volume fractions, rather than the more commonly used mole fractions. Using matrix algebra, explicit expressions are derived for calculation of the trans-membrane fluxes and component permeabilities. The accuracy of the developed procedure is demonstrated by comparison with published experimental data on CO_2/C_2H_6 and water/ethanol mixture permeation.

1. Introduction

Accurate, and robust models to describe the mixture permeation fluxes across polymeric membranes are essential in the design and development of gas separations, pervaporation, dialysis, reverse osmosis processes, and direct methanol fuel cells. It is generally recognized that chemical potential gradients are the proper driving forces for diffusion in polymers [1–7]. The component chemical potentials in the polymer phase are most conveniently described by the Flory-Huggins (F-H) model that relates the component activities to the *volume fractions* of the penetrants [8–11]. For binary mixtures of penetrants, with interaction parameters χ_{12},χ_{1m},χ_{2m} that are composition independent, the F-H model relates the activity, a_i, of penetrant i, to its volume fraction, φ_i, as follows

$$\ln a_1 = \ln(\varphi_1) + (1-\varphi_1) - \varphi_2\frac{\overline{V_1}}{\overline{V_2}} - \varphi_m\frac{\overline{V_1}}{\overline{V_m}} + (\chi_{12}\varphi_2 + \chi_{1m}\varphi_m)(\varphi_2+\varphi_m) - \chi_{2m}\frac{\overline{V_1}}{\overline{V_2}}\varphi_2\varphi_m$$

$$\ln a_2 = \ln(\varphi_2) + (1-\varphi_2) - \varphi_1\frac{\overline{V_2}}{\overline{V_1}} - \varphi_m\frac{\overline{V_2}}{\overline{V_m}} + \left(\chi_{12}\varphi_1\frac{\overline{V_2}}{\overline{V_1}} + \chi_{2m}\varphi_m\right)(\varphi_1+\varphi_m) - \chi_{1m}\frac{\overline{V_2}}{\overline{V_1}}\varphi_1\varphi_m \quad (1)$$

where $\overline{V_i}$ is the partial molar volume of species i. We also note that the membrane volume fraction is $\varphi_m = 1-\varphi_1-\varphi_2$. In general, all three interaction parameters χ_{12},χ_{1m},χ_{2m} will be functions of the volume fractions of the penetrants and Equation (1) needs to be extended [8,9]; detailed discussions on this aspect are included in the Supplementary material accompanying this communication.

The Maxwell-Stefan (M-S) approach, that is firmly rooted in the theory of irreversible thermodynamics, provides a convenient and practical framework for setting up the flux relations for multi-component diffusion; most commonly, the M-S diffusion formulation is set up using *mole fractions* as composition measures [12–15]. The calculation of trans-membrane fluxes of the penetrants requires the combination of M-S and F-H model descriptions; this combination requires re-casting the M-S equations in terms of volume fractions [3,4]. Such a combined model has been set up by

E-mail address: r.krishna@contact.uva.nl.

http://dx.doi.org/10.1016/j.polymer.2016.09.051
0032-3861/

Ribeiro et al. [4] for quantitative description of CO_2/C_2H_6 mixture permeation across a cross-linked polyethylene oxide (XLPEO) membrane; the resulting set of coupled ordinary differential equations (ODEs) were solved using numerical methods.

The primary objective of the present communication is to develop explicit analytic expressions for the trans-membrane fluxes as functions of the volume fraction gradients; this development requires re-casting the M-S equations in two-dimensional matrix notation. The proportionality between fluxes and volume fraction gradients is described by a matrix of effective Fick diffusivities, $[D]=[B]^{-1}[\Gamma]$ where $[\Gamma]$ is a matrix of thermodynamic correction factors, determinable by analytic differentiation of the F-H equations. The elements of $[B]$ can be calculated from information on M-S diffusivities for penetrant i -membrane (m), and penetrant (1) – penetrant (2) frictional interactions. For the scenario in which the Fick matrix $[D]$ can be assumed constant, say by evaluation at the average composition in the membrane, the fluxes, can be determined explicitly, obviating the need for numerical solutions of ODEs; this simplification will be of value to both researchers and practitioners.

The accuracy of the linearized M-S approach is established by comparison with the experimental data of Ribeiro et al. [16] on permeabilities for CO_2/C_2H_6/XLPEO. The linearized M-S approach is also applied to the modelling water/alcohol pervaporation processes, and the immersion precipitation process for membrane preparation.

The Supplementary material accompanying this publication provides: (1) the F-H model parameters used in the phase equilibrium calculations, (2) detailed derivation of the M-S equations using volume fractions, and (3) input data on the M-S diffusivities in the illustrative examples.

2. Matrix formulation of the Maxwell-Stefan equations

The M-S equations represent a balance between the force exerted per mole of species i with the drag, or friction, experienced with each of the partner species in the mixture. We may expect that the frictional drag to be proportional to differences in the velocities of the diffusing species (u_i-u_j). For binary mixture diffusion, the M-S equations written in terms of volume fractions take the form (see detailed derivations in the Supplementary material)

$$-\frac{1}{RT}\frac{d\mu_1}{dz}=\frac{\varphi_2(u_1-u_2)}{Đ^V_{12}}+\frac{\varphi_m(u_1-u_m)}{Đ^V_{1m}}$$
$$-\frac{1}{RT}\frac{d\mu_2}{dz}=\frac{\varphi_1(u_1-u_2)}{Đ^V_{21}}+\frac{\varphi_m(u_2-u_m)}{Đ^V_{2m}} \quad (2)$$

The polymer membrane can be considered to be stagnant, i.e. $u_m = 0$. The superscript V serves as a reminder that the M-S pair diffusivities are not ones that arise in the commonly used M-S formulation in terms of mole fractions [17]. The *modified* M-S diffusivities are related to the ones commonly used: $c_t Đ_{12}\overline{V_2}=\frac{Đ_{12}\overline{V_2}}{\overline{V}}=Đ^V_{12}$, and $c_t Đ_{1m}\overline{V_m}=\frac{Đ_{1m}\overline{V_m}}{\overline{V}}=Đ^V_{1m}$ where $c_t=1/\overline{V}$ is the mixture molar density. We have the symmetry constraint $\frac{Đ^V_{21}}{\overline{V}_1}=\frac{Đ^V_{12}}{\overline{V}_2}$ that is imposed by the Onsager reciprocal relations. The diffusivities $Đ^V_{1m}$, and $Đ^V_{2m}$ may be interpreted as *inverse* drag coefficients for 1-m, and 2-m friction. An important, persuasive, advantage of the M-S formulation is that $Đ^V_{1m}$, and $Đ^V_{2m}$ are relatable to the corresponding M-S diffusivities for *unary* permeation of 1 and 2 across the membrane [4]. For interpretation of binary permeation experimental data, it is common to use the exponential model [4,18].

$$Đ^V_{1m}=Đ^V_{1m,0}\exp[A_1(\varphi_1+C_{12}\varphi_2)]; \quad Đ^V_{2m}=Đ^V_{2m,0}\exp[A_2(\varphi_2+C_{21}\varphi_1)] \quad (3)$$

to describe the composition dependence of the M-S diffusivities for penetrant-membrane frictional interactions. The values of the parameters $Đ^V_{im,0}$ and A_i can be determined by fitting data on unary permeation. The parameter C_{ij} portrays the influence of the influence of the sorption loading of species j on the M-S diffusivity of species i; this parameter must be determined from binary permeation experimental data. The quantity $Đ^V_{12}$ reflects the frictional drag between the two penetrants as they traverse the membrane. There are no reliable estimation procedures for 1–2 friction and, therefore, $Đ^V_{12}$ needs to be fitted to experimental data on binary mixture permeation; we return to this point later in the discussions.

In proceeding further it is convenient to define the *volumetric* flux of component i, $N^V_i=\varphi_i u_i$, that has the units $m^3\ m^{-2}\ s^{-1}$. In terms of the volumetric fluxes of components, Equation (2) is

$$-\frac{\varphi_i}{RT}\frac{d\mu_i}{dz}=\sum_{\substack{j=1\\ j\neq i}}^{2}\frac{\left(\varphi_j N^V_i-\varphi_i N^V_j\right)}{Đ^V_{ij}}+\frac{\left(\varphi_m N^V_i\right)}{Đ^V_{im}}; \quad i=1,2 \quad (4)$$

which is equivalent to Equation (12) of Ribeiro et al. [4], but expressed in terms of volumetric fluxes. In order to explicitly relate the volumetric fluxes to the gradients of the volume fractions, we define a set of two matrices, as follows. Firstly, we define a matrix of thermodynamic factors $[\Gamma]$:

$$\frac{\varphi_i}{RT}\frac{d\mu_i}{dz}=\varphi_i\frac{d\ln a_i}{dz}=\sum_{j=1}^{j=2}\Gamma_{ij}\frac{d\varphi_j}{dz}; \quad \Gamma_{ij}=\frac{\varphi_i}{\varphi_j}\frac{\partial\ln a_i}{\partial\ln\varphi_j}; \quad i,j=1,2 \quad (5)$$

The four elements $\Gamma_{11},\Gamma_{12},\Gamma_{21},\Gamma_{22}$ can be determined by analytic differentiation of the Flory-Huggins relations relating the component activities to the volume fractions; explicit analytic expressions are provided by Mulder and Smolders [6] and Ribeiro et al. [4].

Secondly, we define a matrix of inverse diffusivities $[B]$ whose elements are given by

$$B_{11}=\frac{\varphi_2}{Đ^V_{12}}+\frac{\varphi_m}{Đ^V_{1m}}; \quad B_{12}=-\frac{\varphi_1}{Đ^V_{12}}$$
$$B_{21}=-\frac{\varphi_2}{Đ^V_{21}}; \quad B_{22}=\frac{\varphi_1}{Đ^V_{21}}+\frac{\varphi_m}{Đ^V_{2m}} \quad (6)$$

Using the definitions in Equation (5) and (6), we may re-cast Equation (2) to obtain the following explicit expression for the trans-membrane volumetric fluxes

$$\begin{pmatrix}N^V_1\\N^V_2\end{pmatrix}=-\begin{bmatrix}D_{11}&D_{12}\\D_{21}&D_{22}\end{bmatrix}\begin{pmatrix}\frac{d\varphi_1}{dz}\\\frac{d\varphi_2}{dz}\end{pmatrix}$$
$$=-\begin{bmatrix}B_{11}&B_{12}\\B_{21}&B_{22}\end{bmatrix}^{-1}\begin{bmatrix}\Gamma_{11}&\Gamma_{12}\\\Gamma_{21}&\Gamma_{22}\end{bmatrix}\begin{pmatrix}\frac{d\varphi_1}{dz}\\\frac{d\varphi_2}{dz}\end{pmatrix} \quad (7)$$

where the matrix of Fick diffusivities is the product $[D]=[B]^{-1}[\Gamma]$, demarcating the contributions of "diffusion" and "thermodynamics", respectively. In general, each of the matrices, $[B]^{-1}$ and $[\Gamma]$

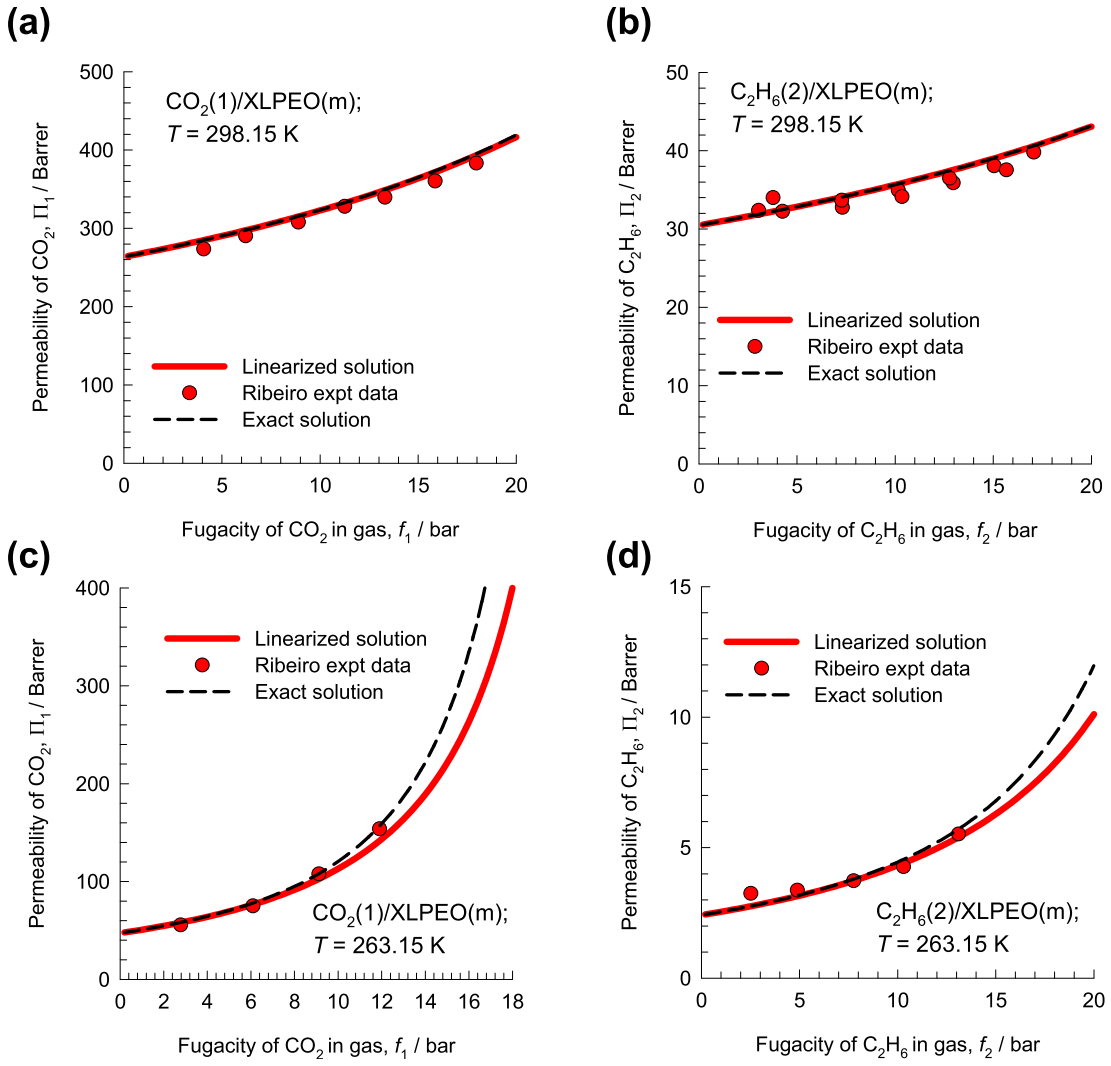

Fig. 1. Permeabilities, expressed in Barrers, for unary permeation of (a, c) CO_2 and (b, d) C_2H_6 across XLPEO membrane at (a, b) 298.15 K, and (c, d) 263.15 K. The simulations details and input data are provided in the Supplementary material.

has significant off-diagonal elements, causing the permeation fluxes N_i^V to be strongly coupled, i.e. the flux of each penetrant is influenced by the volume fraction gradients of both penetrants, not just its own. The molar flux of component i, expressed as mol m^{-2} s^{-1}, is calculated using

$$N_i = c_i u_i = \frac{\varphi_i}{\overline{V_i}} u_i = \frac{N_i^V}{\overline{V_i}} \tag{8}$$

For the special case of unary permeation of component 1 in membrane (m), Equations (7) and (8) degenerate to yield

$$N_1 = -\frac{1}{\overline{V_1}} \frac{1}{1-\varphi_1} Đ_{1m}^V \frac{\partial \ln a_1}{\partial \ln \varphi_1} \frac{d\varphi_1}{dz} \tag{9}$$

Equation (9) is equivalent to that used by Fornasiero et al. [19] for diffusion of water through soft-contact-lens materials and Ribeiro et al. [4] for modelling unary permeation of CO_2 and C_2H_6 across XLPEO membrane. The effective Fick diffusivity for unary permeation is

$$D_{1,eff} = \frac{1}{1-\varphi_1} Đ_{1m}^V \frac{\partial \ln a_1}{\partial \ln \varphi_1} \tag{10}$$

3. Steady-state unary permeation across polymer membrane

At steady-state, the unary permeation flux can be determined by integrating Equation (9) over the membrane thickness, δ,

$$N_1 \delta = -\frac{1}{\overline{V_1}} \int_{\varphi_{10}}^{\varphi_{1\delta}} D_{1,eff} d\varphi_1 = -\frac{1}{\overline{V_1}} \int_{\varphi_{10}}^{\varphi_{1\delta}} \frac{1}{1-\varphi_1} Đ_{1m}^V \frac{\partial \ln a_1}{\partial \ln \varphi_1} d\varphi_1 \tag{11}$$

In Equation (11), φ_{10} and $\varphi_{1\delta}$ are the volume fractions of the penetrant 1 at the upstream and downstream faces, respectively; these volume fractions are determined by equating the activities at the two membrane faces with the activities in the bulk fluid mixtures in the upstream and downstream compartments respectively; the determination of the volume fractions at either membrane face requires the use of an equation solver such as the one available in Microsoft Excel.

In the membrane permeation literature, experimental data for

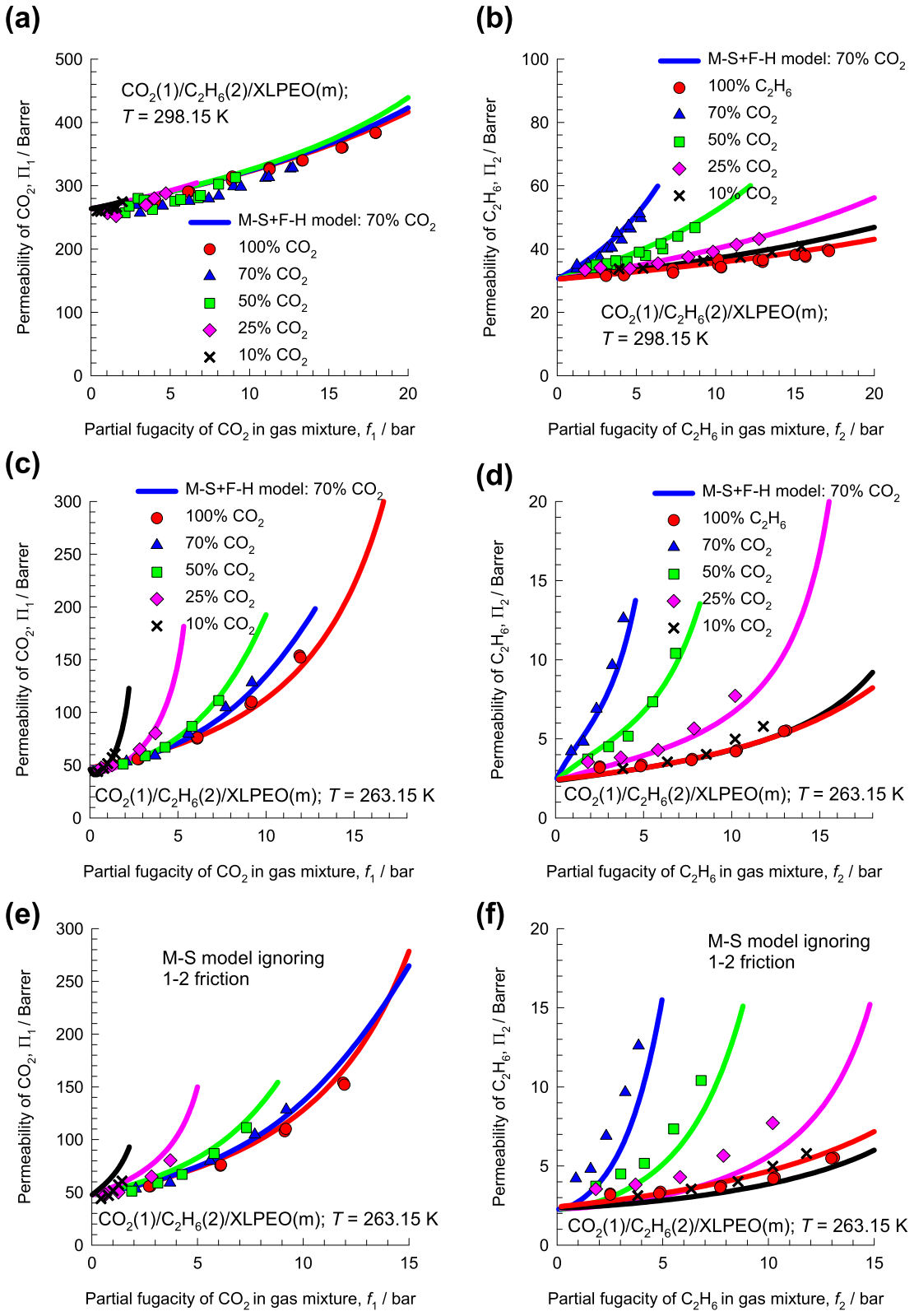

Fig. 2. Permeabilities, expressed in Barrers, of (a, c, e) CO_2, and (b, d, f) C_2H_6 for binary CO_2/C_2H_6 mixture permeation across XLPEO membrane at (a, b) 298.15 K, and (c, d, e, f) 263.15 K. For the simulations presented in (e) and (f), the 1–2 friction is ignored. The simulations details and input data are provided in the Supplementary material.

gas separations are often presented in terms of component permeabilities, defined as

$$\Pi_i = \frac{N_i}{\Delta f_i/\delta} \tag{12}$$

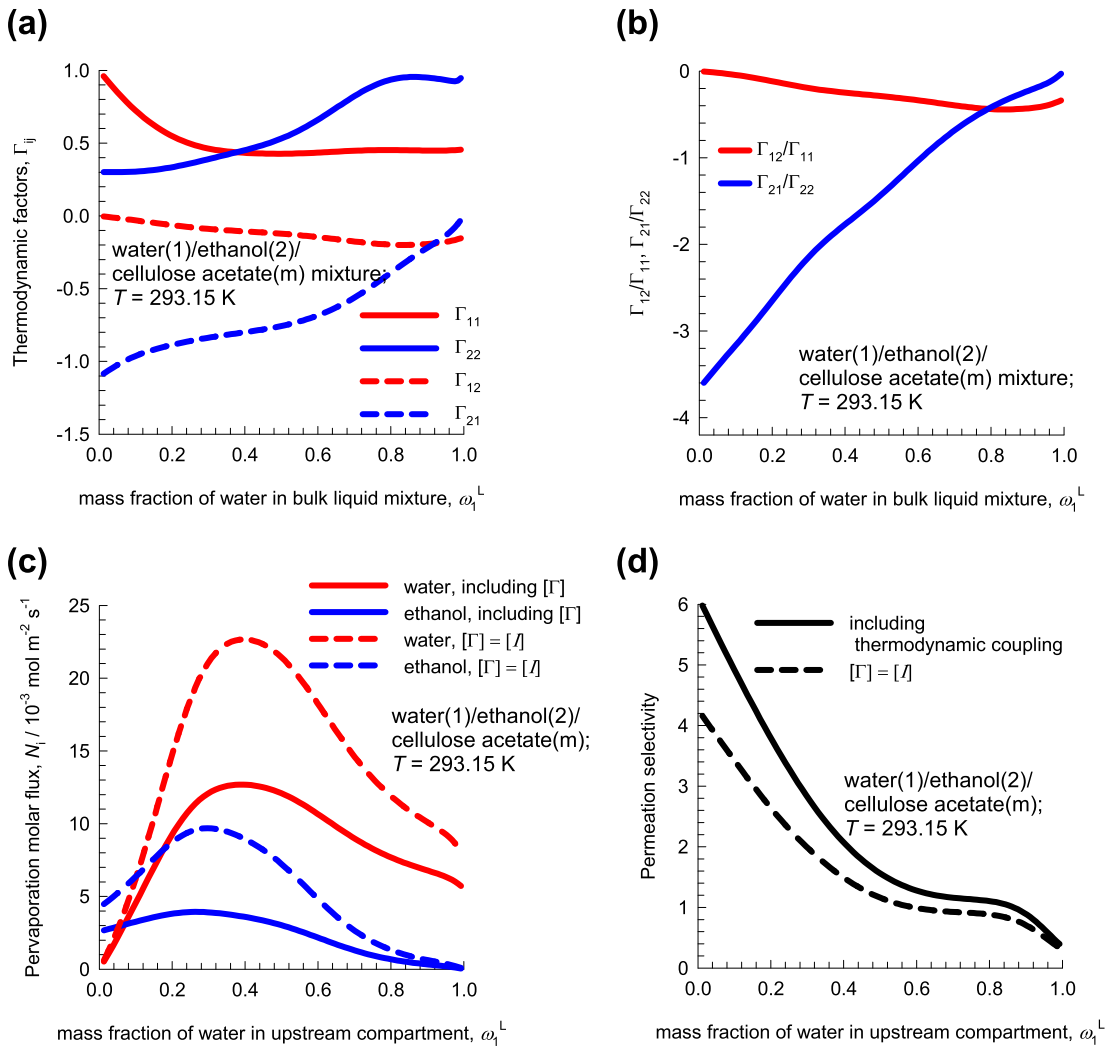

Fig. 3. (a) Thermodynamic correction factors for the ternary mixture consisting of water (1), ethanol (2) and cellulose acetate (m). (b) Ratio of the elements of thermodynamic correction factors. (c) Molar fluxes of water, and ethanol across CA membrane calculated using the linearized M-S equations, using two different scenarios for [Γ] calculations. (d) Water/ethanol permeation selectivity across CA membrane calculated using two different scenarios for [Γ]. The simulations details and input data are provided in the Supplementary material.

In Equation (12), Δf_i is the difference in the fugacities in the upstream and downstream compartments.

If the volume fraction of the component 1 at the downstream face of the polymer membrane are taken to be vanishingly small, i.e. $\varphi_{1\delta} \approx 0; f_{1\delta} \approx 0;$, and $D_{1,eff}$ is evaluated at the arithmetic average volume fraction $(\varphi_{10} + \varphi_{1\delta})/2$, we get

$$\Pi_1 = \frac{N_1}{\Delta f_1} = \frac{1}{\Delta f_1}\frac{1}{V_1}D_{1,eff}(\varphi_{10} - 0) \approx \frac{1}{f_{10}}\frac{1}{V_1}D_{1,eff}(\varphi_{10}) \qquad (13)$$

Equation (13) represents the simplified, i.e. linearized, solution to the Maxwell-Stefan description of unary permeation.

Fig. 1a,b present the experimental data on the permeabilities for unary permeation of CO_2 and C_2H_6 across XLPEO at 298.15 K, as reported by Ribeiro et al. [16] The continuous solid lines are the calculations using the simplified Equation (13), along with the exponential model in Equation (3). The results obtained with the linearized solution are indistinguishable from those obtained from the exact solution given in Equation (11). Both models are in good agreement with the experimental data.

Fig. 1c,d present the corresponding data for permeabilities for unary permeation of CO_2 and C_2H_6 across XLPEO at 263.15 K. At the lower temperature, the volume fractions of the penetrants in the membrane are higher, and interactions between the penetrants and membrane is stronger. Consequently, the linearized solution deviates slightly from the exact analytical solution at high upstream fugacities. Both linearized model, and exact solutions, are in good agreement with the experimental data of Ribeiro et al. [16].

4. Permeation of CO_2/C_2H_6 mixtures across XLPEO membrane

The computational benefits of the linearized model are significant in binary mixture permeation. Fig. 2a,b present experimental data of Ribeiro et al. [16] (indicated by symbols) for the permeabilities of CO_2 and C_2H_6 for CO_2/C_2H_6/XLPEO permeation at 298.15 K. The x-axis represents the partial fugacity of the permeants in the bulk gas phase in the upstream compartment. We note that the permeability of CO_2 is practically unaffected by the mixture composition of the bulk gas phase in the upstream compartment. In sharp contrast, we note that the permeability of C_2H_6 is strongly influenced (increased) by increasing proportion of CO_2 in the bulk gas phase mixture in the upstream compartment. The continuous

solid lines in Fig. 2 are obtained from the flux Equation (7), combined with (8) and (12), wherein $[B]^{-1}[\Gamma]$ is evaluated at the arithmetic average volume fractions $(\varphi_{i0}+\varphi_{i\delta})/2 \approx (\varphi_{i0})/2$. In these calculations, $Đ^{V}_{12}$ is estimated from the fits provided by Ribeiro et al. [4]. The linearized set of M-S equations captures, quantitatively, all the essential features of the composition dependence of the permeabilities of the two penetrants.

Fig. 2c,d compare the experimental data for CO_2/C_2H_6/XLPEO permeation at a lower temperature of 263.15 K at which molecule-molecule and molecule-membrane interactions are significantly stronger, and more strongly composition dependent. At this lower temperature, the permeabilities of both components are influenced by the mixture composition. The linearized M-S model, in combination with F-H, affords a quantitative reproduction of the experimental data.

If the friction between the two penetrants is ignored, i.e. $Đ^{V}_{12} >> Đ^{V}_{1m}$; $Đ^{V}_{12} >> Đ^{V}_{2m}$, then the matrix $[B]$ simplifies to a diagonal matrix

$$B_{ii} = \varphi_m \Big/ Đ^{V}_{im}; \quad B_{ij;i\neq j} = 0 \tag{14}$$

The calculations in Fig. 2e,f are obtained using Equation (14) for binary permeation at 263.15 K. We note that this simplified scenario captures the composition dependence only *qualitatively*, but the quantitative agreement is not as good as in Fig. 2c,d. For a quantitative modelling of mixture permeation, 1–2 friction cannot be ignored.

5. Water/ethanol pervaporation across polymer membranes

The contribution of the off-diagonal elements of $[\Gamma]$ are particularly significant for separation of water/alcohol mixtures by pervaporation. In order to demonstrate this, Fig. 3a presents calculations for the thermodynamic correction factors for the ternary mixture consisting of water (1), ethanol (2) and cellulose acetate (m) using the Flory-Huggins parameters from Refs. [6,7]. Cellulose acetate membranes are hydrophilic, and preferentially adsorb water from water/ethanol bulk liquid mixtures. Fig. 3b plots the ratios Γ_{12}/Γ_{11}, and Γ_{21}/Γ_{22} as a function of the volume fraction of water in the bulk liquid mixture. The large magnitude of Γ_{21}/Γ_{22} implies that the flux of ethanol is strongly influenced by the driving force for water transport. The influence of thermodynamic coupling is to suppress the flux of ethanol and enhance the water flux, a desirable result for pervaporation separations. In order to illustrate the influence of thermodynamic coupling on the pervaporation fluxes, we perform calculations using the input diffusivity data from Ref. [6]. The fluxes are determined from Equations (7) and (14), with evaluation of $[B]^{-1}[\Gamma]$ at the arithmetic average volume fractions $(\varphi_{i0}+\varphi_{i\delta})/2 \approx (\varphi_{i0})/2$; the results are shown by the continuous solid lines in Fig. 3c. The dashed lines in Fig. 3c represent calculations of the permeation fluxes assuming a scenario in which the thermodynamic coupling effects are ignored, i.e. we assume $[\Gamma]$=[*I*], the identity matrix; both fluxes are strongly influenced by this simplifying assumption. Fig. 3d presents calculations of the permeation selectivities; inclusion of thermodynamic coupling effects improves the separation selectivity in favor of water.

We now investigate the importance of 1–2 friction in pervaporation processes by considering the experimental data of Ni et al. [20] for water/ethanol pervaporation across polyimide membrane; their data on volumetric fluxes of water, and ethanol are plotted in Fig. 4a,b. Based on unary permeation experiments, we take $Đ^{V}_{1m} = 25.5\times10^{-13}$, and $Đ^{V}_{2m} = 2.1\times10^{-13}$ m^2 s^{-1}; both these diffusivities are assumed to be composition independent. We estimate $Đ^{V}_{12}$ using the Vignes interpolation formula [21] for diffusion in binary liquid mixtures, adapted as follows

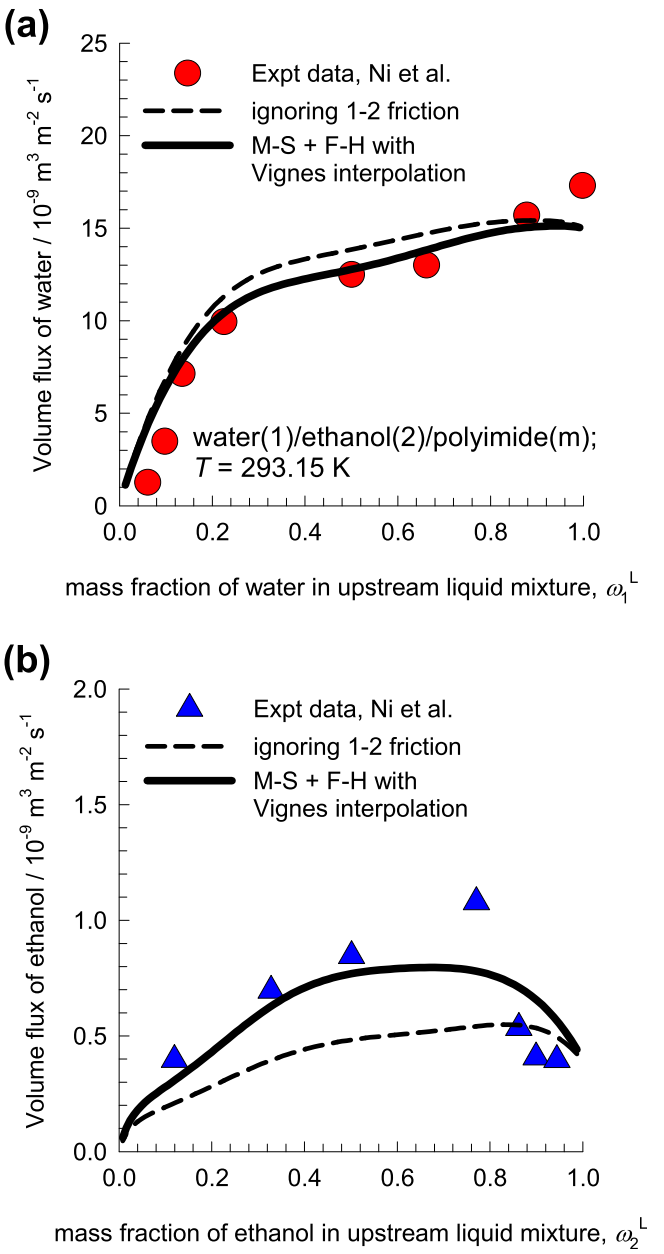

Fig. 4. Volumetric fluxes of (a) water, and (b) ethanol across polyimide membrane. The symbols represent the experimental data of [20]. The continuous solid lines are the flux calculations using the linearized M-S equations, along with the logarithmic interpolation formula. The dashed lines are simulations in which the 1–2 friction is considered to be negligible. The simulations details and input data are provided in the Supplementary material.

$$\left(Đ^{V}_{12}\Big/\overline{V_2}\right) = \left(Đ^{V}_{21}\Big/\overline{V_1}\right) = \left(Đ^{V}_{1m}\Big/\overline{V_2}\right)^{\varphi_1/(\varphi_1+\varphi_2)}\left(Đ^{V}_{2m}\Big/\overline{V_1}\right)^{\varphi_1/(\varphi_1+\varphi_2)} \tag{15}$$

with the limiting scenarios

$$\varphi_2 \to 0, \quad Đ^{V}_{12} = Đ^{V}_{1m}; \quad \varphi_1 \to 0, \quad Đ^{V}_{21} = Đ^{V}_{2m} \tag{16}$$

Equation (15) is also commonly used in the description of binary mixture diffusion in microporous crystalline materials such as zeolites and metal-organic frameworks [22–24]. The flux calculations

using Equations (7) and (15) are shown by the continuous solid lines in Fig. 4. The dependences of the volumetric fluxes on the feed composition, including the maximum in the ethanol flux, are essentially captured by the linearized M-S model that includes 1–2 friction.

The dashed lines in Fig. 4 are the flux calculations assuming that 1–2 friction is negligible, and Equation (14) is invoked; the agreement with experimental data is significantly worsened. Comparing the two sets of simulations in Fig. 4 it can be concluded that the inclusion of 1–2 friction has the effect of reducing the permeation selectivity. In the modeling of direct methanol fuel cells, the influence of 1–2 friction is non-negligible [25,26].

Heintz and Stephan [14] have also underscored the importance of diffusional coupling effects for pervaporation of water/ethanol mixtures across a poly (vinyl alcohol)/poly (acrylonitrile) composite membrane. Their experimental data also show a maximum in the ethanol fluxes, analogous to the observations in Figs. 3c and 4b. Simulation of their experiments using the linearized M-S model is able to capture the maximum in the ethanol flux; see Fig. S25.

6. Conclusions

Mixture permeation across polymer membranes is modelled by combining the Maxwell-Stefan (M-S) diffusion formulation with the Flory-Huggins (F-H) description of phase equilibrium thermodynamics. For compatibility with the F-H model, the M-S equations is re-formulated in terms of volume fractions. The key result of this work is Equation (7), that allows the explicit determination of the fluxes. If the matrix of Fick diffusivities $[D]=[B]^{-1}[\Gamma]$ is assumed constant, and evaluated say at the average composition in the membrane, the flux calculations are further simplified and there is no need for solution of coupled ODEs. Equation (7) can be generalized easily to *n*-component mixture permeation; see derivations in Supplementary material. The developed matrix approach clearly demarcates the contributions of diffusion and thermodynamics, reflected in the matrices, $[B]^{-1}$ and $[\Gamma]$, respectively.

For CO_2/C_2H_6/XLPEO mixture permeation, the calculated permeabilities using the linearized M-S model are in excellent agreement with published experimental data.

Thermodynamic coupling effects, arising from off-diagonal contributions of $[\Gamma]$, have a strong influence in pervaporation processes. Also important in the modelling of pervaporation processes is the contribution of 1–2 friction; neglect of 1–2 friction is not recommended for modelling of pervaporation separations. In this context, the interpolation formula suggested in Equation (15) deserves further scrutiny with regard to its applicability to polymer membranes.

The linearized solution to the M-S equations can also be gainfully employed to model diffusion close to demixing regions, that is encountered in the immersion precipitation process for membrane preparation [27,28]; details are provided in the Supplementary material. In this case, the curvilinear diffusion equilibration trajectories often experience forays into meta-stable regions, lying between the spinodal and binodal curves; see Figs. S29–S40. Such forays signal the phenomenon of uphill diffusion [17,29-33], and have a significant impact on the membrane structure created.

Appendix A. Supplementary data

Supplementary data related to this article can be found at http://dx.doi.org/10.1016/j.polymer.2016.09.051.

Notation

a_i	activity of species *i*, dimensionless
A_i	constant describing the composition dependence of M-S diffusivity, dimensionless
$[B]$	matrix defined by Equation (6), m^{-2} s
c_t	total molar concentration of mixture, mol m^{-3}
C_{ij}	constant describing the composition dependence of M-S diffusivity, dimensionless
$Đ_{ij}$	M-S diffusivity for binary pair *i-j*, m^2 s^{-1}
$Đ^V_{ij}$	modified M-S diffusivity for binary penetrant pair *i-j*, m^2 s^{-1}
$Đ^V_{im}$	modified M-S diffusivity for penetrant *i* in polymer m, m^2 s^{-1}
$D_{i,eff}$	Effective Fick diffusivity of species *i*, m^2 s^{-1}
$[D]$	Fick diffusivity matrix, m^2 s^{-1}
f_i	fugacity of species *i*, Pa
$[I]$	Identity matrix with elements δ_{ij}, dimensionless
N_i	molar flux of species *i*, mol m^{-2} s^{-1}
N_i^V	volumetric flux of species *i*, m^3 m^{-2} s^{-1}
R	gas constant, 8.314 J mol^{-1} K^{-1}
T	absolute temperature, K
u_i	velocity of diffusion of species *i*, m s^{-1}
$\overline{V_i}$	partial molar volume of species *i*, m^3 mol^{-1}
$\overline{V}$	molar volume of mixture, m^3 mol^{-1}
z	direction coordinate, m

Greek letters

δ	membrane thickness, m
δ_{ij}	Kronecker delta, dimensionless
Γ_{ij}	thermodynamic factors, dimensionless
$[\Gamma]$	matrix of thermodynamic factors, dimensionless
μ_i	molar chemical potential, J mol^{-1}
Φ_i	volume fraction of penetrant *i* in polymer, dimensionless
φ_i^L	volume fraction in bulk liquid mixture, dimensionless
χ	interaction parameter in Flory-Huggins model, dimensionless
ω_i	mass fraction of component *i*, dimensionless

Subscripts

i	referring to penetrant *i*
m	referring to membrane
t	referring to total mixture

Superscripts

V	referring to use of volume fractions

References

[1] J.M. Zielinski, B.F. Hanley, Practical friction-based approach to modeling multicomponent diffusion, A. I. Ch. E. J. 45 (1999) 1–12.
[2] J.S. Vrentas, J.L. Duda, Molecular diffusion in polymer solutions, A. I. Ch. E. J. 25 (1979) 1–24.
[3] F. Fornasiero, J.M. Prausnitz, C.J. Radke, Multicomponent diffusion in highly asymmetric systems. An extended maxwell-Stefan model for starkly different-sized, segment-accessible chain molecules, Macromolecules 38 (2005) 1364–1370.
[4] C.P. Ribeiro, B.D. Freeman, D.R. Paul, Modeling of multicomponent mass transfer across polymer Films using a thermodynamically consistent formulation of the Maxwell-Stefan equations in terms of volume fractions, Polymer 52 (2011) 3970–3983.
[5] G.D. Verros, N.A. Malamataris, Multi-component diffusion in polymer solutions, Polymer 46 (2005) 12626–12636.
[6] M.H.V. Mulder, C.A. Smolders, On the mechanism of separation of ethanol/water mixtures by pervaporation. I. Calculation of concentration profiles, J. Membr. Sci. 17 (1984) 289–307.
[7] M.H.V. Mulder, A.C.M. Franken, C.A. Smolders, On the mechanism of separation of ethanol/water mixtures by pervaporation. II. Experimental concentration profiles, J. Membr. Sci. 22 (1985) 41–58.
[8] M.H.V. Mulder, A.C.M. Franken, C.A. Smolders, Preferential sorpton versus preferential permeability in pervaporation, J. Membr. Sci. 22 (1985) 155–178.
[9] T.-H. Yang, J. Lue, Modeling sorption behavior for ethanol/water mixtures in a cross-linked polydimethylsiloxane membrane using the Flory-Huggins

equation, J. Macromol. Sci. Part B Phys. 52 (2013) 1009–1029.
[10] C.P. Ribeiro, B.D. Freeman, Carbon dioxide/ethane mixed-gas sorption and dilation in a cross-linked poly(ethylene oxide) copolymer, Polymer 51 (2010) 1156–1158.
[11] M.J. Varady, T.P. Pearl, S.M. Stevenson, B.A. Mantooth, Decontamination of VX from silicone: characterization of multicomponent diffusion effects, Ind. Eng. Chem. Res. 55 (2016) 3139–3149.
[12] R. Krishna, J.A. Wesselingh, The Maxwell-Stefan approach to mass transfer, Chem. Eng. Sci. 52 (1997) 861–911.
[13] J.A. Wesselingh, R. Krishna, Mass transfer in multicomponent mixtures, VSSD, Delft, 2000.
[14] A. Heintz, W. Stephan, A generalized solution-diffusion model of the pervaporation process through composite membranes Part II. Concentration polarization, coupled diffusion and the influence of the porous support layer, J. Membr. Sci. 89 (1994) 153–169.
[15] A.A. Ghoreyshi, H. Asadi, K. Pirzadeh, A generic transport model for separation of gas mixtures by glassy polymer membranes based on Maxwell–Stefan formulation, RSC Adv. 5 (2015) 48207–48216.
[16] C.P. Ribeiro, B.D. Freeman, D.R. Paul, Pure- and mixed-gas carbon dioxide/ethane permeability and diffusivity in a cross-linked poly(ethylene oxide) copolymer, J. Membr. Sci. 377 (2011) 110–123.
[17] R. Krishna, Uphill diffusion in multicomponent mixtures, Chem. Soc. Rev. 44 (2015) 2812–2836.
[18] J.-P. Brun, C. Larchet, R. Melet, G. Bulvestre, Modelling of the pervaporaion of binary mixtures through moderately swelling, non-reacting membranes, J. Membr. Sci. 23 (1985) 257–283.
[19] F. Fornasiero, F. Krull, J.M. Prausnitz, C.J. Radke, Steady-state diffusion of water through soft-contact-lens materials, Biomaterials 26 (2005) 5704–5716.
[20] X. Ni, X. Sun, D. Ceng, Coupled diffusion of water and ethanol in a polyimide membrane, Polym. Eng. Sci. 41 (2001) 1440–1447.
[21] A. Vignes, Diffusion in binary solutions, Ind. Eng. Chem. Fundam. 5 (1966) 189–199.
[22] R. Krishna, Describing the diffusion of guest molecules inside porous structures, J. Phys. Chem. C 113 (2009) 19756–19781.
[23] R. Krishna, Diffusion in porous crystalline materials, Chem. Soc. Rev. 41 (2012) 3099–3118.
[24] R. Krishna, The Maxwell-Stefan description of mixture diffusion in nanoporous crystalline materials, Microporous Mesoporous Mater 185 (2014) 30–50.
[25] T. Schultz, K. Sundmacher, Rigorous dynamic model of a direct methanol fuel cell based on Maxwell–Stefan mass transport equations and a Flory–Huggins activity model: formulation and experimental validation, J. Power Sources 145 (2005) 435–462.
[26] T. Schultz, K. Sundmacher, Mass, charge and energy transport phenomena in a polymer electrolyte membrane (PEM) used in a direct methanol fuel cell (DMFC): modelling and experimental validation of fluxes, J. Membr. Sci. 276 (2006) 272–285.
[27] G.B. van den Berg, C.A. Smolders, Diffusional phenomena in membrane separation processes, J. Membr. Sci. 73 (1992) 103–118.
[28] A.J. Reuvers, C.A. Smolders, Formation of membranes by means of immersion precipitation Part II. The mechanism of formation of membranes prepared from the system cellulose acetate - acetone - water, J. Membr. Sci. 34 (1987) 67–86.
[29] R. Krishna, Serpentine diffusion trajectories and the Ouzo effect in partially miscible ternary liquid mixtures, Phys. Chem. Chem. Phys. 17 (2015) 27428–27436.
[30] R. Krishna, Highlighting diffusional coupling effects in ternary liquid extraction and comparisons with distillation, Ind. Eng. Chem. Res. 55 (2016) 1053–1063.
[31] R. Krishna, Diffusing uphill with James Clerk Maxwell and Josef Stefan, Curr. Opin. Chem. Eng. 12 (2016) 106–119.
[32] R. Krishna, Tracing the origins of transient overshoots for binary mixture diffusion in microporous crystalline materials, Phys. Chem. Chem. Phys. 18 (2016) 15482–15495.
[33] R. Krishna, Investigating the validity of the Knudsen diffusivity prescription for mesoporous and macroporous materials, Ind. Eng. Chem. Res. 55 (2016) 4749–4759.

Supplementary material to accompany:

Describing Mixture Permeation across Polymeric Membranes by a Combination of Maxwell-Stefan and Flory-Huggins Models

Rajamani Krishna

Van 't Hoff Institute for Molecular Sciences, University of Amsterdam, Science Park 904,

1098 XH Amsterdam, The Netherlands

*email: r.krishna@contact.uva.nl

Table of Contents

1. Preamble

This Supplementary material accompanying the article *Describing Mixture Permeation across Polymeric Membranes by a Combination of Maxwell-Stefan and Flory-Huggins Models* provides: (1) the F-H model parameters used in the phase equilibrium calculations, (2) detailed development of the M-S equations using volume fractions, and (3) input data on the M-S diffusivities.

All the calculations and simulations reported in this article were performed using MathCad 15.[1]

For ease of reading, this Supplementary material is written as a stand-alone document; as a consequence, there is some overlap of material with the main manuscript.

2. The Flory-Huggins description of phase equilibrium thermodynamics

The thermodynamics of sorption equilibrium of penetrants and polymer is most commonly described by the Flory-Huggins relations.[2-4] The Flory-Huggins equation in its simplest form deals with molecules that are similar chemically, but differ greatly in length. An example might be cross-linked polyethylene with the penetrant propane (C_3H_8). The Flory-Huggins model is based on the idea that the chain elements of the polymer arrange themselves randomly (but with the molecules remaining connected) on a three- dimensional lattice; see Figure 1.

The Flory-Huggins model does not take effects of crystallization or other inhomogeneities into account. The resulting equation for the activity of the penetrant is a simple function of the volume fraction of the penetrant in the membrane. We use ϕ_i to denote the volume fraction of the peneterant species *i*; the volume fraction of species *i* is $\phi_i = c_i \overline{V_i}$. The volume fractions are related to the mass fractions, ω_i

$$\omega_i = \frac{\rho_i}{\rho_t} = \frac{\phi_i \rho_{i0}}{\sum_{i=1}^{n} \phi_i \rho_{i0}}; \quad \phi_i = c_i \overline{V_i} = \frac{\frac{\omega_i}{\rho_{i0}}}{\sum_{i=1}^{n} \frac{\omega_i}{\rho_{i0}}} \tag{1}$$

In equation (1), the ρ_{i0} are the pure component mass densities. The use of mole fractions is not convenient for description of the mixture equilibrium in polymers, because the molar mass of the polymer chains are ill defined.[2]

The Flory-Huggins model for binary mixture of penetrant (1) and polymer (indicated by subscript m) is

$$\ln a_1 = \ln(\phi_1) + (1-\phi_1) - \phi_m \frac{\overline{V_1}}{\overline{V_m}} + \chi_{1m}\phi_m^2 \qquad (2)$$
$$\phi_m = 1 - \phi_1$$

Equation (2) contains a non-ideality, or interaction parameter χ_{1m} that is assumed to be independent of the volume fraction. Figure 2 illustrates the influence of the interaction parameter on the activity (a_1) and thermodynamic correction factor, $\Gamma = \frac{\partial \ln a_1}{\partial \ln \phi_1}$, that plays a pivotal role in diffusion (discussions on this are in the following sections). In these calculations, the ratio $\frac{\overline{V_1}}{\overline{V_m}} = 0$, i.e. the molar volume of the penetrant is negligible in comparison to the molar volume of the polymer. If χ is positive, the solution can split into two phases for a range of volume fractions, one rich in polymer and one rich in solvent; the demixing zone is indicated in cyan in Figure 2.

If the interaction parameter χ_{1m} in equation (2) is composition dependent, the F-H model for the activity needs to be extended as follows

$$\ln a_1 = \ln(\phi_1) + (1-\phi_1) - (1-\phi_1)\frac{\overline{V_1}}{\overline{V_m}} + \chi_{1m}(1-\phi_1)^2 + \phi_1(1-\phi_1)^2 \frac{\partial \chi_{1m}}{\partial \phi_1} \qquad (3)$$

Readers are warned that Equation (16) of Verros and Malamataris[5] contains a typo, and Equation (3) above is the correct equation that should be used.

The Flory-Huggins model for binary mixture of penetrants (Components 1, and 2) in a polymer membrane (indicated by subscript m) is[6, 7]

$$\ln a_1 = \ln(\phi_1) + (1-\phi_1) - \phi_2 \frac{\overline{V_1}}{\overline{V_2}} - \phi_m \frac{\overline{V_1}}{\overline{V_m}} + (\chi_{12}\phi_2 + \chi_{1m}\phi_m)(\phi_2 + \phi_m) - \chi_{2m} \frac{\overline{V_1}}{\overline{V_2}} \phi_2 \phi_m$$

$$\ln a_2 = \ln(\phi_2) + (1-\phi_2) - \phi_1 \frac{\overline{V_2}}{\overline{V_1}} - \phi_m \frac{\overline{V_2}}{\overline{V_m}} + \left(\chi_{12}\phi_1 \frac{\overline{V_2}}{\overline{V_1}} + \chi_{2m}\phi_m \right)(\phi_1 + \phi_m) - \chi_{1m} \frac{\overline{V_2}}{\overline{V_1}} \phi_1 \phi_m \quad (4)$$

$$\phi_m = 1 - \phi_1 - \phi_2$$

In the Flory-Huggins formulations presented in Equation (2) and Equation (4), the interaction parameters $\chi_{12}, \chi_{1m}, \chi_{2m}$ are assumed to be constant, i.e. independent of the volume fractions.

In general, all interaction parameters $\chi_{12}, \chi_{1m}, \chi_{2m}$ will be functions of the volume fractions of the penetrants; see discussions in Yang and Lue,[8] and Mulder et al.[9] In this case, the Flory-Huggins model needs to be extended and the more general model equations for the activities are provided by Yang and Lue,[8] Mulder et al.[9] and Varady et al.[10]

3. Equilibrium between bulk fluids and membranes

Polymer membranes are widely used for mixture separations; for an introduction to this topic see Wesselingh and Krishna.[2] The upstream compartment contains fluid mixtures that are in the gaseous state at elevated pressures, or in the liquid state; see schematic in Figure 3. The pressure in the downstream compartment corresponds to ambient pressures or vacuum. Thermodynamic equilibrium is assumed to prevail between the bulk fluid mixture in the upstream compartment and the sorbed mixture in the upstream face of the membrane. An analogous situation prevails in the downstream compartment; there is equilibrium between the bulk fluid mixture in the downstream compartment and the downstream face of the membrane.

Let us first consider the scenario in which the upstream compartment contains a binary *gas* mixture. The equilibrium relation, for either upstream or downstream sides of the membrane, may be written as

$$\mu_i - \mu_{i0} = RT \ln\left(\frac{f_i}{f_{i,sat}} \right) = RT \ln(a_i) \quad (5)$$

where f_i is the partial fugacity of gaseous component i in the bulk fluid mixture, and $f_{i,sat}$ is the fugacity of pure component i at saturation, and a_i is the activity of component i in the sorbed phase in the

polymeric membrane; the activities within the membrane are described by Equation (4). For further discussions on fluid-polymer equilibrium and the interpretation of equation (5), see Ribeiro and Freeman.[3, 4]

For specified set of partial fugacities in the upstream compartment, the volume fractions of the penetrants in the polymer membrane may be calculated by solving equations (4) and (5) simultaneously, using an equation solver. All the calculations presented in this article were implemented in MathCad 15.[1] As illustration, Figure 4 presents calculations of the volume fractions of penetrants CO_2 (component 1) and C_2H_6 (Component 2) in a cross-linked polyethylene oxide (XLPEO) membrane (indicated by subscript m) at 298.15 K; at this temperature all interaction parameters $\chi_{12}, \chi_{1m}, \chi_{2m}$ are independent of the volume fractions in the membrane; the values are specified in Table 1. The upstream face of the membrane is in equilibrium with CO_2/C_2H_6 mixtures of five different compositions. The experimental data (indicated by symbols) on mixed-gas sorption are those presented in Figures 5 and 6 of Ribeiro and Freeman.[11] The simultaneous solution to equations (4) and (5), indicated by the continuous solid lines, are in excellent agreement with the experimental data of Ribeiro and Freeman.[11] This is to be expected because the three interaction parameters $\chi_{12}, \chi_{1m}, \chi_{2m}$ were determined by fitting the experimental data to Equation (4).

Figure 5 presents the experimental data (indicated by symbols) for the volume fractions of penetrants CO_2 (component 1) and C_2H_6 (Component 2) in a cross-linked polyethylene oxide (XLPEO) membrane (indicated by subscript m) at 263.15 K with the F-H model calculations. At this lower temperature, all three interaction parameters $\chi_{12}, \chi_{1m}, \chi_{2m}$ parameters were determined to be dependent on the volume fractions of the penetrants and empirical fits are provided by Ribeiro et al.[7] For convenience to readers, the data fits at 263.15 K are provided in Table 2. It is to be noted that the fitted expressions obtained by Ribeiro et al.[7] are based on the use of Equations (4), and *not* on the extended equations provided by Yang and Lue,[8] Mulder et al.[9] and Varady et al.[10]

The simultaneous solution to equations (4) and (5), indicated by the continuous solid lines, are in excellent agreement with the experimental data of Ribeiro and Freeman.[11]

In a subsequent section, we will compare model calculations of mixture permeation fluxes with experimental data at 298.15 K and at 263.15 K.

Let us now turn our attention to a scenario in which the upstream compartment contains a binary liquid mixture; this scenario is relevant to membrane pervaporation processes. A detailed analysis of the equilibrium between the binary liquid mixture (Components 1, and 2) and the polymer membrane (Penetrants 1, 2, and polymer membrane (m)) is available in the works of Yang and Lue,[8] and Mulder et al.[9]

Let ϕ_1^L, ϕ_2^L represent the volume fractions of components 1 and 2 in the bulk liquid mixture. These volume fractions are related to the mass fractions in the bulk liquid mixture $\phi_i^L = \dfrac{\dfrac{\omega_i^L}{\rho_{i0}}}{\sum_{i=1}^{n} \dfrac{\omega_i^L}{\rho_{i0}}}$. We also have the constraint $\phi_1^L + \phi_2^L = 1$. The component activities in the liquid mixture are described by the F-H model

$$\begin{aligned} \ln a_1^L &= \ln(\phi_1^L) + (1 - \frac{\overline{V_1}}{\overline{V_2}})\phi_2^L + \chi_{12}\left(\phi_2^L\right)^2 - \phi_1^L\left(\phi_2^L\right)^2 \frac{\partial \chi_{12}}{\partial \phi_2^L} \\ \ln a_2^L &= \ln(\phi_2^L) + (1 - \frac{\overline{V_2}}{\overline{V_1}})\phi_1^L + \frac{\overline{V_2}}{\overline{V_1}}\chi_{12}\left(\phi_1^L\right)^2 + \frac{\overline{V_2}}{\overline{V_1}}\phi_2^L\left(\phi_1^L\right)^2 \frac{\partial \chi_{12}}{\partial \phi_2^L} \end{aligned} \tag{6}$$

Equation (6) corresponds precisely with equations (9), and (10) of Mulder et al.[9] The χ_{12} is related to the excess Gibbs free energy

$$\begin{aligned} \chi_{12} &= \frac{1}{x_1 \phi_2^L}\left[x_1 \ln(\frac{x_1}{\phi_1^L}) + x_2 \ln(\frac{x_2}{\phi_2^L}) + \frac{G^{excess}}{RT} \right] \\ \frac{G^{excess}}{RT} &= x_1 \ln(\gamma_1) + x_2 \ln(\gamma_2) \end{aligned} \tag{7}$$

In equation (7), x_1, x_2 are liquid phase mole fractions $x_i = \frac{c_i}{c_t} = \frac{\frac{\omega_i^L}{M_i}}{\sum_{i=1}^{n} \frac{\omega_i^L}{M_i}} = \frac{\omega_i}{M_i}\overline{M}$. The interaction parameter χ_{12} for mixtures such as water/ethanol are strongly dependent on the liquid mixture composition. The excess Gibbs free energy $\frac{G^{excess}}{RT} = x_1 \ln(\gamma_1) + x_2 \ln(\gamma_2)$ can be calculated from activity coefficient models such as that of Wilson, NRTL, and UNIQUAC.[8, 9] Mulder et al.[9] have also shown that the dependence of χ_{12} on the volume fractions of components in the bulk liquid mixture can be expressed as a fourth-order polynomial in $u_2^L = \frac{\phi_2^L}{\phi_1^L + \phi_2^L} = \phi_2^L$

$$\chi_{12} = a + b\left(u_2^L\right) + c\left(u_2^L\right)^2 + d\left(u_2^L\right)^3 + e\left(u_2^L\right)^4; \quad \text{bulk liquid mixture}$$
$$u_2^L = \frac{\phi_2^L}{\phi_1^L + \phi_2^L} = \phi_2^L; u_1^L = \frac{\phi_1^L}{\phi_1^L + \phi_2^L} = \phi_1^L = 1 - u_2^L = 1 - \phi_2^L \qquad (8)$$

Since the proper description of the composition dependence of the interaction factor χ_{12} is of vital importance in the description of phase equilibrium, we need to establish the accuracy of the 4th order polynomial fit suggested by Mulder et al.[9] Figure 6a presents alculations of the interaction factor χ_{12} for ethanol(1)/water(2) mixtures at 298.15 K using equation (7) and the Wilson parameters provided by Yang and Lue.[8] Also shown are the 4-th polynomial fits with coefficients specified in Table 5. There is perfect agreement between the two sets.

Figure 6b presents calculations of the interaction factor χ_{12} for water(1)/ethanol(2) mixtures at 333 K using equation (7) and NRTL parameters from the literature. Also shown are the 4-th polynomial fits with coefficients specified in Table 7. There is perfect agreement between the two sets.

Figure 6c presents calculations of the interaction factor χ_{12} for water(1)/methanol(2) mixtures at 333 K using equation (7) and NRTL parameters. Also shown are the 3rd polynomial fits with coefficients specified in Table 8. There is perfect agreement between the two sets.

In all the Flory-Huggins calculations presented in this article, the 4th order polynomial expressions are used to describe the volume fraction dependence of χ_{12}.

A significant contribution of Mulder et al.[9] is to demonstrate that the interaction parameter χ_{12} for the same two penetrants in the polymer membrane phase shows the same composition dependence on the normalized volume fraction of component 2 within the membrane $u_2 = \dfrac{\phi_2}{\phi_1 + \phi_2}$, i.e.

$$\begin{aligned} &\chi_{12} = a + b(u_2) + c(u_2)^2 + d(u_2)^3 + e(u_2)^4; \quad \text{polymer membrane phase} \\ &u_2 = \frac{\phi_2}{\phi_1 + \phi_2}; u_1 = \frac{\phi_1}{\phi_1 + \phi_2} = 1 - u_2 \end{aligned} \tag{9}$$

It is important to note there that, for convenience, we use the same nomenclature as Mulder et al.[9] However, in the Maxwell-Stefan formulation for diffusion, the quantities u_1 and u_2 refer to the diffusion velocities of the penetrants as they diffuse across the membrane.

In the scenario in which the interaction parameter χ_{12} follows composition dependence following equation (9) in the membrane phase, the Flory-Huggins equation (4) needs to be extended as follows (these equations correspond to equations (6) and (7) of Mulder et al.[9])

$$\begin{aligned} \ln a_1 &= \ln(\phi_1) + (1-\phi_1) - \phi_2 \frac{\overline{V_1}}{\overline{V_2}} - \phi_m \frac{\overline{V_1}}{\overline{V_m}} + (\chi_{12}\phi_2 + \chi_{1m}\phi_m)(\phi_2 + \phi_m) - \chi_{2m} \frac{\overline{V_1}}{\overline{V_2}} \phi_2 \phi_m - u_1 u_2 \phi_2 \frac{\partial \chi_{12}}{\partial u_2} \\ \ln a_2 &= \ln(\phi_2) + (1-\phi_2) - \phi_1 \frac{\overline{V_2}}{\overline{V_1}} - \phi_m \frac{\overline{V_2}}{\overline{V_m}} + \left(\chi_{12}\phi_1 \frac{\overline{V_2}}{\overline{V_1}} + \chi_{2m}\phi_m \right)(\phi_1 + \phi_m) - \chi_{1m} \frac{\overline{V_2}}{\overline{V_1}} \phi_1 \phi_m + \frac{\overline{V_2}}{\overline{V_1}} u_1^2 \phi_2 \frac{\partial \chi_{12}}{\partial u_2} \end{aligned} \tag{10}$$

By equating the activities of the components in the bulk liquid mixture (a_i^L from equation (6)) to the corresponding component activities in the membrane mixture (a_i from equation (10)), we can calculate the volume fractions in the polymer phase, ϕ_i, that is in equilibrium with any specified liquid mixture composition in the upstream face, with volume fractions ϕ_i^L. The determination of the volume fractions in the polymer requires the use of an equation solver, such as MathCad 15[1] that was employed in this work.

As illustration, Figure 7 presents calculations of the volume fractions of penetrants water (component 1), ethanol (component 2) in a cellulose acetate (polymer, component m) at 293.15 K. The upstream face of the membrane is in equilibrium with water/ethanol liquid mixture of varying mass fractions. Water is adsorbed preferentially in hydrophilic cellulose acetate. Another point to note is that the volume fractions of the penetrants in the membrane phase are significantly higher than those for CO_2/C_2H_6/XLPEO system. The calculations of the trans-membrane permeation fluxes will be analyzed and discussed in a subsequent section.

Figure 8 presents calculations of the volume fractions of penetrants water (component 1), ethanol (component 2) in polyimide membrane (polymer, component m) at 293.15 K. The upstream face of the membrane is in equilibrium with water/ethanol liquid mixture of varying mass fractions. In the calculations, χ_{1m}, χ_{2m} are composition dependent, and χ_{12} follows the composition dependence described by equations (8) and (9). The Flory-Huggins model calculations are in reasonable agreement with the experimental sorption data of Ni et al.[12].

Yang and Lue[8] have presented a detailed analysis of the dependence of the interaction parameters $\chi_{12}, \chi_{1m}, \chi_{2m}$ on the volume fractions of the penetrants ethanol (component 1), water (component 2) in polydimethylsiloxane (PDMS) (polymer, component m) membrane film at 298.15 K. Ethanol adsorbs preferentially in PDMS films. As illustration, we consider the scenario in which χ_{1m}, χ_{2m} are composition independent, and χ_{12} follows the composition dependence described by equations (8) and (9). Figure 9a presents calculations of the volume fractions of the penetrants in the polymer film in equilibrium with ethanol/water liquid mixture of varying volume fractions. The uptakes in terms of kg penetrant per kg dry membrane are related to the volume fractions by

$$\phi_i = \frac{\dfrac{Uptake_i}{\rho_{iL}}}{\dfrac{Uptake_1}{\rho_{1L}} + \dfrac{Uptake_2}{\rho_{2L}} + \dfrac{1}{\rho_m}}; \quad Uptake_i = \frac{\phi_i \rho_{iL}}{\phi_m \rho_m} \tag{11}$$

where $\rho_{1L}, \rho_{2L}, \rho_m$ are the densities of the liquid penetrants and membrane. The calculated component uptakes are shown in Figure 9b; these calculations are in perfect agreement to those presented in Figure 7 of Yang and Lue,[8] as is to be expected.

When all three interaction parameters $\chi_{12}, \chi_{1m}, \chi_{2m}$ are dependent on the volume fractions of the penetrants, equation (10) needs to be further extended; these equations are provided in equations (6) and (7) of Mulder et al.[9] The same set of extended equations are given by Yang and Lue.[8] For readers' convenience, the extended F-H model equations are given below:

$$\begin{aligned}
\ln a_1 &= \ln(\phi_1) + (1-\phi_1) - \phi_2 \frac{\overline{V_1}}{V_2} - \phi_m \frac{\overline{V_1}}{V_m} + (\chi_{12}\phi_2 + \chi_{1m}\phi_m)(\phi_2 + \phi_m) - \chi_{2m} \frac{\overline{V_1}}{V_2}\phi_2\phi_m - u_1u_2\phi_2 \frac{\partial \chi_{12}}{\partial u_2} \\
&\quad - u_1u_2\phi_m \frac{\partial \chi_{1m}}{\partial u_2} - \phi_1\phi_m^2 \frac{\partial \chi_{1m}}{\partial \phi_m} + \frac{\overline{V_1}}{V_2} u_2^2\phi_m \frac{\partial \chi_{2m}}{\partial u_1} - \frac{\overline{V_1}}{V_2}\phi_2\phi_m^2 \frac{\partial \chi_{2m}}{\partial \phi_m} \\
\ln a_2 &= \ln(\phi_2) + (1-\phi_2) - \phi_1 \frac{\overline{V_2}}{V_1} - \phi_m \frac{\overline{V_2}}{V_m} + \left(\chi_{12}\phi_1 \frac{\overline{V_2}}{V_1} + \chi_{2m}\phi_m\right)(\phi_1 + \phi_m) - \chi_{1m} \frac{\overline{V_2}}{V_1}\phi_1\phi_m + \frac{\overline{V_2}}{V_1} u_1^2\phi_2 \frac{\partial \chi_{12}}{\partial u_2} \\
&\quad + \frac{\overline{V_2}}{V_1} u_1^2\phi_m \frac{\partial \chi_{1m}}{\partial u_2} - \frac{\overline{V_2}}{V_1}\phi_1\phi_m^2 \frac{\partial \chi_{1m}}{\partial \phi_m} - u_1u_2\phi_m \frac{\partial \chi_{2m}}{\partial u_1} - \phi_2\phi_m^2 \frac{\partial \chi_{2m}}{\partial \phi_m}
\end{aligned} \tag{12}$$

In order to illustrate the influence of the influence of composition dependent χ_{1m}, χ_{2m}, we have recalculated the volume fractions of the penetrants ethanol (component 1), water (component 2) in polydimethylsiloxane (PDMS) (polymer, component m) membrane film using a scenario in which all three parameters $\chi_{12}, \chi_{1m}, \chi_{2m}$ are dependent on the volume fractions of the penetrants; the results are shown in Figure 10a. The uptakes are presented in Figure 10b; these results are in excellent agreement to those presented in Figure 10 of Yang and Lue,[8] as is to be expected. The additional inclusion of the composition dependence of χ_{1m}, χ_{2m} induces a maximum in the volume fraction of water, in accordance with the experimental data of Yang and Lue.[8]

Figure 11 shows the experimental data (symbols) of Heintz and Stephan[13] for binary sorption of water/ethanol mixtures across a poly (vinyl alcohol) /poly (acrylonitrile) (PVA/PAN) composite membrane. The continuous solid lines are the F-H model calculations using the input data in Table 7. The modelling of pervaporation will be presented in a subsequent section.

Figure 12 shows F-H model calculations for binary sorption of water/methanol mixtures in Nafion membrane. A proper description of sorption equilibrium is of vital importance in the modeling of direct methanol fuel cells.[14, 15]

4. Diffusivities in polymers, some introductory remarks

For an elementary introduction to the diffusivity in polymers, see Chapter 16 of Wesselingh and Krishna.[2] Some essential remarks from Wesselingh and Krishna[2] are reproduced below (as indicated in italics).

Figure 13 shows diffusivities of a trace of benzene. These are in a series of polymers with different glass transition temperatures. The diffusivities vary by a factor of 10^{10}, so over ten decades! You cannot expect any general correlation to predict such variation with much accuracy. What we plot along the bottom axis is the difference between the temperature at the measurement, (= 300 K) and the glass transition temperature of the polymer. To the left of the zero point we have glassy polymers, to the right rubbery polymers. We see that diffusivities tend to increase very rapidly above the glass transition point. The highest diffusivity shown (that in silicone rubber) is similar to that of benzene in normal liquids. Except in extremely thin layers, glassy polymers are impermeable for all but the smallest molecules. A good look at the figure shows that some diffusivities lie substantially outside the band drawn. The diffusivities also appear to depend not only on the glass transition temperature, but also on other details of the structure of the polymer.

The effect of the size of the permeant is also extreme (Figure 14) at least near and below the glass transition temperature. The diffusivities of the smallest penetrants are much larger than those of the bulkier penetrants. (Almost) glassy polymers have a low permeability, but an attractive size selectivity. The size selectivity is much less pronounced in the rubbery polymer (although it is still important).

Swelling usually increases diffusivities in a polymer. Figure 15 shows two examples. Again the effect is much larger in the more glassy polymer. This is largely because poly(vinyl acetate) becomes more rubbery as it swells in the solvent. The change in the diffusivity is often exponential in the volume

fraction of the permeant, at least over not-too-large variations. This means that we can use logarithmic interpolation.

5. The Maxwell-Stefan description of *n*-component mixture permeation

The Maxwell-Stefan (M-S) equations represent a balance between the force exerted per mol of species *i* with the drag, or friction, experienced with each of the partner species in the mixture. We may expect that the frictional drag to be proportional to differences in the velocities of the diffusing species $(u_i - u_j)$. For a mixture containing a total of *n* penetrants, 1, 2, 3,..*n* we write

$$
\begin{aligned}
-\frac{d\mu_1}{dz} &= \frac{RT}{Đ_{12}} x_2(u_1 - u_2) + \frac{RT}{Đ_{13}} x_3(u_1 - u_3) + \ldots + \frac{RT}{Đ_{1m}} x_m(u_1 - u_m) \\
-\frac{d\mu_2}{dz} &= \frac{RT}{Đ_{21}} x_1(u_2 - u_1) + \frac{RT}{Đ_{23}} x_3(u_2 - u_3) + \ldots + \frac{RT}{Đ_{2m}} x_m(u_2 - u_m) \\
&\cdots\cdots \\
-\frac{d\mu_n}{dz} &= \frac{RT}{Đ_{n1}} x_1(u_n - u_1) + \frac{RT}{Đ_{n2}} x_2(u_n - u_3) + \ldots + \frac{RT}{Đ_{nm}} x_m(u_n - u_m)
\end{aligned}
\qquad (13)
$$

The left members of equation (13) are the negative of the gradients of the chemical potentials, with the units N mol^{-1}; it represents the driving force acting per mole of species 1, 2, 3,..*n*. The term $RT/Đ_{ij}$ is interpreted as the drag coefficient for the *i-j* pair. The subscript m refers to the polymer membrane, that is regarded as the (*n*+1) th component in the mixture. The multiplier x_j in each of the right members represents the mole fraction of component *j*; this factor is introduced because we expect the friction to be dependent on the number of molecules of *j* relative to that of component *i*. The M-S diffusivity $Đ_{ij}$ has the units m^2 s^{-1} and the physical significance of an *inverse* drag coefficient. The magnitudes of the M-S diffusivities $Đ_{ij}$ do not depend on the choice of the mixture reference velocity because equation (13) is set up in terms of velocity differences.

Only *n* of the chemical potential gradients $\frac{d\mu_i}{dz}$ are independent, because of the Gibbs-Duhem relationship

$$x_1 \frac{d\mu_1}{dz} + x_2 \frac{d\mu_2}{dz} + \cdots x_n \frac{d\mu_n}{dz} + x_m \frac{d\mu_m}{dz} = 0 \tag{14}$$

The Maxwell-Stefan diffusion formulation (13) is consistent with the theory of irreversible thermodynamics. The Onsager Reciprocal Relations imply that the M-S pair diffusivities are symmetric

$$Đ_{ij} = Đ_{ji} \tag{15}$$

For diffusion across polymeric membranes, the velocity of the polymer, $u_m = 0$. For diffusion in multicomponent polymer solutions such as acetone/cellulose acetate, $u_m \neq 0$, i.e. the polymer chains have a finite velocity of diffusion. The discussions in this article are, in the main, focused on polymeric membranes and we proceed further with the assertion $u_m = 0$. In the last section, we will analyze the diffusion processes in the immersion precipitation process for membrane preparation, that involves determining the diffusion equilibration trajectories in polymeric solutions in which $u_m \neq 0$.

For modelling mixture permeation across polymeric membranes, we need to reformulate the Maxwell-Stefan equations using volume fractions instead of mole fractions.[7, 10, 16] The mole fraction is related to the volume fraction by $x_i = \frac{c_i}{c_t} = c_i \overline{V} = \frac{\phi_i}{\overline{V_i}} \overline{V} = \frac{\phi_i}{\overline{V_i}} \frac{1}{c_t} = \frac{\phi_i}{\overline{V_i}} \sum_{k=1}^{m} x_k \overline{V_k}$. We re-write equation (13) in terms of volume fractions by replacing the mole fractions by the volume fractions: $-\frac{\phi_i}{\overline{V_i}} \frac{1}{c_t RT} \frac{d\mu_i}{dz} = \sum_{\substack{j=1 \\ j \neq i}}^{m} \frac{\left(u_i - u_j\right)}{Đ_{ij}} \frac{\phi_i}{\overline{V_i}} \frac{1}{c_t} \frac{\phi_j}{\overline{V_j}} \frac{1}{c_t}$, or $-\frac{\phi_i}{\overline{V_i}} \frac{1}{RT} \frac{d\mu_i}{dz} = \sum_{\substack{j=1 \\ j \neq i}}^{m} \frac{\phi_i \phi_j \left(u_i - u_j\right)}{Đ_{ij}} \frac{1}{\overline{V_i}} \frac{1}{\overline{V_j}} \frac{1}{c_t}$. Let us define modified M-S diffusivities: $c_t Đ_{ij} \overline{V_j} = \frac{Đ_{ij} \overline{V_j}}{\overline{V}} = Đ_{ij}^V$, $c_t Đ_{12} \overline{V_2} = \frac{Đ_{12} \overline{V_2}}{\overline{V}} = Đ_{12}^V$, and $c_t Đ_{1m} \overline{V_m} = \frac{Đ_{1m} \overline{V_m}}{\overline{V}} = Đ_{1m}^V$

We have the symmetry constraint $Đ_{ij} = \frac{Đ_{ij}^V}{\overline{V_j}} \overline{V} = Đ_{ji} = \frac{Đ_{ji}^V}{\overline{V_i}} \overline{V}$; $\frac{Đ_{ji}^V}{\overline{V_i}} = \frac{Đ_{ij}^V}{\overline{V_j}}$.

The M-S equations written in terms of volume fractions take the form

$$-\frac{1}{RT}\frac{d\mu_i}{dz}=\sum_{\substack{j=1\\ j\neq i}}^{n}\frac{\phi_j\left(u_i-u_j\right)}{Đ_{ij}^{V}}+\frac{\phi_m\left(u_i\right)}{Đ_{im}^{V}};\quad i=1,2,...n$$
$$-\phi_i\frac{1}{RT}\frac{d\mu_i}{dz}=\sum_{\substack{j=1\\ j\neq i}}^{n}\frac{\phi_i\phi_j\left(u_i-u_j\right)}{Đ_{ij}^{V}}+\frac{\phi_i\phi_m\left(u_i\right)}{Đ_{im}^{V}};\quad i=1,2,...n \tag{16}$$

We re-write equation (16) as

$$-\phi_i\frac{1}{RT}\frac{d\mu_i}{dz}=\sum_{\substack{j=1\\ j\neq i}}^{n}\frac{\left(\phi_i\phi_j u_i-u_j\phi_i\phi_j\right)}{Đ_{ij}^{V}}+\frac{\left(\phi_i\phi_m u_i\right)}{Đ_{im}^{V}};\quad i=1,2,...n \tag{17}$$

Let us define the *volumetric* flux of component *i*, expressed as $m^3\ m^{-2}\ s^{-1}$ as $N_i^V=\phi_i u_i$. The molar flux of component *i*, expressed as mol $m^{-2}\ s^{-1}$ is $N_i=c_i u_i=\frac{\phi_i}{\overline{V}_i}u_i=\frac{N_i^V}{\overline{V}_i}$. In terms of the volumetric fluxes of components, equation (17) is

$$-\phi_i\frac{1}{RT}\frac{d\mu_i}{dz}=\sum_{\substack{j=1\\ j\neq i}}^{n}\frac{\left(\phi_j N_i^V-\phi_i N_j^V\right)}{Đ_{ij}^{V}}+\frac{\left(\phi_m N_i^V\right)}{Đ_{im}^{V}};\quad i=1,2,...n \tag{18}$$

Let us define a $n\times n$ dimensional matrix of inverse diffusivities $\left[B\right]$ whose elements are given by

$$B_{ii}=\sum_{j=1;j\neq i}^{j=n}\frac{\phi_j}{Đ_{ij}^{V}}+\frac{\phi_m}{Đ_{1m}^{V}};\quad B_{ij;i\neq j}=-\frac{\phi_i}{Đ_{ij}^{V}};\quad i,j=1,2,...n \tag{19}$$

It is helpful to express the left member of equation (17) in terms of the volume fraction gradients by introducing an $n\times n$ dimensional matrix of thermodynamic factors $\left[\Gamma\right]$:

$$\frac{\phi_i}{RT}\frac{d\mu_i}{dz}=\phi_i\frac{d\ln a_i}{dz}=\sum_{j=1}^{j=n}\Gamma_{ij}\frac{d\phi_j}{dz};\quad \Gamma_{ij}=\frac{\phi_i}{\phi_j}\frac{\partial\ln a_i}{\partial\ln\phi_j};\quad i,j=1,,..n \tag{20}$$

Combining Equations (18), (19) and (20) and casting these in *n*-dimensional matrix notation we write

$$\left(N^V\right)=-\left[B\right]^{-1}\left[\Gamma\right]\frac{d\left(\phi\right)}{dz} \tag{21}$$

The corresponding expression for the molar fluxes is obtained from use of the $N_i = \frac{N_i^V}{\overline{V}_i}$; this results in the final expression as follows

$$(N) = -\begin{bmatrix} 1/\overline{V}_1 & 0 & 0 & 0 \\ 0 & 1/\overline{V}_2 & 0 & 0 \\ 0 & 0 & \ddots & 0 \\ 0 & 0 & 0 & 1/\overline{V}_n \end{bmatrix} [B]^{-1}[\Gamma]\frac{d(\phi)}{dz} \tag{22}$$

We now consider the special cases of unary permeation and binary mixture permeation.

6. The Maxwell-Stefan description of unary permeation

For the special case of unary permeation through polymer membrane (indicated with subscript m), $N_m = N_m^V = 0$, we write

$$N_1^V = -\frac{Đ_{1m}^V}{\phi_m}\Gamma\frac{d\phi_1}{dz}; \quad \Gamma = \frac{\partial \ln a_1}{\partial \ln \phi_1}; \quad N_1 = \frac{N_1^V}{\overline{V}_1} = -\frac{1}{\overline{V}_1}\frac{1}{1-\phi_1}Đ_{1m}^V\frac{\partial \ln a_1}{\partial \ln \phi_1}\frac{d\phi_1}{dz}; \tag{23}$$

The thermodynamic correction factor, $\Gamma = \frac{\partial \ln a_1}{\partial \ln \phi_1}$ can be evaluated by analytic differentiation of the Flory-Huggins Equation (2).

The "effective" Fick diffusivity is

$$D_{1,eff} = \frac{1}{1-\phi_1}Đ_{1m}^V\frac{\partial \ln a_1}{\partial \ln \phi_1} \tag{24}$$

We note, in passing, that the Fick diffusivity is defined as $Đ_{1m}^V\frac{\partial \ln a_1}{\partial \ln \phi_1}$ in the works of Fornasiero et al.[16] and Ribeiro et al.[7] We choose to define the effective Fick diffusivity using equation (24), because this allows a more convenient generalization to *n*-component mixtures as discussed in the foregoing section. In order to underscore the differences in the definitions, we have added the adjective "effective" for differentiation purposes.

As illustration of the dependence of the M-S and effective Fick diffusivities on the volume fraction of the penetrant, we present in Figure **16** calculations for (a) thermodynamic correction factor, $\Gamma = \frac{\partial \ln a_1}{\partial \ln \phi_1}$, (b) modified Maxwell-Stefan diffusivity, $Đ_{1m}^{V}$, and (c) effective Fick diffusivity, $D_{1,eff} = \frac{1}{1-\phi_1} Đ_{1m}^{V} \frac{\partial \ln a_1}{\partial \ln \phi_1}$, for water (component 1) in 2-hydroxyethyl methacrylate (HEMA) (indicated by subscript m) at $T = 296.65$ K.

Figure 17a shows calculations of the effective Fick diffusivities for unary permeation of CO_2 and C_2H_6 across a cross-linked polyethylene oxide (XLPEO) membrane at 298.15 K. The *x*-axis represents the volume fraction of the penetrant. The corresponding calculations of the thermodynamic factors are shown in Figure 17b. The influence of the thermodynamic correction factors is particularly strong for C_2H_6; this is because of the large value of the Flory-Huggins interaction parameter $\chi_{2m} = 2.0804$.

The unary molar flux of penetrant 1 can be determined by integrating equation (23) over the membrane thickness, δ.

$$N_1 \delta = -\frac{1}{\overline{V}_1} \int_{\phi_{10}}^{\phi_{1\delta}} D_{1,eff} d\phi_1 = -\frac{1}{\overline{V}_1} \int_{\phi_{10}}^{\phi_{1\delta}} \frac{1}{1-\phi_1} Đ_{1m}^{V} \frac{\partial \ln a_1}{\partial \ln \phi_1} d\phi_1 \tag{25}$$

In equation (25), ϕ_{10} and $\phi_{1\delta}$ are the volume fractions of the penetrant 1 at the upstream and downstream faces, respectively. Fornasiero et al.[17] use Equation (25) to describe the steady-state diffusion of water through soft-contact-lens materials. The integral in Equation (25) can be determined analytically.

In the membrane literature, the experimental data are commonly presented in terms of the permeability of component *i* that is defined as

$$\Pi_i = \frac{N_i}{\Delta f_i / \delta} \tag{26}$$

In equation (26), Δf_i is the difference in the fugacities in the upstream and downstream compartments. The SI units for the permeability is mol m m^{-2} s^{-1} Pa^{-1}. The more commonly used engineering unit for permeability is the Barrer expressed in cm^3 (STP) cm cm^{-2} s^{-1} $(cm\ Hg)^{-1}$. To convert to the commonly used engineering units of Barrers we divide the value in mol m m^{-2} s^{-1} Pa^{-1} by 3.348×10^{-16}.

Combining equation (25) and (26), we obtain

$$\Pi_1 = \frac{N_1}{\Delta f_1} = -\frac{1}{\Delta f_1}\frac{1}{\overline{V}_1}\int_{\phi_{10}}^{\phi_{1\delta}} D_{1,eff}\, d\phi_1 = -\frac{1}{\Delta f_1}\frac{1}{\overline{V}_1}\int_{\phi_{10}}^{\phi_{1\delta}} \frac{1}{1-\phi_1} Đ_{1m}^{V} \frac{\partial \ln a_1}{\partial \ln \phi_1} d\phi_1 \tag{27}$$

The membrane thickness does not appear in the model calculations presented in Equation (27).

If the volume fraction of the component 1 at the downstream face of the polymer membrane is taken to be vanishingly small, i.e. $\phi_{1\delta} \approx 0; f_{1\delta} \approx 0;$, and $D_{1,eff}$ is evaluated at the arithmetic average volume fraction $\frac{(\phi_{10}+\phi_{1\delta})}{2}$, we get

$$\Pi_1 = \frac{N_1}{\Delta f_1} = \frac{1}{\Delta f_1}\frac{1}{\overline{V}_1} D_{1,eff}(\phi_{10} - 0) \approx \frac{1}{f_{10}}\frac{1}{\overline{V}_1} D_{1,eff}(\phi_{10}) \tag{28}$$

Equation (28) represents the simplified, i.e. linearized, solution to the Maxwell-Stefan equations.

In order to demonstrate the accuracy of the linearized solution to the M-S equations, let us consider the unary permeation of penetrants CO_2 and C_2H_6 across a cross-linked polyethylene oxide (XLPEO) membrane (indicated by subscript m). The input data on the Flory-Higgins parameters, and the Maxwell-Stefan diffusivities are culled from the papers by Ribeiro et al.[3, 4, 7, 18] The input data for temperatures of (a) 298.15 K, and (b) 263.15 K are summarized in Table 1, and Table 2

Figures 18a,b present the experimental data, as reported in Figure 2 of Ribeiro et al.,[18] on the permeabilities for unary permeation of CO_2 and C_2H_6 across a cross-linked polyethylene oxide (XLPEO) membrane at 298.15 K. The continuous solid lines are the calculations using the simplified linearized Equation (28). The agreement of the linearized solution is indistinguishable from the exact

solution given in Equation (27). Both models are in excellent agreement with the experimental data of Ribeiro et al.[18]

Figures 18c,d present the corresponding data for permeabilities for unary permeation of CO_2 and C_2H_6 across a cross-linked polyethylene oxide (XLPEO) membrane at 263.15 K. At the lower temperature, the volume fractions of the penetrants in the membrane are higher, and interactions between the penetrants and membrane is stronger. Consquently, the linearized solution deviates slightly from the exact analytical solution at high upstream fugacities. Both linearized model, and exact solutions, are in excellent agreement with the experimental data of Ribeiro et al.[18]

7. The Maxwell-Stefan description of binary mixture permeation

For binary mixture permeation across a polymeric membrane (indicated with subscript m), $N_m = N_m^V = 0$, we write

$$\begin{aligned} -\phi_1 \frac{1}{RT}\frac{d\mu_1}{dz} &= \frac{\left(\phi_2 N_1^V - \phi_1 N_2^V\right)}{Đ_{12}^V} + \frac{\left(\phi_m N_1^V\right)}{Đ_{1m}^V} \\ -\phi_2 \frac{1}{RT}\frac{d\mu_2}{dz} &= \frac{\left(\phi_1 N_2^V - \phi_2 N_1^V\right)}{Đ_{21}^V} + \frac{\left(\phi_m N_2^V\right)}{Đ_{2m}^V} \end{aligned} \tag{29}$$

Let us define a 2 × 2 dimensional matrix of inverse diffusivities $[B]$ whose elements are given by

$$\begin{aligned} B_{11} &= \frac{\phi_2}{Đ_{12}^V} + \frac{\phi_m}{Đ_{1m}^V}; \quad B_{12} = -\frac{\phi_1}{Đ_{12}^V} \\ B_{21} &= -\frac{\phi_2}{Đ_{21}^V}; \quad B_{22} = \frac{\phi_1}{Đ_{21}^V} + \frac{\phi_m}{Đ_{2m}^V} \end{aligned} \tag{30}$$

It is helpful to express the left member of equation (17) in terms of the volume fraction gradients by introducing an 2 × 2 dimensional matrix of thermodynamic factors $[\Gamma]$:

$$\frac{\phi_i}{RT}\frac{d\mu_i}{dz} = \phi_i \frac{d\ln a_i}{dz} = \sum_{j=1}^{2} \Gamma_{ij}\frac{d\phi_j}{dz}; \quad \Gamma_{ij} = \frac{\phi_i}{\phi_j}\frac{\partial \ln a_i}{\partial \ln \phi_j}; \quad i,j = 1,2$$

$$\begin{bmatrix} \Gamma_{11} & \Gamma_{12} \\ \Gamma_{21} & \Gamma_{22} \end{bmatrix} = \begin{bmatrix} \phi_1 \dfrac{\partial \ln a_1}{\partial \phi_1} & \phi_1 \dfrac{\partial \ln \phi_1}{\partial \phi_2} \\ \phi_2 \dfrac{\partial \ln a_2}{\partial \phi_1} & \phi_2 \dfrac{\partial \ln a_2}{\partial \phi_2} \end{bmatrix} \tag{31}$$

The four elements $\Gamma_{11}, \Gamma_{12}, \Gamma_{21}, \Gamma_{22}$ can be determined by analytic differentiation of Equation (4). Explicit analytic expressions are provided by Ribeiro et al.[7]

Combining Equations (29), (30) and (31) and casting these in 2-dimensional matrix notation we write

$$(N^V) = -[B]^{-1}[\Gamma]\frac{d(\phi)}{dz}; \quad \begin{pmatrix} N_1^V \\ N_2^V \end{pmatrix} = -\begin{bmatrix} B_{11} & B_{12} \\ B_{21} & B_{22} \end{bmatrix}^{-1}\begin{bmatrix} \Gamma_{11} & \Gamma_{12} \\ \Gamma_{21} & \Gamma_{22} \end{bmatrix}\frac{d}{dz}\begin{pmatrix} \phi_1 \\ \phi_2 \end{pmatrix} \tag{32}$$

The matrix inversion $\begin{bmatrix} B_{11} & B_{12} \\ B_{21} & B_{22} \end{bmatrix}^{-1}$ can be performed explicitly

$$\begin{bmatrix} B_{11} & B_{12} \\ B_{21} & B_{22} \end{bmatrix}^{-1} = \frac{\begin{bmatrix} \dfrac{\phi_1}{Đ_{21}^V} + \dfrac{\phi_m}{Đ_{2m}^V} & \dfrac{\phi_1}{Đ_{12}^V} \\ \dfrac{\phi_2}{Đ_{21}^V} & \dfrac{\phi_2}{Đ_{12}^V} + \dfrac{\phi_m}{Đ_{1m}^V} \end{bmatrix}}{\phi_m\left(\dfrac{\phi_1}{Đ_{21}^V Đ_{1m}^V} + \dfrac{\phi_2}{Đ_{12}^V Đ_{2m}^V} + \dfrac{\phi_m}{Đ_{1m}^V Đ_{2m}^V}\right)} \tag{33}$$

The 2 × 2 dimensional matrix of Fick diffusivities is

$$[D] = [B]^{-1}[\Gamma] = \frac{\begin{bmatrix} \dfrac{\phi_1}{Đ_{21}^V} + \dfrac{\phi_m}{Đ_{2m}^V} & \dfrac{\phi_1}{Đ_{12}^V} \\ \dfrac{\phi_2}{Đ_{21}^V} & \dfrac{\phi_2}{Đ_{12}^V} + \dfrac{\phi_m}{Đ_{1m}^V} \end{bmatrix}}{\phi_m\left(\dfrac{\phi_1}{Đ_{21}^V Đ_{1m}^V} + \dfrac{\phi_2}{Đ_{12}^V Đ_{2m}^V} + \dfrac{\phi_m}{Đ_{1m}^V Đ_{2m}^V}\right)}\begin{bmatrix} \phi_1 \dfrac{\partial \ln a_1}{\partial \phi_1} & \phi_1 \dfrac{\partial \ln \phi_1}{\partial \phi_2} \\ \phi_2 \dfrac{\partial \ln a_2}{\partial \phi_1} & \phi_2 \dfrac{\partial \ln a_2}{\partial \phi_2} \end{bmatrix} \tag{34}$$

The "effective" Fick diffusivities of components 1 and 2 are

$$D_{1,eff} = D_{11} + D_{12}\frac{d\phi_2/dz}{d\phi_1/dz}; \quad D_{2,eff} = D_{22} + D_{21}\frac{d\phi_1/dz}{d\phi_2/dz} \tag{35}$$

The molar fluxes can be determined from

$$\begin{pmatrix} N_1 \\ N_2 \end{pmatrix} = -\begin{bmatrix} 1/V_1 & 0 \\ 0 & 1/V_2 \end{bmatrix} \frac{\begin{bmatrix} \frac{\phi_1}{\mathcal{D}_{21}^V} + \frac{\phi_m}{\mathcal{D}_{2m}^V} & \frac{\phi_1}{\mathcal{D}_{12}^V} \\ \frac{\phi_2}{\mathcal{D}_{21}^V} & \frac{\phi_2}{\mathcal{D}_{12}^V} + \frac{\phi_m}{\mathcal{D}_{1m}^V} \end{bmatrix}}{\phi_m \left(\frac{\phi_1}{\mathcal{D}_{21}^V \mathcal{D}_{1m}^V} + \frac{\phi_2}{\mathcal{D}_{12}^V \mathcal{D}_{2m}^V} + \frac{\phi_m}{\mathcal{D}_{1m}^V \mathcal{D}_{2m}^V} \right)} \begin{bmatrix} \phi_1 \frac{\partial \ln a_1}{\partial \phi_1} & \phi_1 \frac{\partial \ln \phi_1}{\partial \phi_2} \\ \phi_2 \frac{\partial \ln a_2}{\partial \phi_1} & \phi_2 \frac{\partial \ln a_2}{\partial \phi_2} \end{bmatrix} \frac{d}{dz} \begin{pmatrix} \phi_1 \\ \phi_2 \end{pmatrix} \tag{36}$$

In the linearized solution, the 2-dimensional matrix $\begin{bmatrix} B_{11} & B_{12} \\ B_{21} & B_{22} \end{bmatrix}^{-1} \begin{bmatrix} \Gamma_{11} & \Gamma_{12} \\ \Gamma_{21} & \Gamma_{22} \end{bmatrix}$ is evaluated at the at the arithmetic average volume fractions $\frac{(\phi_{i0} + \phi_{i\delta})}{2}$. Furthermore, the gradients of the volume fraction are evaluated using the linearized relation: $-\frac{d\begin{pmatrix} \phi_1 \\ \phi_2 \end{pmatrix}}{dz} = \frac{\begin{pmatrix} \phi_{10} - \phi_{1\delta} \\ \phi_{20} - \phi_{2\delta} \end{pmatrix}}{\delta}$.

8. Permeation of CO_2/C_2H_6 mixtures across XLPEO membrane

Generally speaking, thermodynamic coupling effects are important in mixture permeation across polymer membranes. In order to highlight the importance of thermodynamic coupling effects, let us consider the permeation of penetrants CO_2 (component 1) and C_2H_6 (Component 2) across a cross-linked polyethylene oxide (XLPEO) membrane (indicated by subscript m) at 263.15 K. The upstream face of the membrane is in equilibrium with 70% CO_2 gas mixture. In the calculations, the partial fugacity of CO_2 is increased, keeping the gas mixture composition constant. The input data on the Flory-Higgins parameters are culled from the papers by Ribeiro et al.[3, 4, 7, 18]. Figure 19a shows the calculations of the four elements of the matrix of thermodynamic factors Γ_{ij}. Particularly noteworthy is the large magnitude of Γ_{12}. The significance of thermodynamic coupling may be quantified by the ratio $\frac{\Gamma_{11}\phi_1 + \Gamma_{12}\phi_2}{\Gamma_{21}\phi_1 + \Gamma_{22}\phi_2}$; see calculations in Figure 19b. For thermodynamically ideal mixtures, this ratio should be constant. Thermodynamic coupling effects strongly influence trans-membrane fluxes and permeatbilities, as we shall see below.

Figure 19c presents calculations of the effective Fick diffusivities of CO_2 (component 1) and C_2H_6 (Component 2). Both effective diffusivities show strong increases with increasing partial fugacities of CO_2 in the gas mixture in the upstream compartment.

Figures 20a and 20b present experimental data (indicated by symbols) of Ribeiro et al.[18] for the permeabilities, expressed in Barrers, of CO_2 and C_2H_6 for binary CO_2/C_2H_6 mixture permeation across a cross-linked polyethylene oxide (XLPEO) membrane at 298.15 K. The *x*-axis represents the partial fugacity of the permeants in the bulk gas phase in the upstream compartment. Five different mixture compositions are considered. We note that the permeability of CO_2 is practically unaffected by the mixture composition of the bulk gas phase in the upstream compartment. In sharp contrast, we note that the permeability of C_2H_6 is strongly influenced (increased) by increasing proportion of CO_2 in the bulk gas phase mixture in the upstream compartment. The continuous solid lines in Figures 20a and 20b are the permeabilities calculated using equation (36), wherein $\begin{bmatrix} B_{11} & B_{12} \\ B_{21} & B_{22} \end{bmatrix}^{-1} \begin{bmatrix} \Gamma_{11} & \Gamma_{12} \\ \Gamma_{21} & \Gamma_{22} \end{bmatrix}$ is evaluated at the arithmetic average volume fractions $\frac{(\phi_{i0} + \phi_{i\delta})}{2} \approx \frac{(\phi_{i0} + 0)}{2}$. The linearized set of M-S equations captures, quantitatively, all the essential features of the composition dependence of the permeabilities of CO_2 and C_2H_6.

Figures 21a, and 21b compare the experimental data CO_2, and C_2H_6 for binary mixture permeation across a XLPEO at a lower temperature of 263.15 K at which molecule-molecule and molecule-membrane interactions are significantly stronger, and composition dependent. At this lower temperature, the permeabilities of both components are influenced by the mixture composition. The linearized M-S model, in combination with F-H, affords a quantitative reproduction of all the essential features of the experimental data as presented in Figure 4b and Figure 5b of Ribeiro et al.[18]

If the friction between the two penetrants is ignored, i.e. $Đ_{12}^V >> Đ_{1m}^V; Đ_{12}^V >> Đ_{2m}^V$ then the matrix $[B]$ simplifies to a diagonal matrix

$$B_{ii} = \frac{\phi_m}{Đ_{im}^V}; \quad B_{ij;i\neq j} = 0; \quad \text{negligible 1 - 2 friction scenario} \tag{37}$$

The calculations in Figure 22a,b are obtained with equation (37) for binary permeation at 263.15 K. We note that this simplified scenario captures the composition dependence *qualitatively*, but the quantitative agreement is not as good as in Figures 21a, and 21b

9. Water/ethanol pervaporation across cellulose acetate membrane

Thermodynamic coupling effects also strongly influence the separation of water/alcohol mixtures by pervaporation. In order to demonstrate this, Figure 23a presents calculations for the thermodynamic correction factors for the ternary mixture consisting of water (component 1), ethanol (component 2) and cellulose acetate (polymer, component m) using the Flory-Huggins parameters from Mulder et al.[6, 19] Cellulose acetate membranes are hydrophilic, and preferentially adsorb water from water/ethanol bulk liquid mixtures. Figure 23b plots the ratios $\frac{\Gamma_{12}}{\Gamma_{11}}$, and $\frac{\Gamma_{21}}{\Gamma_{22}}$ as a function of the volume fraction of water in the bulk liquid mixture. The large magnitude of $\frac{\Gamma_{21}}{\Gamma_{22}}$ implies that the flux of ethanol is strongly influenced by the driving force for water transport.

The influence of thermodynamic coupling is to suppress the flux of ethanol and enhance the water flux, a desirable result for pervaporation separations. In order to illustrate the influence of thermodynamic coupling on the pervaporation fluxes, we perform calculations using the input diffusivity data from Mulder et al;[19] see data summary in Table 3. The pervaporation fluxes are determined from:

$$\begin{pmatrix} N_1 \\ N_2 \end{pmatrix} = -\begin{bmatrix} 1/V_1 & 0 \\ 0 & 1/V_2 \end{bmatrix} \begin{bmatrix} D_{11} & D_{12} \\ D_{21} & D_{22} \end{bmatrix} \frac{\begin{pmatrix} \phi_{10} - \phi_{1\delta} \\ \phi_{20} - \phi_{2\delta} \end{pmatrix}}{\delta}. \tag{38}$$

The expression for the Fick diffusivity matrix, ignoring the 1-2 interactions is

$$\begin{bmatrix} D_{11} & D_{12} \\ D_{21} & D_{22} \end{bmatrix} = \begin{bmatrix} \dfrac{\phi_m}{Đ_{1m}^V} & 0 \\ 0 & \dfrac{\phi_m}{Đ_{2m}^V} \end{bmatrix}^{-1} \begin{bmatrix} \Gamma_{11} & \Gamma_{12} \\ \Gamma_{21} & \Gamma_{22} \end{bmatrix} = \frac{1}{(1-\phi_1-\phi_2)} \begin{bmatrix} Đ_{1m}^V & 0 \\ 0 & Đ_{2m}^V \end{bmatrix} \begin{bmatrix} \Gamma_{11} & \Gamma_{12} \\ \Gamma_{21} & \Gamma_{22} \end{bmatrix} \tag{39}$$

In the linearized approach, equation (39) is estimated at the arithmetic average volume fractions $\frac{(\phi_{i0}+\phi_{i\delta})}{2} \approx \frac{\phi_{i0}}{2}$.

The continuous solid lines in Figure 23c are the calculations of the permeation fluxes using equations (38) and (39). The origin of the maximum in the water flux can be traced to the corresponding maximum in the volume fractions of water penetrant, as observed in Figure 7.

The dashed lines in Figure 23c represent calculations of the permeation fluxes assuming a scenario in which the thermodynamic coupling effects are ignored and we assume $\begin{bmatrix} \Gamma_{11} & \Gamma_{12} \\ \Gamma_{21} & \Gamma_{22} \end{bmatrix} \approx \begin{bmatrix} 1 & 0 \\ 0 & 1 \end{bmatrix}$, the identity matrix [*I*], and therefore the Fick diffusivity matrix is uncoupled

$$\begin{bmatrix} D_{11} & D_{12} \\ D_{21} & D_{22} \end{bmatrix} = \frac{1}{(1-\phi_1-\phi_2)} \begin{bmatrix} Đ_{1m}^V & 0 \\ 0 & Đ_{2m}^V \end{bmatrix}. \tag{40}$$

Neglect of thermodynamic coupling has a relatively stronger effect on the ethanol fluxes. Figure 23d presents calculations of the permeation selectivities defined by $\frac{(N_1 M_1)/(N_2 M_2)}{\omega_1^L/\omega_2^L}$. Inclusion of thermodynamic coupling effects improves the separation selectivity in favor of water.

Heintz and Stephan[20] have also underscored the importance of diffusional coupling effects for pervaporation of water/ethanol mixtures across a poly (vinyl alcohol) /poly (acrylonitrile) (PVA/PAN) composite membrane. Interestingly, their experimental data also show a maximum in the ethanol fluxes, analogous to the observations in Figure 23c.

10. Water/ethanol pervaporation across polyimide membrane

Thermodynamic coupling effects are also significant for water/ethanol pervaporation across polyimide membrane. Figure 24a shows the calculations of the elements of $[\Gamma]$ as function of the mass

fraction of water in the bulk liquid mixture in the upstream compartment. The off-diagonal elements are non-negligible in comparison with the diagonal elements; see Figure 24b.

The experimental data of Ni et al.[12] on the volumetric fluxes of water, and ethanol are plotted in Figures 24c, and 24d. Based on unary permeation, the input data values for binary mixture simulations are the ones provided in Table 1 of Ni et al.[12]: $Đ_{1m}^{V} = 25.5\times10^{-13}$, and $Đ_{2m}^{V} = 2.1\times10^{-13}$ m^2 s^{-1}; both these diffusivities are assumed to be composition independent.

Since no data on $Đ_{12}^{V}$ is available, we use the approach of Mulder et al.[6, 19] and use equation(39), ignoring 1-2 frictional contribution; the calculations are presented by the dashed lines in Figures 24c, and 24d. The flux of water is slightly over-predicted, and the ethanol flux is significantly under-predicted.

In Figure 5 of Ni et al.[12] the $Đ_{12}^{V}$ is determined to be composition dependent, lying between $Đ_{1m}^{V}$ and $Đ_{2m}^{V}$ at either ends of the composition scale. For our purposes here, we estimate $Đ_{12}^{V}$ using the logarithmic interpolation formula of Vignes [21] that has its origins in diffusion in binary liquid mixtures

$$\left(Đ_{12}^{V}/\overline{V_2}\right) = \left(Đ_{21}^{V}/\overline{V_1}\right) = \left(Đ_{1m}^{V}/\overline{V_2}\right)^{\phi_1/(\phi_1+\phi_2)}\left(Đ_{2m}^{V}/\overline{V_1}\right)^{\phi_2/(\phi_1+\phi_2)} \tag{41}$$

The limiting scenarios are

$$\begin{aligned} Đ_{12}^{V} &= Đ_{1m}^{V}; \quad \phi_2 \to 0 \\ Đ_{21}^{V} &= Đ_{2m}^{V}; \quad \phi_1 \to 0 \end{aligned} \tag{42}$$

Equation (41) is commonly used in the description of binary mixture diffusion in microporous crystalline materials.[22-24]

The inclusion of 1-2 fraction using Equation (41) provides improved agreement with the experimental data on ethanol fluxes. In particular the maximum in the ethanol flux is reasonably well captured. Ni et al.[12] also concluded that 1-2 friction cannot be ignored.

11. Water/ethanol pervaporation across PVA/PAN membrane

Heintz and Stephan[20] have also underscored the importance of diffusional coupling effects for pervaporation of water/ethanol mixtures across a poly (vinyl alcohol) /poly (acrylonitrile) (PVA/PAN) composite membrane. Interestingly, their experimental data (see Figure 25a) also show a maximum in the ethanol fluxes, analogous to the observations in Figure 23c and Figures 24d.

They have modelled their experiments using a combination of the Maxwell-Stefan model with the UNIQUAC description of phase equilibrium. For our purposes here, we use the M-S + F-H combination to model their pervaporation experiments with the objective of demonstrating the significance of 1-2 friction. The Flory-Huggins model provides a reasonably good descripition of phase equilibrium; see Figure 11.

Figure 25b shows the M-S+F-H model calculations assuming strong 1-2 friction, taking $Đ_{1m}^{V} = 5\times10^{-13}$ m^2 s^{-1}; $Đ_{2m}^{V} = Đ_{12}^{V} = 5\times10^{-14}$ m^2 s^{-1}; the matrix of Fick diffusivities is evaluated at the average volume fractions in the membrane layer. The maximum in the ethanol fluxes is reasonably well captured in the simulations with strong 1-2 friction. If the value of $Đ_{12}^{V}$ is assumed to be ten times larger, i.e. $Đ_{1m}^{V} = Đ_{12}^{V} = 5\times10^{-13}$ m^2 s^{-1}; $Đ_{2m}^{V} = 5\times10^{-14}$ m^2 s^{-1}, the maximum in the ethanol flux practically disappears; see the simulation results in Figure 25c.

For proper modelling of pervaporation processes, 1-2 friction is strong and cannot be ignored.

12. The M-S formulation for diffusion in multicomponent polymer solutions

We now turn our attention to the description of diffusion processes in which the polymer is dissolved in a homogeneous solution. The analysis of the diffusion process is important in a wide variety of contexts including that for membrane preparation, discussed in the foregoing sections. The diffusion velocity of the polymer molecules is finite, and equation (16) needs to be modified as follows

$$-\frac{1}{RT}\frac{d\mu_i}{dz}=\sum_{\substack{j=1\\ j\neq i}}^{n}\frac{\phi_j\left(u_i-u_j\right)}{Đ_{ij}^{V}}+\frac{\phi_m\left(u_i-u_m\right)}{Đ_{im}^{V}};\quad i=1,2,...n$$
$$-\phi_i\frac{1}{RT}\frac{d\mu_i}{dz}=\sum_{\substack{j=1\\ j\neq i}}^{n}\frac{\phi_i\phi_j\left(u_i-u_j\right)}{Đ_{ij}^{V}}+\frac{\phi_i\phi_m\left(u_i-u_m\right)}{Đ_{im}^{V}};\quad i=1,2,...n \tag{43}$$

The modified M-S diffusivities are the same as encountered in the foregoing analyses of membrane permeation; they are related to the more common M-S diffusivities defined in terms of mole fractions by: $c_t Đ_{ij}\overline{V_j}=\frac{Đ_{ij}\overline{V_j}}{\overline{V}}=Đ_{ij}^{V}$, and $c_t Đ_{1m}\overline{V_m}=\frac{Đ_{1m}\overline{V_m}}{\overline{V}}=Đ_{1m}^{V}$.

Let us define the volumetric diffusion fluxes relative to the volume average velocity of the mixture

$$J_i^V=\phi_i\left(u_1-u\right);\quad J_m^V=\phi_m\left(u_m-u\right)=-J_1-J_2-...-J_n;\quad u=\phi_1u_1+\phi_2u_2...+\phi_nu_n+\phi_mu_m \tag{44}$$

Equation (43) can be re-written in terms of the diffusion fluxes

$$-\phi_i\frac{1}{RT}\frac{d\mu_i}{dz}=\sum_{\substack{j=1\\ j\neq i}}^{n}\frac{\left(\phi_jJ_i^V-\phi_iJ_j^V\right)}{Đ_{ij}^{V}}+\frac{\left(\phi_mJ_i^V-\phi_iJ_m^V\right)}{Đ_{im}^{V}};\quad i=1,2,...n \tag{45}$$

Let us start by considering a binary solution consisting of solvent (1) and polymer (m). Equation (43) simplifies to yield

$$-\phi_1\frac{1}{RT}\frac{d\mu_1}{dz}=\frac{\left(\phi_1\phi_mu_1-\phi_1\phi_mu_m\right)}{Đ_{1m}^{V}}=\frac{\left(\phi_mN_1^V-\phi_1N_m^V\right)}{Đ_{1m}^{V}}=\frac{\left(\phi_mJ_1^V-\phi_1J_m^V\right)}{Đ_{1m}^{V}} \tag{46}$$

The J_1^V, J_m^V are the volumetric diffusion fluxes relative to the volume average velocity of the mixture

$$J_1^V=\phi_1\left(u_1-u\right);\quad J_m^V=\phi_m\left(u_m-u\right);\quad u=\phi_1u_1+\phi_mu_m;\quad J_1^V=-J_m^V;\quad \phi_1+\phi_m=1 \tag{47}$$

In view of equation (47), we may re-write equation (46) as

$$J_1^V=-Đ_{1m}^{V}\phi_1\frac{1}{RT}\frac{d\mu_1}{dz}=-Đ_{1m}^{V}\Gamma\frac{d\phi_1}{dz}=-D_1^V\frac{d\phi_1}{dz} \tag{48}$$

where $\Gamma=\frac{\partial\ln a_1}{\partial\ln\phi_1}$ is the thermodynamic correction factor as before, and $D_1^V=Đ_{1m}^{V}\frac{\partial\ln a_1}{\partial\ln\phi_1}$ is the Fick diffusivity.

13. Comparison of M-S and Bearman formulations for diffusion

In the vast literature on diffusion in polymer solutions,[25, 26] it is customary to use the friction formulation for multicomponent diffusion, normally credited to Bearman,[27] written in a manner such as in equation (1) of Price and Romdhane[26]

$$-\frac{d\mu_i}{dz}=\sum_{\substack{j=1\\ j\neq i}}^{n}\frac{\rho_j}{M_j}\varsigma_{ij}\left(u_i-u_j\right)+\frac{\rho_m}{M_m}\varsigma_{im}\left(u_i-u_m\right) \tag{49}$$

or equivalently, as $-\frac{d\mu_i}{dz}=\sum_{\substack{j=1\\ j\neq i}}^{n}c_j\varsigma_{ij}\left(u_i-u_j\right)+c_m\varsigma_{im}\left(u_i-u_m\right)$.

In equation (49), the $\varsigma_{ij},\varsigma_{im}$ are friction coefficients that are related to the modified Maxwell-Stefan diffusivities

$$\frac{\rho_j}{M_j}\varsigma_{ij}=\frac{RT\phi_j}{Đ_{ij}^{V}};\frac{\rho_m}{M_m}\varsigma_{im}=\frac{RT\phi_m}{Đ_{im}^{V}} \tag{50}$$

Furthermore, an alternative flux expression is used to describe for diffusion in polymer solutions; the mass fluxes, j_i, kg m^{-2} s^{-1}, relative to the volume average velocity of the mixture, are expressed as a linear function of the mass concentration gradients.[26] For the specific case of a binary solvent/polymer system

$$j_1=\rho_1\left(u_1-u\right)=\phi_1\frac{M_1}{\overline{V_1}}\left(u_1-u\right)=\frac{M_1}{\overline{V_1}}J_1^{V}=-D_1\frac{d\rho_1}{dz} \tag{51}$$

The Fick diffusivity, D_1, defined above in the volume average reference velocity frame, is related to the Bearman friction coefficient, and the modified Maxwell-Stefan diffusivity:

$$D_1=\frac{\overline{V_m}\rho_1}{\varsigma_{1m}}\frac{\partial\mu_1}{\partial\rho_1}=\frac{\overline{V_m}RT}{\varsigma_{1m}}\left(\frac{\rho_1}{RT}\frac{\partial\mu_1}{\partial\rho_1}\right)=\frac{\overline{V_m}\rho_m}{\phi_m M_m}Đ_{1m}^{V}\left(\frac{\rho_1}{RT}\frac{\partial\mu_1}{\partial\rho_1}\right)=Đ_{1m}^{V}\left(\frac{\rho_1}{RT}\frac{\partial\mu_1}{\partial\rho_1}\right) \tag{52}$$

In equation (52) we have used the equalities $\phi_m=c_m\overline{V_m}=\frac{\overline{V_m}\rho_m}{M_m}$.

14. Self-diffusivity in binary solvent/polymer solutions: Free-volume theory

It is also common in the polymer diffusion literature, to relate the Fick diffusivity D_1 to the self-diffusivity, $D_{1,self}$. The rationale for this is that the free volume theory allows prediction of self-diffusivity, $D_{1,self}$.[2, 25, 28] The relation between D_1 and $D_{1,self}$ requires careful and rigorous derivation.

We start with the Bearman equation (49) and apply it to a ternary mixture containing species 1, tagged species 1*, and polymer (m). The tagged species 1* is identical to species 1 with respect to thermodynamics and diffusion. This results in the following expression for $D_{1,self}$

$$\frac{1}{D_{1,self}} = \frac{\rho_1}{RTM_1}\varsigma_{11} + \frac{\rho_m}{RTM_m}\varsigma_{1m} \tag{53}$$

From the equalities $\frac{\rho_m}{RTM_m}\varsigma_{1m} = \frac{\phi_m}{Đ_{1m}^V}; \frac{\rho_1}{RTM_1}\varsigma_{11} = \frac{\phi_1}{Đ_{11}^V}$ we derive the following expression in terms of the M-S diffusivities

$$\frac{1}{D_{1,self}} = \frac{\phi_1}{Đ_{11}^V} + \frac{\phi_m}{Đ_{1m}^V} \tag{54}$$

The $Đ_{11}^V$ is the self-diffusivity of species 1 in pure 1; this can be estimated using the procedure such as Wilke-Chang.[29-31]

The corresponding expressions for the self-diffusivity of the polymer (m) are

$$\frac{1}{D_{m,self}} = \frac{\rho_m}{RTM_m}\varsigma_{mm} + \frac{\rho_1}{RTM_1}\varsigma_{1m} = \frac{\phi_m}{Đ_{mm}^V} + \frac{\phi_1}{Đ_{1m}^V} \tag{55}$$

Combining equation (52) and (54) we obtain

$$D_1 = Đ_{1m}^V\left(\frac{\rho_1}{RT}\frac{\partial\mu_1}{\partial\rho_1}\right) = \frac{\phi_m}{\left(\frac{1}{D_{1,self}} - \frac{\phi_1}{Đ_{11}^V}\right)}\left(\frac{\rho_1}{RT}\frac{\partial\mu_1}{\partial\rho_1}\right) \tag{56}$$

Equation (56) is precisely equivalent to equation (8) of Price and Romdhane.[26] For the limiting case of dilute solvent (species 1) in polymer (m) solutions, i.e. $\phi_1 << \phi_m$, we obtain

$$D_1 = Đ_{1m}^{V}\left(\frac{\rho_1}{RT}\frac{\partial\mu_1}{\partial\rho_1}\right) \approx \phi_m D_{1,self}\left(\frac{\rho_1}{RT}\frac{\partial\mu_1}{\partial\rho_1}\right) \tag{57}$$

In view of equation (57), we find $Đ_{1m}^{V} = \phi_m D_{1,self}$ for the case of negligible 1-1 friction.

The thermodynamic correction factor $\left(\frac{\rho_1}{RT}\frac{\partial\mu_1}{\partial\rho_1}\right) = \left(\frac{\partial \ln a_1}{\partial \ln \phi_1}\right)\left(\frac{\partial \ln \phi_1}{\partial \ln \rho_1}\right)$ can be determined from the Flory-Huggins theory; the correction factor $\left(\frac{\partial \ln \phi_1}{\partial \ln \rho_1}\right) \approx 1$.

From experiments, we can determine the Fick diffusivity D_1, along with the self-diffusivities $D_{1,self}$, and $D_{m,self}$ of solvent (1) and polymer (m). As illustration, Figure 26a shows the experimental data as reported in Figure 6 of Zielinski[32] for the self-diffusivities of toluene (1), and polystyrene (m) in polystyrene at 383 K as a function of the mass fraction of toluene. Also shown are the data for the Fick (mutual) diffusivity, D_1. The plotted data are those obtained from *five* different types of measurement techniques. There is a variation of about six orders of magnitude in the diffusivity values as a function of the mass fraction, ω_1. This strong variation make the task of predicting, or estimating, diffusivities in polymer solutions an extremely difficult one.

A further point to note in the experimental data for $0.5 < \omega_1 < 1.0$ is that Fick diffusivity is lower than the self-diffusivity of toluene, $D_{1,self}$ by about 1-2 orders of magnitude. We calculate the thermodynamic correction factor, $\left(\frac{\rho_1}{RT}\frac{\partial\mu_1}{\partial\rho_1}\right)$, taking $\chi = 0.354$; see Figure 26b. There is a strong reduction in $\left(\frac{\rho_1}{RT}\frac{\partial\mu_1}{\partial\rho_1}\right)$, by about 1-3 orders of magnitude as $\omega_1 \to 1$. Figure 26c compares the M-S

diffusivity, calculated using $Đ_{1m}^{V} = D_1 \Big/ \left(\frac{\rho_1}{RT} \frac{\partial \mu_1}{\partial \rho_1} \right)$, with D_1, $D_{1,\text{self}}$, and $D_{2,\text{self}}$. We note that $Đ_{1m} \approx D_{1,self}$; this implies that the 1-1 friction is not of significant importance.

The free-volume theory[2, 25, 28] is commonly used for estimation of the self-diffusivity, $D_{1,self}$. The expression for the self-diffusivity for solvent(1)/polymer(2) system is commonly written as[5]

$$D_{1,self} = D_{1,self,0} \exp\left(\frac{-E}{RT} \right) \exp\left(- \frac{\left(\omega_1 V_1^* + \omega_2 \xi V_2^* \right)}{\omega_1 \left(\frac{K_{11}}{\gamma} \right) \left(K_{21} - T_{g1} + T \right) + \omega_2 \left(\frac{K_{12}}{\gamma} \right) \left(K_{22} - T_{g2} + T \right)} \right) \tag{58}$$

For the system toluene/polystyrene, the free-volume parameters are provided in Table 2 of Alsoy and Duda.[33] The continuous solid line in Figure 26c are the estimations of the self-diffusivity for toluene in polystyrene using equation (58). The excellent agreement is no surprise, because the free-volume parameters, totaling 12 in number, have been determined by fitting to experimental data on self-diffusivities.

Broadly speaking, self-diffusivities display an exponential increase with increasing volume fractions. This provides the rationale for the use of the exponential model[7, 34]

$$Đ_{im}^{V} = Đ_{im,0}^{V} \exp\left[A_i \left(\phi_i + C_{ij} \phi_j \right) \right] \tag{59}$$

for describing the composition dependence of the M-S diffusivity.

Verros and Malamataris[5] provide a further illustration of use of the free-volume theory for estimation of the diffusivity of acetone (component 1) in cellulose acetate (indicated by subscript m) at T = 298.15 K. Calculations, using the input data provided in their paper, are presented in Figure 27. For this system, the penetrant (1) –membrane (m) interaction parameter is dependent on the volume fraction and the activities are calculated according to equation (3). The thermodynamic correction factor $\left(\frac{\rho_1}{RT} \frac{\partial \mu_1}{\partial \rho_1} \right)$

is a strongly decreasing function of the volume fraction, ϕ_1, and mass fraction ω_1; see Figure 27a. The Fick diffusivity is calculated using the approximation $D_1 = \phi_m D_{1,self}\left(\frac{\rho_1}{RT}\frac{\partial \mu_1}{\partial \rho_1}\right)$.

15. The Fick diffusivity matrix for diffusion in polymer solutions

For diffusion in a ternary mixture consisting of two solvent species (1, 2) and polymer (m), equations (45) and (44) yield

$$\begin{aligned} -\phi_1 \frac{1}{RT}\frac{d\mu_1}{dz} &= \frac{\left(\phi_2 J_1^V - \phi_1 J_2^V\right)}{Đ_{12}^V} + \frac{\left((1-\phi_1-\phi_2)J_1^V - \phi_1\left(-J_1^V - J_2^V\right)\right)}{Đ_{1m}^V} \\ -\phi_2 \frac{1}{RT}\frac{d\mu_2}{dz} &= \frac{\left(\phi_1 J_2^V - \phi_2 J_1^V\right)}{Đ_{21}^V} + \frac{\left((1-\phi_1-\phi_2)J_2^V - \phi_2\left(-J_1^V - J_2^V\right)\right)}{Đ_{2m}^V} \end{aligned} \tag{60}$$

For the case of negligible 1-2 friction equation (60) simplifies to yield

$$\begin{aligned} -\phi_1 \frac{1}{RT}\frac{d\mu_1}{dz} &= \frac{(1-\phi_2)J_1^V}{Đ_{1m}^V} + \frac{\phi_1 J_2^V}{Đ_{1m}^V} \\ -\phi_2 \frac{1}{RT}\frac{d\mu_2}{dz} &= \frac{\phi_2 J_1^V}{Đ_{2m}^V} + \frac{(1-\phi_1)J_2^V}{Đ_{2m}^V} \end{aligned} \tag{61}$$

We define the matrix of thermodynamic factor as in equation (20). In 2-dimensional matrix notation, equation (61) takes the form

$$\left(J^V\right) = -[D]\frac{d(\phi)}{dz}; \quad [D] = \begin{bmatrix} \frac{(1-\phi_2)}{Đ_{1m}^V} & \frac{\phi_1}{Đ_{1m}^V} \\ \frac{\phi_2}{Đ_{2m}^V} & \frac{(1-\phi_1)}{Đ_{2m}^V} \end{bmatrix}^{-1} \begin{bmatrix} \phi_1 \frac{\partial \ln a_1}{\partial \phi_1} & \phi_1 \frac{\partial \ln \phi_1}{\partial \phi_2} \\ \phi_2 \frac{\partial \ln a_2}{\partial \phi_1} & \phi_2 \frac{\partial \ln a_2}{\partial \phi_2} \end{bmatrix} \tag{62}$$

The matrix inversion can be performed analytically, and we get the following explicit expression for the Fick diffusivity matrix

$$[D]=\frac{Đ_{1m}^{V}Đ_{2m}^{V}}{\phi_m}\begin{bmatrix}\dfrac{(1-\phi_1)}{Đ_{2m}^{V}} & -\dfrac{\phi_1}{Đ_{1m}^{V}}\\ -\dfrac{\phi_2}{Đ_{2m}^{V}} & \dfrac{(1-\phi_2)}{Đ_{1m}^{V}}\end{bmatrix}\begin{bmatrix}\phi_1\dfrac{\partial \ln a_1}{\partial \phi_1} & \phi_1\dfrac{\partial \ln \phi_1}{\partial \phi_2}\\ \phi_2\dfrac{\partial \ln a_2}{\partial \phi_1} & \phi_2\dfrac{\partial \ln a_2}{\partial \phi_2}\end{bmatrix}$$

$$=\frac{1}{\phi_m}\begin{bmatrix}(1-\phi_1)Đ_{1m}^{V} & -\phi_1 Đ_{2m}^{V}\\ -\phi_2 Đ_{1m}^{V} & (1-\phi_2)Đ_{2m}^{V}\end{bmatrix}\begin{bmatrix}\phi_1\dfrac{\partial \ln a_1}{\partial \phi_1} & \phi_1\dfrac{\partial \ln \phi_1}{\partial \phi_2}\\ \phi_2\dfrac{\partial \ln a_2}{\partial \phi_1} & \phi_2\dfrac{\partial \ln a_2}{\partial \phi_2}\end{bmatrix} \tag{63}$$

$$\frac{1}{\phi_m}\begin{bmatrix}(1-\phi_1)Đ_{1m}^{V}\phi_1\dfrac{\partial \ln a_1}{\partial \phi_1}-\phi_1 Đ_{2m}^{V}\phi_2\dfrac{\partial \ln a_2}{\partial \phi_1} & (1-\phi_1)Đ_{1m}^{V}\phi_1\dfrac{\partial \ln \phi_1}{\partial \phi_2}-\phi_1 Đ_{2m}^{V}\phi_2\dfrac{\partial \ln a_2}{\partial \phi_2}\\ -\phi_2 Đ_{1m}^{V}\phi_1\dfrac{\partial \ln a_1}{\partial \phi_1}+(1-\phi_2)Đ_{2m}^{V}\phi_2\dfrac{\partial \ln a_2}{\partial \phi_1} & -\phi_2 Đ_{1m}^{V}\phi_1\dfrac{\partial \ln \phi_1}{\partial \phi_2}+(1-\phi_2)Đ_{2m}^{V}\phi_2\dfrac{\partial \ln a_2}{\partial \phi_2}\end{bmatrix}$$

Table 1 of Alsoy and Duda[33] provides four different scenarios (called Cases 1, 2, 3, and 4 in their paper) for estimation of the elements of the Fick diffusivity matrix; their expressions are in terms of the self-diffusivities in the *ternary* mixture.

The expression for the self-diffusivities in a mixture of 1,2 and polymer (m) are

$$\frac{1}{D_{1,self}}=\frac{\phi_1}{Đ_{11}^{V}}+\frac{\phi_2}{Đ_{12}^{V}}+\frac{\phi_m}{Đ_{1m}^{V}};\quad \frac{1}{D_{2,self}}=\frac{\phi_2}{Đ_{22}^{V}}+\frac{\phi_1}{Đ_{12}^{V}}+\frac{\phi_m}{Đ_{2m}^{V}} \tag{64}$$

For the case of negligible 1-2, 2-2, and 1-2 friction, equation (64) simplifies to yield

$$Đ_{1m}^{V}=\phi_m D_{1,self};\quad Đ_{2m}^{V}=\phi_m D_{2,self} \tag{65}$$

In view of equation (65), it is noted that Equation (63) is precisely equivalent to their Case 4.

The free-volume theory[2, 25, 28] is commonly used for estimation of the self-diffusivity, $D_{1,self}$, and $D_{2,self}$ in the mixture of 1/2/polymer mixture. The expression for the self-diffusivities for 1, and 2 in the solvent(1)/solvent(2)/polymer(3) system are given by equations (23), (24) and (25) of Zielinski and Hanley,[35] as reproduced below using their nomenclature.

$$D_{1,self} = D_{1,self,0} \exp\left(\frac{-E}{RT}\right) \exp\left(- \frac{\left(\omega_1 V_1^* + \omega_2 \frac{\xi_{13}}{\xi_{23}} V_2^* + \omega_3 \xi_{13} V_3^*\right)}{\omega_1\left(\frac{K_{11}}{\gamma}\right)\left(K_{21} - T_{g1} + T\right) + \omega_2\left(\frac{K_{12}}{\gamma}\right)\left(K_{22} - T_{g2} + T\right) + \omega_3\left(\frac{K_{13}}{\gamma}\right)\left(K_{23} - T_{g3} + T\right)} \right) \tag{66}$$

$$D_{2,self} = D_{2,self,0} \exp\left(\frac{-E}{RT}\right) \exp\left(- \frac{\left(\omega_1 V_1^* \frac{\xi_{23}}{\xi_{13}} + \omega_2 V_2^* + \omega_3 \xi_{23} V_3^*\right)}{\omega_1\left(\frac{K_{11}}{\gamma}\right)\left(K_{21} - T_{g1} + T\right) + \omega_2\left(\frac{K_{12}}{\gamma}\right)\left(K_{22} - T_{g2} + T\right) + \omega_3\left(\frac{K_{13}}{\gamma}\right)\left(K_{23} - T_{g3} + T\right)} \right) \tag{67}$$

We shall illustrate the estimations of the use of the free-volume theory by estimating the matrix of Fick diffusivities $[D]$, for methanol (component 1)/toluene (2)/poly(vinylacetate) (PVAc, subscript m) at T = 333.15 K. Figure 28a presents calculations for (a) matrix of thermodynamic correction factors, $[\Gamma]$, using equation (31) along with the Flory-Huggins parameters $\chi_{12} = 1; \chi_{1m} = 1.19; \chi_{2m} = 0.78$. Particularly note-worthy are the negative values of the off-diagonal elements Γ_{12}, Γ_{21}. The self-diffusivities are estimated using the equations (66) and (67) along with free-volume parameters provided in Table 1 of Zielinski and Hanley.[35] The Fick diffusivity matrix $[D]$ can then be calculated by combination of Equation (63) and equation (65); the results are presented in Figure 28b. Both the off-diagonal elements D_{12}, D_{21} are negative. It is also noteworthy that the magnitude of D_{21} is comparable to the magnitude of D_{22}; this implies that the flux of toluene will be strongly influenced by the driving force of methanol.

In their Table IV, Cussler and Lightfoot[36] report experimental data for the Fick diffusivity matrix $[D]$ for polystyrene(1)/cyclohexane(2)/toluene(3) mixtures. At composition mass fractions $\omega_1 = 0.05; \omega_2 = 0.05; \omega_3 = 0.95$, they report $[D] = \begin{bmatrix} 8.9 & -1.6 \\ -8.9 & 203.1 \end{bmatrix} \times 10^{-11}$ m^2 s^{-1}. It is to be stressed that the values of the Fick diffusivity matrix depending on the component numbering. For the same compositions, if the numbering is chosen as cyclohexane(1)/toluene(2)/polystyrene(3), the values of the Fick matrix can be re-calculated, using the basis of the data on the partial specific volumes provided in Table IV of Cussler and Lightfoot,[36] we obtain $[D] = \begin{bmatrix} 212 & 8.9 \\ -235.8 & -3.26 \end{bmatrix} \times 10^{-11}$ m^2 s^{-1}. In order to understand the large negative value of D_{21}, we estimated the matrix of thermodynamic factors for cyclohexane(1)/toluene(2)/polystyrene(3), using F-H parameters $\chi_{12} = 0.476; \chi_{13} = 0.51; \chi_{23} = 0.3548$, we obtain $[\Gamma] = \begin{bmatrix} 0.93 & -0.03 \\ -0.877 & 0.054 \end{bmatrix}$. The large negative value of Γ_{21} is the main cause of the large negative value of D_{21}.

In the literature on diffusion in multicomponent polymer solutions, equation (63) is often further simplified and used in the following form[19]

$$\left(J^V\right) = -[D]\frac{d(\phi)}{dz}; \quad [D] = \begin{bmatrix} Đ_{1m}^V & 0 \\ 0 & Đ_{2m}^V \end{bmatrix}[\Gamma] \tag{68}$$

We shall use Equation (68) for the analysis of equilibration trajectories in the immersion precipitation process for membrane preparation. Essentially, we make the assumption that all diffusional coupling effects accrue from the off-diagonal elements Γ_{12}, Γ_{21}.

16. Immersion precipitation process for preparation of cellulose acetate membrane

The influence of the thermodynamic correction factors is particularly strong in composition regions close to demixing regions. Diffusion close to demixing regions is of importance in membrane preparation by immersion precipitation.[37, 38] In order to illustrate this, let us consider diffusion in the

ternary mixture consisting of water (non-solvent, component 1), acetone (solvent, component 2) and cellulose acetate (polymer, component m). The binodal and spinodal curves for this ternary mixture are shown in Figure 29. The spinodal curve defines the limit of phase stability, and along the spinodal curve, the condition $|\Gamma| = 0$ must be satisfied, i.e. we must have $\Gamma_{11}\Gamma_{22} = \Gamma_{12}\Gamma_{21}$, the product of the off-diagonal elements is equal in magnitude to the product of the diagonal elements.[39, 40] This situation implies a significant degree of thermodynamic coupling.

The inset to Figure 29 shows calculations of the elements of the matrix of thermodynamic factors $[\Gamma]$ as a function of the volume fraction of acetone, keeping the ratio $\frac{\phi_1}{\phi_3} = \frac{25}{75}$. We note that the value of Γ_{21} becomes increasingly negative as the binodal curve is approached. This implies that the flux of acetone is strongly coupled with the flux of water. Strong thermodynamic coupling will induce strong diffusional coupling.

In order to demonstrate the influence of thermodynamic coupling, let us consider transient inter-diffusion between two compartments for the mixture water/acetone/CA. The binodal and spinodal curves for this system were determined using the numerical procedures outlined in Altena and Smolders.[41] The right compartment (R) contains the polymer solution with initial volume fractions $\phi_{1R} = 0.0; \phi_{2R} = 0.7; \phi_{mR} = 0.3$. The left compartment (L) is the coagulation bath with initial volume fractions $\phi_{1L} = 0.26; \phi_{2L} = 0.507; \phi_{mL} = 0.233$, that lie on the binodal curve. The matrix of thermodynamic correction factors at this composition in the coagulation bath is $[\Gamma] = \begin{bmatrix} 0.1682 & -0.0865 \\ -0.5624 & 0.543 \end{bmatrix}$. Note the large negative value of Γ_{21} in relation to Γ_{22}; this implies that the flux of acetone is strongly influenced by the driving force for water. The transient equilibration process is described by the coupled two-dimensional matrix equation

$$\begin{pmatrix} \phi_1 \\ \phi_2 \end{pmatrix} = \frac{1}{2}\begin{pmatrix} \phi_{1L} + \phi_{1R} \\ \phi_{2L} + \phi_{2R} \end{pmatrix} + \frac{1}{2} erf\left[-\frac{z}{\sqrt{4t}} [D]^{-1/2} \right] \begin{pmatrix} \phi_{1R} - \phi_{1L} \\ \phi_{2R} - \phi_{2L} \end{pmatrix} \tag{69}$$

The Sylvester theorem, detailed in Appendix A of Taylor and Krishna,[42] is required for explicit determination of the 2-dimensional square matrix $[Q] = erf\left[-\frac{z}{\sqrt{4t}}[D]^{-1/2} \right]$. The matrix of diffusivities are calculated from equation (62), at the average composition $\frac{1}{2}\begin{pmatrix} \phi_{1L} + \phi_{1R} \\ \phi_{2L} + \phi_{2R} \end{pmatrix}$. The Fick diffusivity matrix is calculated using equation (62), i.e. in the scenario of negligible 1-2 friction.

For the case of two distinct eigenvalues, λ_1, and λ_2 of the 2-dimensional Fick matrix $[D]$, the Sylvester theorem yields

$$[Q] = \frac{f(\lambda_1)[[D] - \lambda_2[I]]}{(\lambda_1 - \lambda_2)} + \frac{f(\lambda_2)[[D] - \lambda_1[I]]}{(\lambda_2 - \lambda_1)} \tag{70}$$

In equation (70), $[I]$ is the identity matrix with elements δ_{ik}. The functions $f(\lambda_i)$ are calculated from

$$f(\lambda_i) = erf\left[\frac{z}{\sqrt{4t}} \lambda_i^{-1/2} \right] \tag{71}$$

For calculation of the diffusional equilibration trajectories, we assume that the modified M-S diffusivities are the same as for water/ethanol/CA. The calculations can be easily implemented in MathCad 15.[1]

Figure 30 shows the equilibration trajectory followed in the two compartments, plotted in ternary volume fraction space. We note that equilibration trajectory follows a strongly curvilinear path. The volume fraction profiles on either side of the interface, at time t = 1 s, are plotted in the inset to Figure 30. During transient equilibration, both acetone and CA experience overshoots, and undershoots; these overshoots/undershoots signify the phenomenon of uphill diffusion that is commonly observed for transient uptake in micro-porous and macro-porous adsorbents.[43-46] The diffusional equilibration trajectory follows a strongly curvilinear path in ternary composition space.

Curvilinear equilibration trajectories for water/acetone/CA have been reported in the immersion precipitation process for membrane preparation.[37, 38] Figure 31 shows the equilibration trajectories when a 10% solution of Cellulose Acetate (CA) in acetone is immersed in a bath of pure water; the

trajectories at three different times, t = 10 s, t = 25 s, and t = 50 s are depicted. We note the curvilinear trajectory at t = 50 s has entered the meta-stable region. This foray into the meta-stable region impacts on the membrane structure.[37, 38] Tsay and McHugh[47] present detailed modelling of the transient equilibration trajectories for water/acetone/CA systems.

In order to demonstrate the foray into the meta-stable region, we perform transient diffusion from a well-stirred coagulation bath of constant composition (left compartment) into a polymer solution (right compartment) in the homogeneous single-phase region of the ternary diagram. The left compartment is the coagulation bath of constant composition $\phi_{1L} = 0.18067; \phi_{2L} = 0.10078; \phi_{mL} = 0.71855$; this composition lies on the binodal curve. The right compartment is the polymer solution of initial composition $\phi_{1R} = 0.24; \phi_{2R} = 0.6; \phi_{mR} = 0.16$. We focus on the transient equilibration in the right compartment, $z \geq 0$. The transient development of concentrations of the ions in the Right compartment is described by

$$\begin{pmatrix} \phi_1 \\ \phi_2 \end{pmatrix} = \begin{pmatrix} \phi_{1L} \\ \phi_{2L} \end{pmatrix} + erf\left[-\frac{z}{\sqrt{4t}} [D]^{-1/2} \right] \begin{pmatrix} \phi_{1R} - \phi_{1L} \\ \phi_{2R} - \phi_{2L} \end{pmatrix} \tag{72}$$

The transient volume fraction profiles in the right compartment is determined using essentially the same procedure as described above. A step-wise numerical scheme is used in which the matrix of diffusivity values is re-calculated at the values of volume fractions available for the previous position, z, as the volume fractions approach the values correspond to those in the left compartment. We note that the equilibration trajectory experiences a foray into the meta-stable region that lies between the binodal and spinodal curves. The profiles at time t = 1 s are plotted in the inset to Figure 32; the equilibration of water shows a distinct ϕ_1 overshoot, that is indicative of uphill diffusion.

For the ternary system water (non-solvent, component 1), 1,4 dioxane (solvent, component 2) and cellulose acetate (polymer, component m), the Flory-Huggins parameters as provided by Altena and Smolders[41] produce binodal and spinodal curves that have similar shapes and characteristics as those for the water/acetone/CA system. Also, in this case forays into the meta-stable region are observable as

indicated by the results in Figures 33a,b. In this case, the left compartment is the coagulation bath of constant composition $\phi_{1L} = 0.181; \phi_{2L} = 0.113; \phi_{mL} = 0.706$; this composition lies on the binodal curve. The right compartment is the polymer solution of initial composition $\phi_{1R} = 0.24; \phi_{2R} = 0.5; \phi_{mR} = 0.26$. The equilibration trajectory is indicated by the blue line in Figure 33a; this indicates a clear incursion into the meta-stable region. The volume fraction profiles in the polymer solution (right compartment) at time t = 1 s after the start are shown in Figure 33b. The equilibration of water shows a distinct ϕ_1 overshoot, that is indicative of uphill diffusion.

17. Immersion precipitation process for preparation of poly(ether)sulfone (PES) membrane

Thermodynamic coupling effects and curvilinear diffusional equilibration trajectories are generic characteristics of ternary membrane forming systems. As further demonstration, Figure 34 shows the diffusional equilibration trajectory in a ternary system consisting of water (non-solvent, component 1), N-methyl-2-pyrrolidone (NMP) (solvent, component 2) and poly(ether)sulfone (PES) (polymer, component m). The calculations are analogous to those presented in Figure 30. At time t = 0, the composition of the polymer solution in the right compartment is: ϕ_{1L} = 0.0, ϕ_{2L} = 0.5. The initial composition of the coagulation bath (left compartment) is ϕ_{1R} = 0.18, ϕ_{2R} = 0.21; these compositions lie on the binodal curve. The equilibration trajectory follows a strongly curvilinear path in ternary composition space. The inset to Figure 34 shows the transient volume fractions in either compartment, monitored at t = 1 s. Note the overshoots and undershoots in the volume fraction of PES polymer.

Also for this ternary mixture, forays into meta-stable region is possible. In order to demonstrate the foray into the meta-stable region, we perform transient diffusion from a well-stirred coagulation bath of constant composition (left compartment) into a polymer solution (right compartment) in the homogeneous single-phase region of the ternary diagram. The left compartment is the coagulation bath of constant composition $\phi_{1L} = 0.1782; \phi_{2L} = 0.2007; \phi_{mL} = 0.6211$; this composition lies on the binodal curve. The right compartment is the polymer solution of initial composition

$\phi_{1R} = 0.1; \phi_{2R} = 0.7; \phi_{mR} = 0.2$. We focus on the transient equilibration in the right compartment, $z \geq 0$. The transient development of concentrations of the ions in the right compartment is described by equation (72).

The transient volume fraction profiles in the right compartment is determined using the same procedure as described for water/acetone/CA; see Figure 35. The profiles at time t = 1 s are plotted in the inset to Figure 35. We note that the equilibration trajectory experiences a foray into the meta-stable region that lies between the binodal and spinodal curves.

18. Immersion precipitation process for preparation of poly(vinylidine fluoride) (PVDF) membrane

For the ternary system water (non-solvent, component 1), dimethyl formamide (DMF, solvent, component 2) and poly(vinylidine fluoride) (PVDF, polymer, component m), the binodal and spinodal curves are shown in Figure 36. Also, in this case forays into the meta-stable region are observable in the diffusion equilibration trajectories. In this case, the left compartment is the coagulation bath of constant composition $\phi_{1L} = 0.0631; \phi_{2L} = 0.072498; \phi_{mL} = 0.864402$; this composition lies on the binodal curve. The right compartment is the polymer solution of initial composition $\phi_{1R} = 0.02; \phi_{2R} = 0.6; \phi_{mR} = 0.38$. The equilibration trajectory is indicated by the blue line in Figure 36; this indicates a clear incursion into the meta-stable region. The volume fraction profiles in the polymer solution (right compartment) at time t = 1 s after the start are shown in the inset to Figure 36. The equilibration of water shows a perceptible overshoot in volume fraction, that is indicative of uphill diffusion.

19. Immersion precipitation process for preparation of polysulfone (PSF) membrane

For the ternary system water (non-solvent, component 1), NMP (solvent, component 2) and polysulfone (PSF, polymer, component m), the binodal and spinodal curves are shown in Figure 37. Also, in this case forays into the meta-stable region are observable in the diffusion equilibration trajectories. In this case, the left compartment is the coagulation bath of constant composition

$\phi_{1L} = 0.015568; \phi_{2L} = 0.200073; \phi_{mL} = 0.784359$; this composition lies on the binodal curve. The right compartment is the polymer solution of initial composition $\phi_{1R} = 0.01; \phi_{2R} = 0.6; \phi_{mR} = 0.39$. The equilibration trajectory is shown by the blue line in Figure 37; this indicates a clear incursion into the meta-stable region. The volume fraction profiles in the polymer solution (right compartment) at time *t* = 1 s after the start are shown in the inset to Figure 37. The equilibration of water shows a sharp overshoot in volume fraction, that is indicative of uphill diffusion.

20. Immersion precipitation process for preparation of poly(etherimide) (PEI) membrane

For the ternary system water (non-solvent, component 1), NMP (solvent, component 2) and poly(etherimide) (PEI, polymer, component m), the binodal and spinodal curves are shown in Figure 38. Also, in this case forays into the meta-stable region are observable in the diffusion equilibration trajectories. In this case, the left compartment is the coagulation bath of constant composition $\phi_{1L} = 0.078955; \phi_{2L} = 0.200545; \phi_{mL} = 0.7205$; this composition lies on the binodal curve. The right compartment is the polymer solution of initial composition $\phi_{1R} = 0.06; \phi_{2R} = 0.6; \phi_{mR} = 0.34$. The equilibration trajectory is shown by the blue line in Figure 38; this indicates a clear incursion into the meta-stable region. The volume fraction profiles in the polymer solution (right compartment) at time *t* = 1 s after the start are shown in the inset to Figure 38. The equilibration of water shows a distinct overshoot in volume fraction, that is indicative of uphill diffusion.

21. Forays into meta-stable region of methanol/acetone/CA

Forays into meta-stable zones are also feasible for non-solvents other than water. We demonstrate this for the ternary system methanol (non-solvent, component 1), acetone (solvent, component 2) and cellulose acetate (CA, polymer, component m), the binodal and spinodal curves are shown in Figure 39. In this case, the left compartment is the coagulation bath of constant composition $\phi_{1L} = 0.35447; \phi_{2L} = 0.00224; \phi_{mL} = 0.743295$; this composition lies on the binodal curve. The right compartment is the polymer solution of initial composition $\phi_{1R} = 0.36; \phi_{2R} = 0.52; \phi_{mR} = 0.12$. The

equilibration trajectory is shown by the blue line in Figure 39; this indicates a clear incursion into the meta-stable region. The volume fraction profiles in the polymer solution (right compartment) at time t = 1 s after the start are shown in the inset to Figure 39. The equilibration of methanol shows a distinct overshoot in volume fraction, that is indicative of uphill diffusion.

22. Forays into meta-stable region of 2-propanol/DMSO/EVAL

We demonstrate forays into meta-stable region for the ternary system 2-propanol (non-solvent, component 1), DMSO (solvent, component 2) and poly(ethylene-co-vinylalcohol) (EVAL, polymer, component m); the binodal and spinodal curves are shown in Figure 40. In this case, the left compartment is the coagulation bath of constant composition $\phi_{1L} = 0.19626; \phi_{2L} = 0.12796; \phi_{mL} = 0.67578$; this composition lies on the binodal curve. The right compartment is the polymer solution of initial composition $\phi_{1R} = 0.15; \phi_{2R} = 0.45; \phi_{mR} = 0.4$. The equilibration trajectory is shown by the blue line in Figure 40; this indicates a clear incursion into the meta-stable region. The volume fraction profiles in the polymer solution (right compartment) at time t = 1 s after the start are shown in the inset to Figure 40. The equilibration of 2-propanol shows a distinct overshoot in volume fraction, that is indicative of uphill diffusion.

23. Notation

a_i activity of species *i*, dimensionless

$[B]$ matrix defined by Equations (30), m^{-2} s

c_i molar concentration of species *i*, mol m^{-3}

c_t total molar concentration of mixture, mol m^{-3}

D_1 Fick diffusivity for unary penetrant 1, m^2 s^{-1}

$Đ_{1m}$ M-S diffusivity for unary penetrant 1, m^2 s^{-1}

$Đ_{ij}$ M-S diffusivity for binary pair *i*-*j*, m^2 s^{-1}

$Đ_{ij}^V$ modified M-S diffusivity for binary penetrant pair *i*-*j*, m^2 s^{-1}

$Đ_{im}^V$ modified M-S diffusivity for penetrant *i* in polymer m, m^2 s^{-1}

$D_{i,eff}$ Effective diffusivity in mixture, m^2 s^{-1}

$D_{i,self}$ self-diffusivity in mixture, m^2 s^{-1}

$[D]$ Fick diffusivity matrix, m^2 s^{-1}

f_i fugacity of species *i*, Pa

$f_{i,sat}$ saturation fugacity of species *i*, Pa

$[I]$ Identity matrix with elements δ_{ij}, dimensionless

J_i^V volumetric flux of species *i* relative to volume average velocity, m^3 m^{-2} s^{-1}

M_i molar mass of species *i*, kg mol^{-1}

$\overline{M}$ mean molar mass of mixture, kg mol^{-1}

n number of penetrants, dimensionless

m refers to polymer membrane (= species n+1), dimensionless

N_i molar flux of species *i*, mol m^{-2} s^{-1}

N_i^V volumetric flux of species *i*, m^3 m^{-2} s^{-1}

p total system pressure, Pa

$[Q]$ matrix quantifying fractional unaccomplished change, dimensionless

R gas constant, 8.314 J mol^{-1} K^{-1}

t time, s

T absolute temperature, K

T_g glass transition temperature of polymer, K

x_i mole fraction of component *i* in fluid phase, dimensionless

u_i velocity of diffusion of species *i*, m s^{-1}

$u_2^L = \frac{\phi_2^L}{\phi_1^L + \phi_2^L}$ relative volume fractions in bulk liquid mixture, dimensionless

$u_2 = \frac{\phi_2}{\phi_1 + \phi_2}$ relative volume fractions in polymer phase, dimensionless

$\overline{V_i}$ partial molar volume of species *i,* m^3 mol^{-1}

$\overline{V}$ molar volume of mixture*,* m^3 mol^{-1}

z direction coordinate, m

Greek letters

δ membrane or slab thickness, m

δ_{ij} Kronecker delta, dimensionless

Γ_{ij} thermodynamic factors, dimensionless

$[\Gamma]$ matrix of thermodynamic factors, dimensionless

μ_i molar chemical potential, J mol^{-1}

μ_i^0 molar chemical potential at standard state, J mol^{-1}

ρ_i mass density of component *i*, kg m^{-3}

ρ_{i0} mass density of pure component *i*, kg m^{-3}

ϕ_i volume fraction of penetrant *i* in polymer, dimensionless

ϕ_m volume fraction of polymer, dimensionless

ϕ_1^L, ϕ_2^L volume fraction in bulk liquid mixture, dimensionless

ρ_i mass density of penetrant *i*, kg m^{-3}

ρ_t mass density of mixture, kg m^{-3}

χ	interaction parameter in Flory-Huggins model, dimensionless
ω_i	mass fraction of component *i*, dimensionless

Subscripts

i	referring to penetrant *i*
m	referring to membrane
t	referring to total mixture

Superscripts

V	referring to use of volume fractions

Table 1. Flory-Huggins parameters for permeation of penetrants CO_2 (component 1) and C_2H_6 (Component 2) across a cross-linked polyethylene oxide (XLPEO) membrane (indicated by subscript m) at T = 298.15 K. The input parameters are based on calculations using the information presented in Appendix A of Ribeiro et al.[7]

Input data:

$f_{1,sat} = 43 \times 10^5$ Pa
$f_{2,sat} = 28 \times 10^5$ Pa
$\chi_{12} = 1.52$
$\chi_{1m} = 0.9085$
$\chi_{2m} = 2.0804$
$\overline{V_1} = 4.174 \times 10^{-5}$ m^3 mol^{-1}
$\overline{V_2} = 6.04 \times 10^{-5}$ m^3 mol^{-1}

Modified Maxwell-Stefan diffusivities for permeation of penetrants CO_2 (component 1) and C_2H_6 (Component 2) across a cross-linked polyethylene oxide (XLPEO) membrane (indicated by subscript m) at T = 298.15 K. The data are taken from Table 6 of Ribeiro et al.[7]

Input data:

$Đ_{1m}^{V} = 1.069 \times 10^{-10} \exp(6.86\phi_1)$
$Đ_{2m}^{V} = 3.756 \times 10^{-11} \exp(11.4(\phi_2 + \phi_1))$ m^2 s^{-1}.
$Đ_{12}^{V} = 2.82 \times 10^{-11}$

Table 2. Flory-Huggins parameters for permeation of penetrants CO_2 (component 1) and C_2H_6 (Component 2) across a cross-linked polyethylene oxide (XLPEO) membrane (indicated by subscript m) at T = 263.15 K. The input parameters are based on calculations using the information presented in Appendix A of Ribeiro et al.[7]

$f_{1,sat} = 21\times10^5$ Pa

$f_{2,sat} = 14.5\times10^5$ Pa

$\chi_{12} = -28.2 - \dfrac{44.3}{\ln(\phi_1)}$

$\chi_{1m} = 1.0421 + 12.3\phi_2$

$\chi_{2m} = 2.421 + 4.76\sqrt{\phi_1}$

$\overline{V_1} = 3.31\times10^{-5}$ m^3 mol^{-1}

$\overline{V_2} = 4.14\times10^{-5}$ m^3 mol^{-1}

Modified Maxwell-Stefan diffusivities for permeation of penetrants CO_2 (component 1) and C_2H_6 (Component 2) across a cross-linked polyethylene oxide (XLPEO) membrane (indicated by subscript m) at T = 263.15 K. The data are taken from Table 6 of Ribeiro et al.[7]

Input data:

$Đ_{1m}^{V} = 8.5\times10^{-12}\exp(18.45(\phi_1 + 0.76\phi_2))$ m^2 s^{-1}

$Đ_{2m}^{V} = 1.489\times10^{-12}\exp(37.7(\phi_2 + 0.832\phi_1))$ m^2 s^{-1}

$Đ_{12}^{V} = 4.3\times10^{-14}\exp(109(\phi_1 + \phi_2))$ m^2 s^{-1}

Table 3. The Flory-Huggins parameters for penetrants water (component 1) and ethanol (Component 2) in cellulose acetate (CA) membrane (indicated by subscript m) at T = 293.15 K. The data are taken from Mulder et al.:[6, 9, 19]

$$\chi_{12} = a + b(u_2) + c(u_2)^2 + d(u_2)^3 + e(u_2)^4; \quad u_2 = \frac{\phi_2}{\phi_1 + \phi_2}$$
$$a = 0.9820; b = -1.3483; c = 4.15; d = -3.3116; e = 0.8897;$$
$$\chi_{1m} = 1.4; \chi_{2m} = 1.1;$$
$$\overline{V_1} = 18 \times 10^{-6} \text{ m}^3 \text{ mol}^{-1}$$
$$\frac{\overline{V_1}}{\overline{V_2}} = 0.309; \frac{\overline{V_1}}{\overline{V_m}} = 0.002; \frac{\overline{V_2}}{\overline{V_m}} = 0.00647;$$

Modified Maxwell-Stefan diffusivities for permeation of penetrants water (component 1) and ethanol (Component 2) across a cellulose acetate (CA) membrane (indicated by subscript m) at T = 293.15 K. The data are taken from the legend to Figure 5 of Mulder and Smolders.[19]

$$Đ_{1m}^{V} = 8.8 \times 10^{-12} \exp(7.3\phi_1 + 7.3\phi_2) \quad \text{m}^2 \text{ s}^{-1}$$
$$Đ_{2m}^{V} = 6 \times 10^{-12} \exp(7.3\phi_1 + 7.3\phi_2) \quad \text{m}^2 \text{ s}^{-1}$$
$$\delta = 20 \times 10^{-6} \quad \text{m}$$

Table 4. The Flory-Huggins parameters for penetrants water (component 1) and ethanol (Component 2) in Polyimide membrane (indicated by subscript m) at T = 293.15 K. The data are based on the information provided from Ni et al.[12] The χ_{12} parameters were taken to be the same as for water/ethanol/CA. The values of χ_{1m}, χ_{2m} were chosen so that $\chi_{1m} - \frac{\overline{V_1}}{\overline{V_2}}\chi_{2m}$ lies between 0.75 and 1.1, as recommended by Ni et al.[12]

$$\chi_{12} = a + b(u_2) + c(u_2)^2 + d(u_2)^3 + e(u_2)^4; \quad u_2 = \frac{\phi_2}{\phi_1 + \phi_2}$$

$$a = 0.9820; b = -1.3483; c = 4.15; d = -3.3116; e = 0.889;$$

$$\chi_{1m} = 1.45; \chi_{2m} = 2.4 - 1.5\left(\frac{\phi_1}{\phi_1 + \phi_2}\right)$$

$$\overline{V_1} = 18 \times 10^{-6} \text{ m}^3 \text{ mol}^{-1}$$

$$\frac{\overline{V_1}}{\overline{V_2}} = 0.309; \frac{\overline{V_1}}{\overline{V_m}} \approx 0.002; \frac{\overline{V_2}}{\overline{V_m}} = 0.00649;$$

Modified Maxwell-Stefan diffusivities for permeation of penetrants water (component 1) and ethanol (Component 2) across the polyimide membrane (indicated by subscript m) at T = 293.15 K. The data are taken from Table 1 of Ni et al.[12].

$$Đ_{1m}^{V} = 25.5 \times 10^{-13} \quad \text{m}^2 \text{ s}^{-1}$$

$$Đ_{2m}^{V} = 2.1 \times 10^{-13} \quad \text{m}^2 \text{ s}^{-1}$$

$$\delta = 20 \times 10^{-6} \quad \text{m}$$

Table 5. Flory-Huggins parameters for permeation of penetrants ethanol (component 1) and water (Component 2) across a PDMS membrane (indicated by subscript m) at T = 298.15 K. The Flory-Huggins parameters are taken from Yang and Lue[8] (specifically; from the legend to their Figure 7).

$$\chi_{12} = a + b(u_2) + c(u_2)^2 + d(u_2)^3 + e(u_2)^4; \quad u_2 = \frac{\phi_2}{\phi_1 + \phi_2}$$

$$a = 4.969; b = -5.889; c = 8.056; d = -6.941; e = 2.468;$$

$$\chi_{1m} = 2.05; \chi_{2m} = 5.65;$$

$$\overline{V_1} = 58.69 \times 10^{-6} \text{ m}^3 \text{ mol}^{-1}; \overline{V_2} = 18 \times 10^{-6} \text{ m}^3 \text{ mol}^{-1}$$

$$\frac{\overline{V_1}}{V_m} \approx 0; \frac{\overline{V_2}}{V_m} \approx 0; \rho_{1L} = 785; \rho_{2L} = 997; \rho_m = 965 \quad \text{kg m}^{-3}$$

The uptakes in terms of kg penetrant per kg dry membrane are related to the volume fractions by

$$\phi_i = \frac{\frac{Uptake_i}{\rho_{iL}}}{\frac{Uptake_1}{\rho_{1L}} + \frac{Uptake_2}{\rho_{2L}} + \frac{1}{\rho_m}}; \quad Uptake_i = \frac{\phi_i \rho_{iL}}{\phi_m \rho_m}$$

Table 6. Flory-Huggins parameters for permeation of penetrants ethanol (component 1) and water (Component 2) across a PDMS membrane (indicated by subscript m) at T = 298.15 K. The Flory-Huggins parameters are taken from Yang and Lue[8] (specifically, from the legend to their Figure 7).

$$\chi_{12} = a + b(u_2) + c(u_2)^2 + d(u_2)^3 + e(u_2)^4; \quad u_2 = \frac{\phi_2}{\phi_1 + \phi_2}$$

$$a = 4.969; b = -5.889; c = 8.056; d = -6.941; e = 2.468;$$

$$\chi_{1m} = 1.28 + \frac{0.02}{(1 - 0.897\phi_m)^2}; \chi_{2m} = 3.064 + \frac{0.013}{(1 - 0.93\phi_m)^2}$$

$$\overline{V_1} = 58.69 \times 10^{-6} \text{ m}^3 \text{ mol}^{-1}; \overline{V_2} = 18 \times 10^{-6} \text{ m}^3 \text{ mol}^{-1}$$

$$\frac{\overline{V_1}}{V_m} \approx 0; \frac{\overline{V_2}}{V_m} \approx 0; \rho_{1L} = 785; \rho_{2L} = 997; \rho_m = 965 \quad \text{kg m}^{-3}$$

Table 7. Flory-Huggins parameters for permeation of penetrants water (component 1) and ethanol (Component 2) across a poly (vinyl alcohol) /poly (acrylonitrile) (PVA/PAN) composite membrane (indicated by subscript m) at T = 333 K. The χ_{12} parameters, in the form of a 4-th order polynomial were determined from the NRTL model parameters for water/ethanol mixtures at 333 K. The values of χ_{1m}, χ_{2m} were chosen to match the experimental sorption data presented in Figure 2 of Heintz and Stephan.[13]

$$\chi_{12} = a + b(u_2) + c(u_2)^2 + d(u_2)^3 + e(u_2)^4; \quad u_2 = \frac{\phi_2}{\phi_1 + \phi_2}$$

$$a = 0.8801; b = 0.3362; c = 0.1695; d = 0.006046; e = 0.0862;$$

$$\chi_{1m} = 0.79 + \frac{0.01}{(1 - 0.8\phi_m)^2}; \chi_{2m} = 1.6 - \frac{0.008}{(1 - 0.8\phi_m)^2}$$

$$\overline{V_1} = 18 \times 10^{-6} \text{ m}^3 \text{ mol}^{-1}; \overline{V_2} = 58.4 \times 10^{-6} \text{ m}^3 \text{ mol}^{-1}$$

$$\frac{\overline{V_1}}{V_m} \approx 0; \frac{\overline{V_2}}{V_m} \approx 0; \rho_{1L} = 1000; \rho_{2L} = 789; \rho_m = 1200 \quad \text{kg m}^{-3}$$

Membrane thickness: $\delta = 1.3 \times 10^{-7}$ m. Modified Maxwell-Stefan diffusivities for permeation of penetrants water (component 1) and ethanol (Component 2) across the PVA/PAN (indicated by subscript m) at T = 333 K. Two sets of values were used in the simulations:

Strong 1:2 friction: $Đ_{1m}^V = 5 \times 10^{-13}$ m^2 s^{-1}; $Đ_{2m}^V = 5 \times 10^{-14}$ m^2 s^{-1}; $Đ_{12}^V = 5 \times 10^{-14}$ m^2 s^{-1}

Weaker 1-2 friction: $Đ_{1m}^V = 5 \times 10^{-13}$ m^2 s^{-1}; $Đ_{2m}^V = 5 \times 10^{-14}$ m^2 s^{-1}; $Đ_{12}^V = 50 \times 10^{-14}$ m^2 s^{-1}

Table 8. Flory-Huggins parameters for permeation of penetrants water (component 1) and methanol (Component 2) across a poly (vinyl alcohol) /poly (acrylonitrile) (PVA/PAN) composite membrane (indicated by subscript m) at T = 333 K. The χ_{12} parameters, in the form of a 3-rd order polynomial were determined from the NRTL model parameters for water/methanol mixtures at 333 K. The values of χ_{1m}, χ_{2m} were culled from Asai et al.[48]

$$\chi_{12} = a + b(u_2) + c(u_2)^2 + d(u_2)^3; \quad u_2 = \frac{\phi_2}{\phi_1 + \phi_2}$$

$$a = 0.6831948; b = 0.4103115; c = -1.0144535; d = 1.2600830;$$

$$\chi_{1m} = 1.57; \chi_{2m} = 1.14;$$

$$\overline{V_1} = 18 \times 10^{-6} \text{ m}^3 \text{ mol}^{-1}; \overline{V_2} = 40.45 \times 10^{-6} \text{ m}^3 \text{ mol}^{-1}; \frac{\overline{V_1}}{V_m} = 0.002;$$

$$\rho_{1L} = 1000; \rho_{2L} = 792; \rho_m = 1000 \quad \text{kg m}^{-3}$$

Table 9. Modified Maxwell-Stefan diffusivity for water (component 1) in 2-hydroxyethyl methacrylate (HEMA) (indicated by subscript m) at T = 296.65 K. The data are culled from Fornasiero et al.[17]

$$Đ_{1m}^{V} = 4\times10^{-12}\exp(9.2\phi_1) \quad \mathrm{m^2\ s^{-1}}$$

The Flory-Huggins parameters are taken from from Fornasiero et al.[17]

$$\chi_{1m} = 0..82;$$
$$\overline{V_1} = 18\times10^{-6}\ \mathrm{m^3\ mol^{-1}}.$$

Table 10. The Flory-Huggins parameters for penetrants water (anti-solvent, component 1) and acetone (solvent, Component 2) in cellulose acetate (CA) (polymer, indicated by subscript m) at T = 298.15 K. The Flory-Huggins parameters are taken from Altena and Smolders[41] and Altinkaya and Ozbas.[49]

$$\chi_{12} = a + b(u_2) + c(u_2)^2 + d(u_2)^3 + e(u_2)^4; \quad u_2 = \frac{\phi_2}{\phi_1 + \phi_2}$$

$$a = 1.1; b = -0.42; c = 4.09; d = -6.7; e = 4.28;$$

$$\chi_{1m} = 1.4; \chi_{2m} = 0.45;$$

$$\overline{V_1} = 18 \times 10^{-6} \text{ m}^3 \text{ mol}^{-1}$$

$$\overline{V_2} = 73.92 \times 10^{-6} \text{ m}^3 \text{ mol}^{-1}$$

$$\overline{V_m} = 0.030532 \text{ m}^3 \text{ mol}^{-1}$$

Modified Maxwell-Stefan diffusivities for permeation of penetrants water (component 1) and acetone (Component 2) are taken to be the same as for water/ethanol/CA system.[19]

$$Đ_{1m}^{V} = 8.8 \times 10^{-12} \exp(7.3\phi_1 + 7.3\phi_2) \quad \text{m}^2 \text{ s}^{-1}$$

$$Đ_{2m}^{V} = 6 \times 10^{-12} \exp(7.3\phi_1 + 7.3\phi_2) \quad \text{m}^2 \text{ s}^{-1}$$

The 1-2 friction is considered to be negligible.

Table 11. The Flory-Huggins parameters for penetrants water (anti-solvent, component 1) and 1,4 dioxane (solvent, Component 2) in cellulose acetate (CA) (polymer, indicated by subscript m) at T = 298.15 K. The Flory-Huggins parameters are taken from Altena and Smolders[41] and Altinkaya and Ozbas.[49]

$$\chi_{12} = a + b(u_2) + c(u_2)^2 + d(u_2)^3 + e(u_2)^4; \quad u_2 = \frac{\phi_2}{\phi_1 + \phi_2}$$

$$a = 0.92; b = -0.69; c = 7.15; d = -12.91; e = 8.17;$$

$$\chi_{1m} = 1.4; \chi_{2m} = 0.4;$$

$$\overline{V_1} = 18 \times 10^{-6} \text{ m}^3 \text{ mol}^{-1}$$

$$\overline{V_2} = 85.3 \times 10^{-6} \text{ m}^3 \text{ mol}^{-1}$$

$$\overline{V_m} = 0.030532 \text{ m}^3 \text{ mol}^{-1}$$

Modified Maxwell-Stefan diffusivities for permeation of penetrants water (component 1) and acetone (Component 2) are taken to be the same as for water/ethanol/CA system.[19]

$$Đ_{1m}^{V} = 8.8 \times 10^{-12} \exp(7.3\phi_1 + 7.3\phi_2) \quad \text{m}^2 \text{ s}^{-1}$$

$$Đ_{2m}^{V} = 6 \times 10^{-12} \exp(7.3\phi_1 + 7.3\phi_2) \quad \text{m}^2 \text{ s}^{-1}$$

The 1-2 friction is considered to be negligible.

Table 12. The Flory-Huggins parameters for penetrants water (anti-solvent, component 1) and NMP (solvent, Component 2) in polyethersulfone (PES, polymer, indicated by subscript m) at T = 298.15 K. The Flory-Huggins parameters are taken from Zeman and Tkacik.[50]

$\chi_{12} = 1.0; \chi_{1m} = 1.5; \chi_{2m} = 0.5;$
$\overline{V_1} = 18.07 \times 10^{-6}\ \mathrm{m^3\ mol^{-1}}$
$\overline{V_2} = 96.52 \times 10^{-6}\ \mathrm{m^3\ mol^{-1}}$
$\overline{V_m} = 0.033869\ \mathrm{m^3\ mol^{-1}}$

Modified Maxwell-Stefan diffusivities for permeation of penetrants water (component 1) and NMP (Component 2) are taken to be the same as for water/ethanol/CA system.[19]

$Đ_{1m}^{V} = 8.8 \times 10^{-12} \exp\left(7.3\phi_1 + 7.3\phi_2\right)\quad \mathrm{m^2\ s^{-1}}$
$Đ_{2m}^{V} = 6 \times 10^{-12} \exp\left(7.3\phi_1 + 7.3\phi_2\right)\quad \mathrm{m^2\ s^{-1}}$

The 1-2 friction is considered to be negligible.

Table 13. The Flory-Huggins parameters for penetrants water (anti-solvent, component 1) and DMF (solvent, Component 2) in PVDF (polymer, indicated by subscript m) at T = 298.15 K. The Flory-Huggins parameters are taken from Yip,[51] and Matsuyama et al.[52]

$$\chi_{12} = a + b(u_2) + c(u_2)^2 + d(u_2)^3 + e(u_2)^4; \quad u_2 = \frac{\phi_2}{\phi_1 + \phi_2}$$

$$a = 0.5; b = 0.04; c = 0.8; d = -1.2; e = 0.8;$$

$$\chi_{1m} = 2.09; \chi_{2m} = 0.43;$$

$$\overline{V_1} = 18 \times 10^{-6} \text{ m}^3 \text{ mol}^{-1}$$

$$\overline{V_2} = 77.4 \times 10^{-6} \text{ m}^3 \text{ mol}^{-1}$$

$$\overline{V_m} = 0.307 \text{ m}^3 \text{ mol}^{-1}$$

Modified Maxwell-Stefan diffusivities for permeation of penetrants water (component 1) and acetone (Component 2) are taken to be the same as for water/ethanol/CA system.[19]

$$Đ_{1m}^V = 8.8 \times 10^{-12} \exp(7.3\phi_1 + 7.3\phi_2) \quad \text{m}^2 \text{ s}^{-1}$$

$$Đ_{2m}^V = 6 \times 10^{-12} \exp(7.3\phi_1 + 7.3\phi_2) \quad \text{m}^2 \text{ s}^{-1}$$

The 1-2 friction is considered to be negligible.

Table 14. The Flory-Huggins parameters for penetrants water (anti-solvent, component 1) and NMP (solvent, Component 2) in Polysulfone (PSF, polymer, indicated by subscript m) at T = 298.15 K. The Flory-Huggins parameters are taken from Yip,[51] and Kim et al.[53]

$$\chi_{12} = a + b(u_2) + c(u_2)^2 + d(u_2)^3 + e(u_2)^4; \quad u_2 = \frac{\phi_2}{\phi_1 + \phi_2}$$

$a = 0.785; b = 0.66; c = 0; d = 0; e = 0;$

$\chi_{1m} = 3.7; \chi_{2m} = 0.24;$

$\overline{V_1} = 18 \times 10^{-6}$ m^3 mol^{-1}

$\overline{V_2} = 96.2 \times 10^{-6}$ m^3 mol^{-1}

$\overline{V_m} = 0.016$ m^3 mol^{-1}

Modified Maxwell-Stefan diffusivities for permeation of penetrants water (component 1) and acetone (Component 2) are taken to be the same as for water/ethanol/CA system.[19]

$$Đ_{1m}^{V} = 8.8 \times 10^{-12} \exp(7.3\phi_1 + 7.3\phi_2) \quad \text{m}^2\ \text{s}^{-1}$$

$$Đ_{2m}^{V} = 6 \times 10^{-12} \exp(7.3\phi_1 + 7.3\phi_2) \quad \text{m}^2\ \text{s}^{-1}$$

The 1-2 friction is considered to be negligible.

Table 15. The Flory-Huggins parameters for penetrants water (anti-solvent, component 1) and NMP (solvent, Component 2) in Poly(etherimide) (PEI, polymer, indicated by subscript m) at T = 298.15 K. The Flory-Huggins parameters are taken from Yip,[51] Kim et al.,[53] and Fernandes et al.[54]

$$\chi_{12} = a + b(u_2) + c(u_2)^2 + d(u_2)^3 + e(u_2)^4; \quad u_2 = \frac{\phi_2}{\phi_1 + \phi_2}$$

$a = 0.785; b = 0.66; c = 0; d = 0; e = 0;$

$\chi_{1m} = 2.1; \chi_{2m} = 0.507;$

$\overline{V_1} = 18 \times 10^{-6}$ m^3 mol^{-1}

$\overline{V_2} = 96.2 \times 10^{-6}$ m^3 mol^{-1}

$\overline{V_m} = 0.0176$ m^3 mol^{-1}

Modified Maxwell-Stefan diffusivities for permeation of penetrants water (component 1) and acetone (Component 2) are taken to be the same as for water/ethanol/CA system.[19]

$$Đ_{1m}^{V} = 8.8 \times 10^{-12} \exp(7.3\phi_1 + 7.3\phi_2) \quad \text{m}^2\ \text{s}^{-1}$$

$$Đ_{2m}^{V} = 6 \times 10^{-12} \exp(7.3\phi_1 + 7.3\phi_2) \quad \text{m}^2\ \text{s}^{-1}$$

The 1-2 friction is considered to be negligible.

Table 16. The Flory-Huggins parameters for penetrants methanol (anti-solvent, component 1) and acetone (solvent, Component 2) in cellulose acetate (CA) (polymer, indicated by subscript m) at T = 298.15 K. The Flory-Huggins parameters are taken from Table 5 of Dabral et al.[55]

$\chi_{12} = 1.38; \chi_{1m} = 0.942; \chi_{2m} = 0.042;$
$\overline{V_1} = 40.4 \times 10^{-6}$ m^3 mol^{-1}
$\overline{V_2} = 73.32 \times 10^{-6}$ m^3 mol^{-1}
$\overline{V_m} = 0.030534$ m^3 mol^{-1}

Modified Maxwell-Stefan diffusivities for permeation of penetrants water (component 1) and acetone (Component 2) are taken to be the same as for water/ethanol/CA system.[19]

$Đ_{1m}^{V} = 8.8 \times 10^{-12} \exp\left(7.3\phi_1 + 7.3\phi_2\right)$ m^2 s^{-1}
$Đ_{2m}^{V} = 6 \times 10^{-12} \exp\left(7.3\phi_1 + 7.3\phi_2\right)$ m^2 s^{-1}

The 1-2 friction is considered to be negligible.

Table 17. The Flory-Huggins parameters for penetrants 2-propanol (anti-solvent, component 1) and DMSO (solvent, Component 2) in EVAL (polymer, indicated by subscript m) at T = 298.15 K. The Flory-Huggins parameters are taken from Table 1 and Table 2 of Cheng et al.[56]

$$\chi_{12} = 0.11 - \frac{1.376}{1 + 0.702u_2}; \quad u_2 = \frac{\phi_2}{\phi_1 + \phi_2};$$
$$\chi_{1m} = 1.35; \chi_{2m} = -1 + 0.9\phi_m;$$
$$\overline{V_1} = 76.56 \times 10^{-6} \text{ m}^3 \text{ mol}^{-1}$$
$$\overline{V_2} = 70.96 \times 10^{-6} \text{ m}^3 \text{ mol}^{-1}$$
$$\overline{V_m} = 0.047836 \text{ m}^3 \text{ mol}^{-1}$$

Modified Maxwell-Stefan diffusivities for permeation of penetrants water (component 1) and acetone (Component 2) are taken to be the same as for water/ethanol/CA system.[19]

$$Đ_{1m}^{V} = 8.8 \times 10^{-12} \exp(7.3\phi_1 + 7.3\phi_2) \quad \text{m}^2 \text{ s}^{-1}$$
$$Đ_{2m}^{V} = 6 \times 10^{-12} \exp(7.3\phi_1 + 7.3\phi_2) \quad \text{m}^2 \text{ s}^{-1}$$

The 1-2 friction is considered to be negligible.

24. References

(1) PTC MathCad 15.0. http://www.ptc.com/, PTC Corporate Headquarters, Needham, 3 November 2015.

(2) Wesselingh, J. A.; Krishna, R. *Mass transfer in multicomponent mixtures*; VSSD: Delft, 2000.

(3) Ribeiro, C. P.; Freeman, B. D. Sorption, Dilation, and Partial Molar Volumes of Carbon Dioxide and Ethane in Cross-Linked Poly(ethylene oxide). *Macromolecules* **2008**, *41*, 9458-9468.

(4) Ribeiro, C. P.; Freeman, B. D. Solubility and Partial Molar Volume of Carbon Dioxide and Ethane in Crosslinked Poly(ethylene oxide) Copolymer. *J. Polym. Sci.: Part B: Polym. Phys.* **2010**, *41*, 9458-9468.

(5) Verros, G. D.; Malamataris, N. A. Estimation of Diffusion Coefficients in Acetone-Cellulose Acetate Solutions. *Ind. Eng. Chem. Res.* **1999**, *38*, 3572-3580.

(6) Mulder, M. H. V.; Franken, A. C. M.; Smolders, C. A. On the Mechanism of Separation of Ethanol/Water Mixtures by Pervaporation. II. Experimental Concentration Profiles *J. Membr. Sci.* **1985**, *22*, 41-58.

(7) Ribeiro, C. P.; Freeman, B. D.; Paul, D. R. Modeling of Multicomponent Mass Transfer across Polymer Films using a Thermodynamically Consistent Formulation of the Maxwell-Stefan Equations in terms of Volume Fractions. *Polymer* **2011**, *52*, 3970-3983.

(8) Yang, T.-H.; Lue, J. Modeling Sorption Behavior for Ethanol/Water Mixtures in a Cross-linked Polydimethylsiloxane Membrane Using the Flory-Huggins Equation. *J. Macromol. Sci., Part B: Phys* **2013**, *52*, 1009-1029.

(9) Mulder, M. H. V.; Franken, A. C. M.; Smolders, C. A. Preferential Sorpton versus Preferential Permeability in Pervaporation. *J. Membr. Sci.* **1985**, *22*, 155-178.

(10) Varady, M. J.; Pearl, T. P.; Stevenson, S. M.; Mantooth, B. A. Decontamination of VX from Silicone: Characterization of Multicomponent Diffusion Effects. *Ind. Eng. Chem. Res.* **2016**, *55*, 3139-3149.

(11) Ribeiro, C. P.; Freeman, B. D. Carbon Dioxide/ethane Mixed-gas Sorption and Dilation in a Cross-linked Poly(ethylene oxide) Copolymer. *Polymer* **2010**, *51*, 1156-1158.

(12) Ni, X.; Sun, X.; Ceng, D. Coupled Diffusion of Water and Ethanol in a Polyimide Membrane. *Polymer Eng. Sci.* **2001**, *41*, 1440-1447.

(13) Heintz, A.; Stephan, W. A generalized solution-diffusion model of the pervaporation process through composite membranes Part I. Prediction of mixture solubilities in the dense active layer using the UNIQUAC model. *J. Membr. Sci.* **1994**, *89*, 143-151.

(14) Schultz, T.; Sundmacher, K. Rigorous dynamic model of a direct methanol fuel cell based on Maxwell–Stefan mass transport equations and a Flory–Huggins activity model: Formulation and experimental validation. *J. Power Sources* **2005**, *145*, 435-462.

(15) Schultz, T.; Sundmacher, K. Mass, charge and energy transport phenomena in a polymer electrolyte membrane (PEM) used in a direct methanol fuel cell (DMFC): Modelling and experimental validation of fluxes. *J. Membr. Sci.* **2006**, *276*, 272-285.

(16) Fornasiero, F.; Prausnitz, J. M.; Radke, C. J. Multicomponent Diffusion in Highly Asymmetric Systems. An Extended Maxwell-Stefan Model for Starkly Different-Sized, Segment-Accessible Chain Molecules. *Macromolecules* **2005**, *38*, 1364-1370.

(17) Fornasiero, F.; Krull, F.; Prausnitz, J. M.; Radke, C. J. Steady-state Diffusion of Water through Soft-contact-lens Materials. *Biomaterials* **2005**, *26*, 5704-5716.

(18) Ribeiro, C. P.; Freeman, B. D.; Paul, D. R. Pure- and Mixed-Gas Carbon Dioxide/Ethane Permeability and Diffusivity in a Cross-linked Poly(ethylene oxide) Copolymer. *J. Membr. Sci.* **2011**, *377*, 110-123.

(19) Mulder, M. H. V.; Smolders, C. A. On the Mechanism of Separation of Ethanol/Water Mixtures by Pervaporation. I. Calculation of Concentration Profiles *J. Membr. Sci.* **1984**, *17*, 289-307.

(20) Heintz, A.; Stephan, W. A generalized solution-diffusion model of the pervaporation process through composite membranes Part II. Concentration polarization, coupled diffusion and the influence of the porous support layer. *J. Membr. Sci.* **1994**, *89*, 153-169.

(21) Vignes, A. Diffusion in binary solutions. *Ind. Eng. Chem. Fundamentals* **1966**, *5*, 189-199.

(22) Krishna, R. Describing the Diffusion of Guest Molecules inside Porous Structures. *J. Phys. Chem. C* **2009**, *113*, 19756-19781.

(23) Krishna, R. Diffusion in Porous Crystalline Materials. *Chem. Soc. Rev.* **2012**, *41*, 3099-3118.

(24) Krishna, R. The Maxwell-Stefan Description of Mixture Diffusion in Nanoporous Crystalline Materials. *Microporous Mesoporous Mater.* **2014**, *185*, 30-50.

(25) Vrentas, J. S.; Duda, J. L. Molecular diffusion in polymer solutions. *A.I.Ch.E.J.* **1979**, *25*, 1-24.

(26) Price, P. E.; Romdhane, I. H. Multicomponent Diffusion Theory and Its Applications to Polymer-Solvent Systems. *A.I.Ch.E.J.* **2003**, *49*, 309-322.

(27) Bearman, R. J. On the Molecular Basis of some Current Theories of Diffusion. *J. Phys. Chem.* **1961**, *65*, 1961-1968.

(28) Wesselingh, J. A.; Bollen, A. M. Multicomponent Diffusivities from the Free Volume Theory. *Trans. Inst. Chem. Eng.* **1997**, *75, Part A*, 590-602.

(29) Wilke, C. R.; Chang, P. Correlation of Diffusion Coefficients in Dilute Solutions. *A.I.Ch.E.J.* **1955**, *1*, 264-270.

(30) Krishna, R.; van Baten, J. M. Describing Diffusion in Fluid Mixtures at Elevated Pressures by Combining the Maxwell-Stefan Formulation with an Equation of State *Chem. Eng. Sci.* **2016**, *153*, 174-187.

(31) Reid, R.C.; Prausnitz, J. M.; Poling, B. E. *The Properties of Gases and Liquids*; 4th Edition, McGraw-Hill: New York, 1986.

(32) Zielinski, J. M. A Friction Factor Analysis of the Coupling between Polymer/Solvent Self- and Mutual-Diffusion: Pol ystyrene/Toluene. *J. Polym. Sci.: Part B: Polym. Phys.* **1996**, *24*, 2759-2766.

(33) Alsoy, S.; Duda, J. L. Modeling of Multicomponent Drying of Polymer Films. *A.I.Ch.E.J.* **1999**, *45*, 896-905.

(34) Brun, J.-P.; Larchet, C.; Melet, R.; Bulvestre, G. Modelling of the Pervaporaion of Binary Mixtures through Moderately Swelling, Non-Reacting Membranes. *J. Membr. Sci.* **1985**, *23*, 257-283.

(35) Zielinski, J. M.; Hanley, B. F. Practical Friction-Based Approach to Modeling Multicomponent Diffusion. *A.I.Ch.E.J.* **1999**, *45*, 1-12.

(36) Cussler, E. L.; Lightfoot, E. N. Multicomponent Diffusion Involving High Polymers. I. Diffusion of Monodisperse Polystyrene in Mixed Solvents. *J. Phys. Chem.* **1965**, *69*, 1135-1144.

(37) van den Berg, G. B.; Smolders, C. A. Diffusional phenomena in membrane separation processes. *J. Membr. Sci.* **1992**, *73*, 103-118.

(38) Reuvers, A. J.; Smolders, C. A. Formation of membranes by means of immersion precipitation Part II. The mechanism of formation of membranes prepared from the system cellulose acetate - acetone - water. *J. Membr. Sci.* **1987**, *34*, 67-86.

(39) Krishna, R. Serpentine Diffusion Trajectories and the Ouzo Effect in Partially Miscible Ternary Liquid Mixtures. *Phys. Chem. Chem. Phys.* **2015**, *17*, 27428-27436.

(40) Krishna, R. Highlighting Diffusional Coupling Effects in Ternary Liquid Extraction and Comparisons with Distillation. *Ind. Eng. Chem. Res.* **2016**, *55*, 1053-1063.

(41) Altena, F. W.; Smolders, C. A. Calculation of Liquid-Liquid Phase Separation in a Ternary System of a Polymer in a Mixture of a Solvent and a Nonsolvent. *Macromolecules* **1982**, *15*, 1491-1497.

(42) Taylor, R.; Krishna, R. *Multicomponent mass transfer*; John Wiley: New York, 1993.

(43) Krishna, R. Diffusing Uphill with James Clerk Maxwell and Josef Stefan. *Curr. Opin. Chem. Eng.* **2016**, *12*, 106-119.

(44) Krishna, R. Tracing the Origins of Transient Overshoots for Binary Mixture Diffusion in Microporous Crystalline Materials. *Phys. Chem. Chem. Phys.* **2016**, *18*, 15482-15495.

(45) Krishna, R. Uphill Diffusion in Multicomponent Mixtures. *Chem. Soc. Rev.* **2015**, *44*, 2812-2836.

(46) Krishna, R. Investigating the Validity of the Knudsen Diffusivity Prescription for Mesoporous and Macroporous Materials. *Ind. Eng. Chem. Res.* **2016**, *55*, 4749-4759.

(47) Tsay, C. S.; McHugh, A. J. Mass Transfer Modeling of Asymmetric Membrane Formation by Phase Inversion. *J. Polym. Sci.: Part B: Polym. Phys.* **1990**, *28*, 1327-1365.

(48) Asai, H.; Kato, S.; Nagahama, K. Solubilities of Aqueous Alcohol Solutions in a Nafion Membrane. *Kagaku Kogaku Ronbunshu* **1989**, *15*, 1172-1178.

(49) Altinkaya, S. A.; Ozbas, B. Modeling of Asymmetric Membrane Formation by Dry-casting Method. *J. Membr. Sci.* **2004**, *230*, 71-89.

(50) Zeman, L.; Tkacik, G. Thermodynamic Analysis of a Membrane-Forming System Water/N-methyl-2-Pyrrolidone/PolyetherSulfone. *J. Membr. Sci.* **1988**, *36*, 119-140.

(51) Yip, Y.-L. *Modeling of dry-casting and non-solvent vapor induced phase separation*. Theses and Dissertations, Lehigh University, Lehigh, 2005. http://preserve.lehigh.edu/cgi/viewcontent.cgi?article=1888&context=etd

(52) Matsuyama, H.; Teramoto, M.; Nakatani, R.; Maki, T. Membrane Formation via Phase Separation Induced by Penetrationof Nonsolvent from Vapor Phase. I. Phase Diagram and Mass Transfer Process. *J. Appl. Polymer Sci.* **1999**, *74*, 159-170.

(53) Kim, J. Y.; Lee, H. K.; Baik, K. J.; Kim, S. C. Liquid–Liquid Phase Separation in Polysulfone/Solvent/Water Systems. *J. Appl. Polymer Sci.* **1997**, *65*, 2643-2653.

(54) Fernandes, G. R.; PIinto, J. C.; Nobrega, R. Modeling and Simulation of the Phase-Inversion Process During Membrane Preparation. *J. Appl. Polymer Sci.* **2001**, *82*, 3036-3051.

(55) Dabral, M.; Francis, L. F.; Scriven, L. E. Drying Process Paths of Ternary Polymer Solution Coating. *A.I.Ch.E.J.* **2002**, *48*, 25-37.

(56) Cheng, L.-P.; Young, T.-H.; Chuang, W.-Y.; Chen, L.-Y.; Chen, L.-W. The Formation Mechanism of Membranes Prepared from the Nonsolvent–Solvent–Crystalline Polymer Systems. *Polymer* **2001**, *42*, 443-451.

25. Captions for Figures

Figure 1. Schematic of Flory-Huggins lattice model.

Figure 2. Influence of the interaction parameter on the activity (a_1) and thermodynamic correction factor, Γ. In these calculations, the ratio $\frac{\overline{V_1}}{V_m} = 0$, i.e. the molar volume of the penetrant is negligible in comparison to the molar volume of the polymer.

Figure 3. Schematic showing mixture permeation across polymeric membrane.

Figure 4. Calculations of the volume fractions of penetrants (a) CO_2 (component 1) and (b) C_2H_6 (Component 2) in a cross-linked polyethylene oxide (XLPEO) membrane (indicated by subscript m) at 298.15 K. The upstream face of the membrane is in equilibrium with CO_2/C_2H_6 mixtures of five different compositions. The experimental data (symbols) on mixed-gas sorption are those presented in Figures 5 and 6 of Ribeiro and Freeman.[11] Note that the experimental component solubility data are converted to volume fractions of penetrants, using the molar volumes. The continuous solid lines are the the simultaneous solutions to equations (4) and (5). The input data are summarized in Table 1. In these calculations, the ratio $\frac{\overline{V_1}}{V_m} = 0$, i.e. the molar volume of the penetrant is negligible in comparison to the molar volume of the polymer.

Figure 5. Calculations of the volume fractions of penetrants (a) CO_2 (component 1) and (b) C_2H_6 (Component 2) in a cross-linked polyethylene oxide (XLPEO) membrane (indicated by subscript m) at 263.15 K. The upstream face of the membrane is in equilibrium with CO_2/C_2H_6 mixtures of five different compositions. The experimental data (symbols) on mixed-gas sorption are those presented in Figures 5 and 6 of Ribeiro and Freeman.[11] Note that the experimental component solubility data are converted to volume fractions of penetrants, using the molar volumes. The continuous solid lines are the the simultaneous solutions to equations (4) and (5). The input data are summarized in Table 2. In these calculations, the ratio $\frac{\overline{V_1}}{\overline{V_m}} = 0$, i.e. the molar volume of the penetrant is negligible in comparison to the molar volume of the polymer.

Figure 6. (a) Calculations of the interaction factor χ_{12} for ethanol(1)/water(2) mixtures at 298.15 K using equation (7) and the Wilson parameters provided by Yang and Lue.[8] Also shown are the 4-th polynomial fits with coefficients specified in Table 5. (b) Calculations of the interaction factor χ_{12} for water(1)/ethanol(2) mixtures at 333 K using equation (7) and NRTL parameters. Also shown are the 4-th polynomial fits with coefficients specified in Table 7. (c) Calculations of the interaction factor χ_{12} for water(1)/methanol(2) mixtures at 333 K using equation (7) and NRTL parameters. Also shown are the 3rd polynomial fits with coefficients specified in Table 8.

Figure 7. Calculations of the volume fractions of penetrants water (component 1), ethanol (component 2) in a cellulose acetate membrane (polymer, component m) at 293.15 K. The upstream face of the membrane is in equilibrium with water/ethanol liquid mixture of varying mass fractions. In the

calculations, χ_{1m}, χ_{2m} are composition independent, and χ_{12} follows the composition dependence described by equations (8) and (9). The Flory-Huggins parameters are specified in Table 3.

Figure 8. Calculations of the volume fractions of penetrants water (component 1), ethanol (component 2) in polyimide membrane (polymer, component m) at 293.15 K. The upstream face of the membrane is in equilibrium with water/ethanol liquid mixture of varying mass fractions. The Flory-Huggins parameters are specified in Table 4.

Figure 9. Calculations of the (a) volume fractions, and (b) uptakes per kg dry PDMS, of penetrants ethanol (component 1), water (component 2) in polydimethylsiloxane (PDMS) membrane (polymer, component m) at 298.15 K. The upstream face of the membrane is in equilibrium with ethanol/water liquid mixture of varying volume fractions. In the calculations, χ_{1m}, χ_{2m} are composition independent, and χ_{12} follows the composition dependence described by equations (8) and (9). The Flory-Huggins parameters are specified in Table 5.

Figure 10. Calculations of the (a) volume fractions, and (b) uptakes per kg dry PDMS, of penetrants ethanol (component 1), water (component 2) in polydimethylsiloxane (PDMS) (polymer, component m) at 298.15 K. The upstream face of the membrane is in equilibrium with ethanol/water liquid mixture of varying volume fractions. In the calculations, all three interaction parameters $\chi_{12}, \chi_{1m}, \chi_{2m}$ are

dependent on the volume fractions of the penetrants. The Flory-Huggins parameters are specified in Table 6.

Figure 11. Experimental data (symbols) of Heintz and Stephan[13] for binary sorption of water/ethanol mixtures in poly (vinyl alcohol) /poly (acrylonitrile) (PVA/PAN) composite membrane. The continuous solid lines are the F-H model calculations using the input data in Table 7.

Figure 12. Binary sorption of water/methanol mixtures in Nafion membrane. The continuous solid lines are the F-H model calculations using the input data in Table 8.

Figure 13. Diffusivity of a trace of benzene in different polymers at 300 K. The effect of the glass transition temperature. The artwork is based on Wesselingh and Krishna.[2]

Figure 14. Effect of permeant volume in a rubbery and an almost glassy polymer. The artwork is based on Wesselingh and Krishna.[2]

Figure 15. The effect of swelling. The artwork is based on Wesselingh and Krishna.[2]

Figure 16. Calculations for (a) thermodynamic correction factor, $\Gamma = \frac{\partial \ln a_1}{\partial \ln \phi_1}$, (b) Modified Maxwell-Stefan diffusivity, $Đ_{1m}^{V}$, and (c) Effective Fick diffusivity, $D_{1,eff} = \frac{1}{1-\phi_1} Đ_{1m}^{V} \frac{\partial \ln a_1}{\partial \ln \phi_1}$, for water (component 1) in 2-hydroxyethyl methacrylate (HEMA) (indicated by subscript m) at T = 296.65 K. The input data are provided in Table 9. In these calculations the volume fractions, ϕ_1, are related to the mass fractions ω_1 by $\phi_1 = \frac{1}{1+\frac{\rho_{10}}{\rho_{20}}\frac{1-\omega_1}{\omega_1}}$, and $\omega_1 = \frac{1}{1+\frac{\rho_{20}}{\rho_{10}}\frac{1-\phi_1}{\phi_1}}$ where the ρ_{i0} are pure component mass densities.

Figure 17. (a) Fick diffusivities for unary permeation of CO_2 and C_2H_6 across a cross-linked polyethylene oxide (XLPEO) membrane at 298.15 K. The *x*-axis represents the volume fraction of the penetrant. (b) Calculations of the thermodynamic factor as a function of the volume fraction of the penetrant. The input data are summarized in Table 1. Furthermore, in these calculations, the ratio $\frac{\overline{V_1}}{\overline{V_m}} = 0$, i.e. the molar volume of the penetrant is negligible in comparison to the molar volume of the polymer.

Figure 18. Permeabilities, expressed in Barrers, for unary permeation of (a, c) CO_2 and (b, d) C_2H_6 across a cross-linked polyethylene oxide (XLPEO) membrane at (a, b) 298.15 K, and (c, d) 263.15 K. The input data are summarized in Table 1, and Table 2. Furthermore, in these calculations, the ratio

$\frac{\overline{V_1}}{\overline{V_m}} = 0$, i.e. the molar volume of the penetrant is negligible in comparison to the molar volume of the polymer. The experimental data on component permeabilities are those presented in Figure 2 of Ribeiro et al.[18]

Figure 19. (a) Calculations of the elements of the matrix of thermodynamic factors for penetrants CO_2 (component 1) and C_2H_6 (Component 2) in a cross-linked polyethylene oxide (XLPEO) membrane (indicated by subscript m) at 263.15 K. The upstream face of the membrane is in equilibrium with a 70% CO_2 gas mixture. In the calculations, the partial fugacity of CO_2 is increased, keeping the gas mixture composition constant. (b) Calculations of the ratio $\frac{\Gamma_{11}\phi_1 + \Gamma_{12}\phi_2}{\Gamma_{21}\phi_1 + \Gamma_{22}\phi_2}$. (c) Calculation of the effective Fick diffusivities of CO_2 (component 1) and C_2H_6 (Component 2). The input data are summarized in Table 2. In these calculations, the ratio $\frac{\overline{V_1}}{\overline{V_m}} = 0$, i.e. the molar volume of the penetrant is negligible in comparison to the molar volume of the polymer.

Figure 20. Permeabilities, expressed in Barrers, of (a) CO_2, and (b) C_2H_6 for binary CO_2/C_2H_6 mixture permeation across a cross-linked polyethylene oxide (XLPEO) membrane at 298.15 K. The *x*-axis represents the partial fugacity of (a) CO_2, and (b) C_2H_6 in the bulk gas phase in the upstream compartment. Five different mixture compositions are considered. The input data are summarized in Table 1. Furthermore, in these calculations, the ratio $\frac{\overline{V_1}}{\overline{V_m}} = 0$, i.e. the molar volume of the penetrant is negligible in comparison to the molar volume of the polymer. The experimental data (symbols) on

component permeabilities are those presented in Figures 2, 4, and 5 of Ribeiro et al.[18] The continuous solid lines are the calculations using the linearized M-S equations, along with the F-H model.

Figure 21. Permeabilities, expressed in Barrers, of (a) CO_2, and (b) C_2H_6 for binary CO_2/C_2H_6 mixture permeation across a cross-linked polyethylene oxide (XLPEO) membrane at 263.15 K. The *x*-axis represents the partial fugacity of (a) CO_2, and (b) C_2H_6 in the bulk gas phase in the upstream compartment. Five different mixture compositions are considered. The input data are summarized in Table 2. Furthermore, in these calculations, the ratio $\frac{\overline{V_1}}{\overline{V_m}} = 0$, i.e. the molar volume of the penetrant is negligible in comparison to the molar volume of the polymer. The experimental data (symbols) on component permeabilities are those presented in Figures 2, 4, and 5 of Ribeiro et al.[18] The continuous solid lines are the calculations using the linearized M-S equations, along with the F-H model.

Figure 22. Permeabilities, expressed in Barrers, of (a) CO_2, and (b) C_2H_6 for binary CO_2/C_2H_6 mixture permeation across a cross-linked polyethylene oxide (XLPEO) membrane at 263.15 K. The *x*-axis represents the partial fugacity of (a) CO_2, and (b) C_2H_6 in the bulk gas phase in the upstream compartment. Five different mixture compositions are considered. The experimental data (symbols) on component permeabilities are those presented in Figures 2, 4, and 5 of Ribeiro et al.[18] The continuous solid lines are the calculations in which the 1-2 friction between the two penetrants is ignored.

Figure 23. (a) Thermodynamic correction factors for the ternary mixture consisting of water (component 1), ethanol (component 2) and cellulose acetate (polymer, component m). (b) Ratio of the elements of thermodynamic correction factors. (c) Molar fluxes of water, and ethanol across CA membrane

calculated using the linearized M-S equations, using two different scenarios for [Γ] calculations. (d) Water/ethanol permeation selectivity, defined as $\frac{(N_1M_1)/(N_2M_2)}{\omega_1^L/\omega_2^L}$, across CA membrane calculated using the linearized M-S equations, using two different scenarios for [Γ] calculations. The Flory-Huggins parameters and modified M-S diffusivities are as specified in Table 3. The 1-2 friction is considered to be negligible.

Figure 24. (a) Thermodynamic correction factors for the ternary mixture consisting of water (component 1), ethanol (component 2) and polyimide (polymer, component m). (b) Ratio of the elements of thermodynamic correction factors. (c, d) Volumetric fluxes of (c) water, and (d) ethanol across polyimide membrane calculated using the linearized M-S equations. The symbols represent the experimental data as presented in Figure 3 and Figure 4 of Ni et al.[12]. The continuous solid lines are the flux calculations using the linearized M-S equations, along with the logarithmic interpolation formula. The dashed lines are simulations in which the 1-2 friction is considered to be negligible. The Flory-Huggins parameters, and diffusivity input data are provided in Table 4.

Figure 25. (a) Experimental data (symbols) of Heintz and Stephan[20] for permeation of water/ethanol mixtures across a poly (vinyl alcohol) /poly (acrylonitrile) (PVA/PAN) composite membrane. The input data are provided in Table 7. (b) M-S+F-H model calculations assuming strong 1-2 friction, taking $Đ_{1m}^V = 5\times10^{-13}$ m^2 s^{-1}; $Đ_{2m}^V = 5\times10^{-14}$ m^2 s^{-1}; $Đ_{12}^V = 5\times10^{-14}$ m^2 s^{-1}. (c) M-S+F-H model calculations assuming weak 1-2 friction, taking: $Đ_{1m}^V = 5\times10^{-13}$ m^2 s^{-1}; $Đ_{2m}^V = 5\times10^{-14}$ m^2 s^{-1}; $Đ_{12}^V = 50\times10^{-14}$ m^2 s^{-1}.

Figure 26. (a) Experimental data as reported in Figure 6 of Zielinski[32] for the self-diffusivities of toluene (1), and polystyrene (m) in polystyrene at 383 K as a function of the mass fraction of toluene. Also shown are the data for the Fick (mutual) diffusivity, D_1. (b) Calculations of the thermodynamic correction factor, $\left(\frac{\rho_1}{RT}\frac{\partial \mu_1}{\partial \rho_1}\right)$, taking $\chi = 0.354$. (c) Comparison of the M-S diffusivity, calculated using $Đ_{1m}^{V} = D_1 \Big/ \left(\frac{\rho_1}{RT}\frac{\partial \mu_1}{\partial \rho_1}\right)$, with D_1, $D_{1,\text{self}}$, and $D_{2,\text{self}}$. The continuous solid line is the estimation of the self-diffusivity using the free-volume theory.

Figure 27. Calculations for (a) thermodynamic correction factor, $\Gamma = \frac{\partial \ln a_1}{\partial \ln \phi_1}$, (b) Fick diffusivity, $D_1 = Đ_{1m}^{V}\frac{\partial \ln a_1}{\partial \ln \phi_1}$, and self-diffusivity, $D_{1,self}$, for acetone (component 1) in cellulose acetate (indicated by subscript m) at T = 298.15 K. The input data are taken from the Verros and Malamataris.[5] In these calculations the volume fractions, ϕ_1, are related to the mass fractions ω_1 by $\phi_1 = \frac{1}{1+\frac{\rho_{10}}{\rho_{20}}\frac{1-\omega_1}{\omega_1}}$, and $\omega_1 = \frac{1}{1+\frac{\rho_{20}}{\rho_{10}}\frac{1-\phi_1}{\phi_1}}$ where the ρ_{i0} are the mass densities of pure components. Also, $\frac{\overline{V_1}}{V_m} = 0.008$.

Figure 28. Calculations for (a) matrix of thermodynamic correction factors, $[\Gamma]$, (b) Fick diffusivity matrix $[D]$, for methanol (component 1)/toluene (2)/poly(vinylacetate)(m) at T = 333.15 K. The calculations are based on the predictions of the self-diffusivities using the free-volume parameters

provided in Table 1 of Zielinski and Hanley, [35] along with the Flory-Huggins parameters also provided in page 6 of their paper: $\chi_{12} = 1; \chi_{1m} = 1.19; \chi_{2m} = 0.78$. In these calculations, the mass fractions of methanol and toluene are taken to equal each other, i.e. $\omega_1 = \omega_2$.

Figure 29. The binodal and spinodal curves, plotted in volume fraction space, for the ternary mixture consisting of water (non-solvent, component 1), acetone (solvent, component 2) and cellulose acetate (polymer, component m). The inset to the Figure are calculations of the thermodynamic correction factors at compositions that lie along the dotted line indicated in the ternary diagram. The Flory-Huggins parameters are provided in Table 10.

Figure 30. Diffusional equilibration trajectory in a ternary system consisting of water (non-solvent, component 1), acetone (solvent, component 2) and cellulose acetate (polymer, component m). The plotted data in ternary composition space are in terms of volume fractions. The equilibration trajectory is indicated by the blue line in ternary composition space. The inset shows the volume fraction profiles in the coagulation bath (left compartment) and in the polymer solution (right compartment) at time t = 1 s after the start. The Flory-Huggins parameters and diffusivity data are provided in Table 10.

Figure 31. Diffusion trajectories during the immersion precipitation process for membrane preparation; adapted from the papers of van den Berg and Smolders,[37] and Reuvers and Smolders.[38] A 10% solution of Cellulose Acetate (CA) in acetone is immersed in a bath of pure water. The transient equilibration trajectories at three different times, t =10 s, t = 25 s, and t = 50 s are depicted.

Figure 32. Diffusional equilibration trajectory in a ternary system consisting of water (non-solvent, component 1), acetone (solvent, component 2) and cellulose acetate (polymer, component m). The plotted data in ternary composition space are in terms of volume fractions. The equilibration trajectory is indicated by the blue line in ternary composition space. The inset shows the volume fraction profiles in the polymer solution (right compartment) at time t = 1 s after the start. The Flory-Huggins parameters and diffusivity data are provided in Table 10.

Figure 33. (a) Diffusional equilibration trajectory in a ternary system consisting of water (non-solvent, component 1), 1,4 dioxane (solvent, component 2) and cellulose acetate (polymer, component m). The equilibration trajectory is indicated by the blue line. (b) Volume fraction profiles in the polymer solution (right compartment) at time t = 1 s after the start. The Flory-Huggins parameters and diffusivity data are provided in Table 11.

Figure 34. Diffusional equilibration trajectory in a ternary system consisting of water (non-solvent, component 1), N-methyl-2-pyrrolidone (NMP) (solvent, component 2) and poly(ether)sulfone (PES) (polymer, component m). The plotted data in ternary composition space are in terms of volume fractions. The equilibration trajectory is indicated by the blue line in ternary composition space. The inset shows the volume fraction profiles in the polymer solution and in the coagulation bath at time t = 1 s. The Flory-Huggins parameters and diffusivity data are provided in Table 12.

Figure 35. Diffusional equilibration trajectory in a ternary system consisting of water (non-solvent, component 1), N-methyl-2-pyrrolidone (NMP) (solvent, component 2) and poly(ether)sulfone (PES) (polymer, component m). The plotted data in ternary composition space are in terms of volume fractions. The equilibration trajectory is indicated by the blue line in ternary composition space. The inset shows the volume fraction profiles in the polymer solution (right compartment) at time t = 1 s. The Flory-Huggins parameters and diffusivity data are provided in Table 12.

Figure 36. Diffusional equilibration trajectory in a ternary system consisting of water (non-solvent, component 1), DMF (solvent, component 2) and PVDF (polymer, component m). The plotted data in ternary composition space are in terms of volume fractions. The equilibration trajectory is indicated by the blue line. The insets show the volume fraction profiles in the polymer solution (right compartment) at time t = 1 s after the start. The Flory-Huggins parameters and diffusivity data are provided in Table 13.

Figure 37. Diffusional equilibration trajectory in a ternary system consisting of water (non-solvent, component 1), NMP (solvent, component 2) and Polysulfone (PSF, polymer, component m). The plotted data in ternary composition space are in terms of volume fractions. The equilibration trajectory is indicated by the blue line. The insets show the volume fraction profiles in the polymer solution (right compartment) at time t = 1 s after the start. The Flory-Huggins parameters and diffusivity data are provided in Table 14.

Figure 38. Diffusional equilibration trajectory in a ternary system consisting of water (non-solvent, component 1), NMP (solvent, component 2) and Pol(etherimide) (PEI, polymer, component m). The

plotted data in ternary composition space are in terms of volume fractions. The equilibration trajectory is indicated by the blue line. The insets show the volume fraction profiles in the polymer solution (right compartment) at time t = 1 s after the start. The Flory-Huggins parameters and diffusivity data are provided in Table 15.

Figure 39. Diffusional equilibration trajectory in a ternary system consisting of methanol (non-solvent, component 1), acetone (solvent, component 2) and cellulose acetate (polymer, component m). The plotted data in ternary composition space are in terms of volume fractions. The equilibration trajectory is indicated by the blue line in ternary composition space. The inset shows the volume fraction profiles in the polymer solution (right compartment) at time t = 1 s after the start. The Flory-Huggins parameters and diffusivity data are provided in Table 16.

Figure 40. Diffusional equilibration trajectory in a ternary system consisting of 2-propanol (non-solvent, component 1), DMSO (solvent, component 2) and EVAL (polymer, component m). The plotted data in ternary composition space are in terms of volume fractions. The equilibration trajectory is indicated by the blue line in ternary composition space. The inset shows the volume fraction profiles in the polymer solution (right compartment) at time t = 1 s after the start. The Flory-Huggins parameters and diffusivity data are provided in Table 17.

Fig. S1

Flory-Huggins

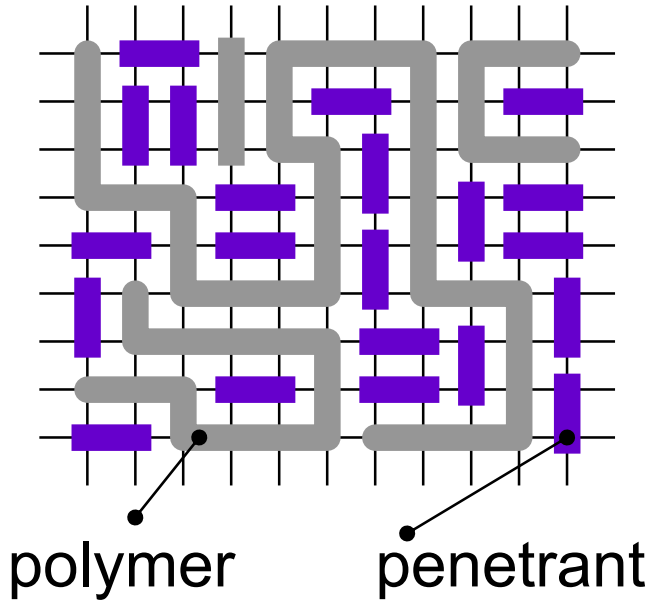

penetrant and polymer fit on a 3D lattice

Fig. S2

Influence of interaction parameter on activity

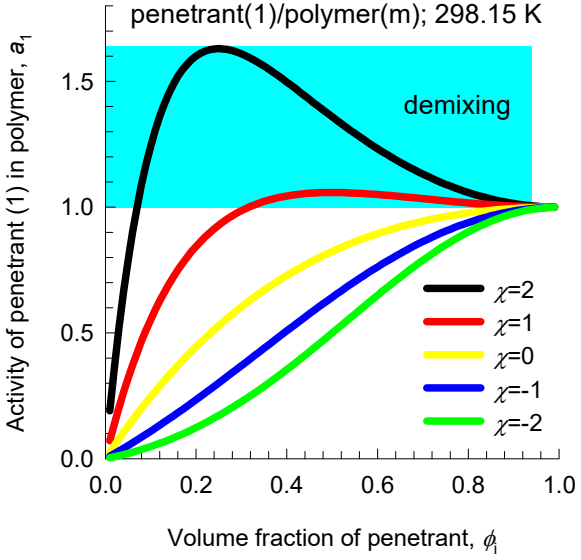

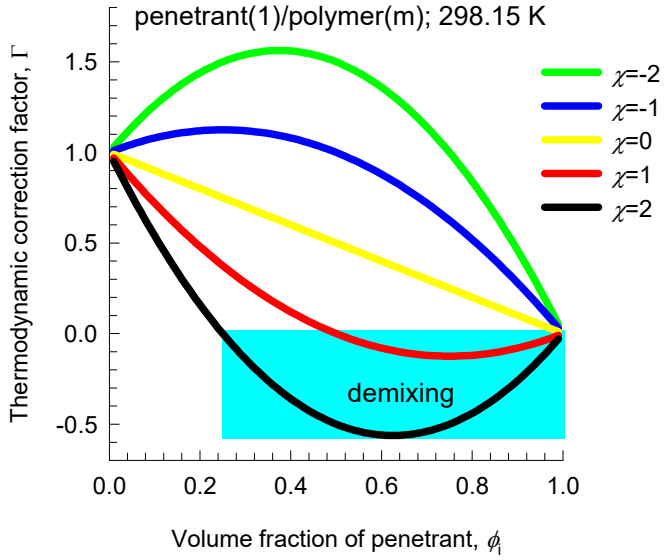

$\chi > 0$ *solvent and polymer dislike each other*

$\chi = 0$ *solvent and polymer are similar*

$\chi < 0$ *solvent and polymer attract each other*

Fig. S3

Permeation across polymeric membrane

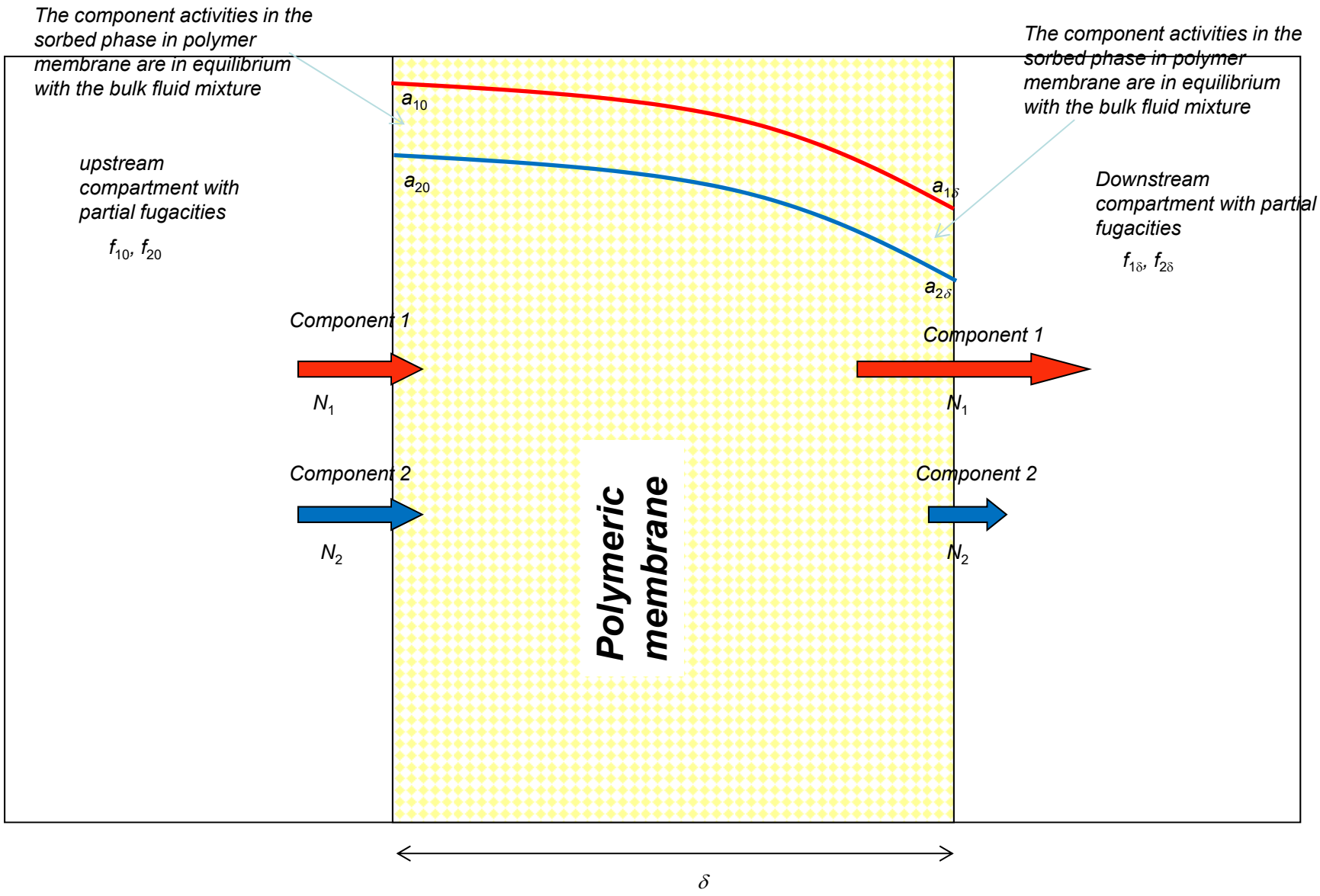

Fig. S4

CO_2/C_2H_6/XLPEO equilibrium

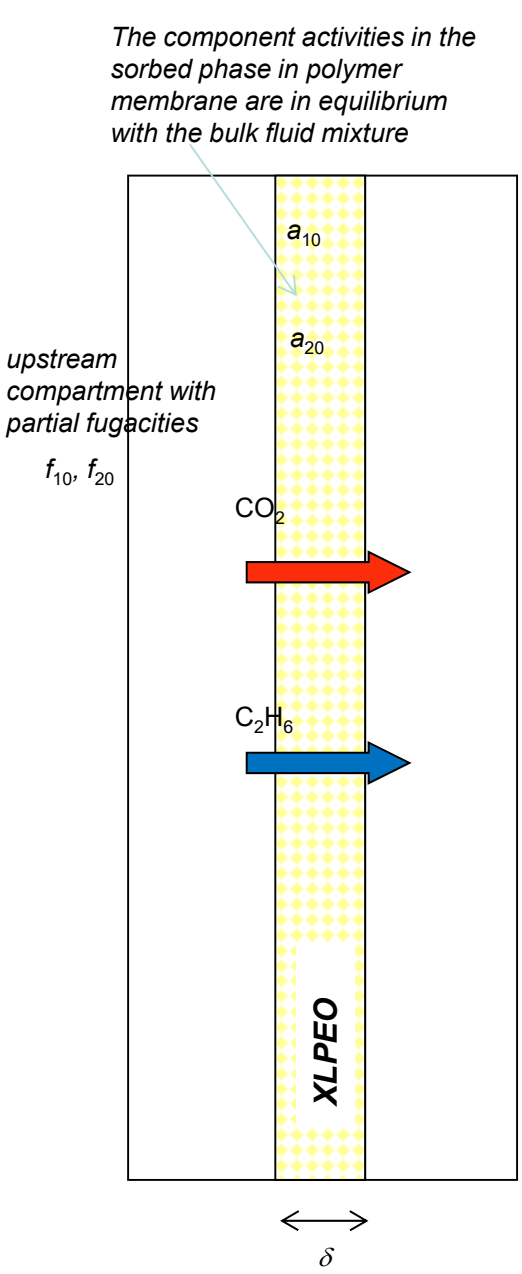

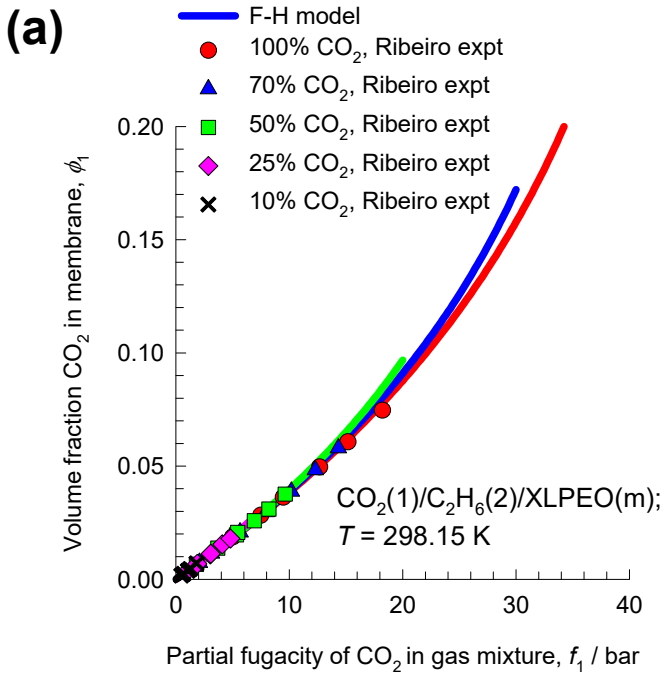

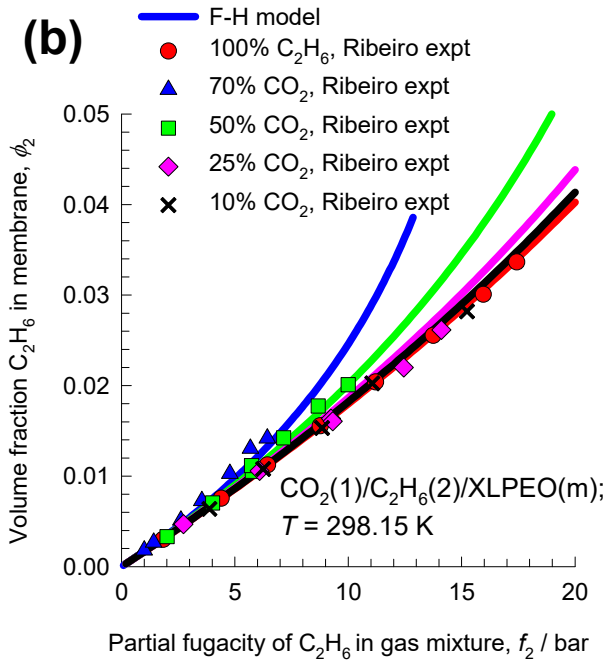

Fig. S5

CO_2/C_2H_6/XLPEO equilibrium

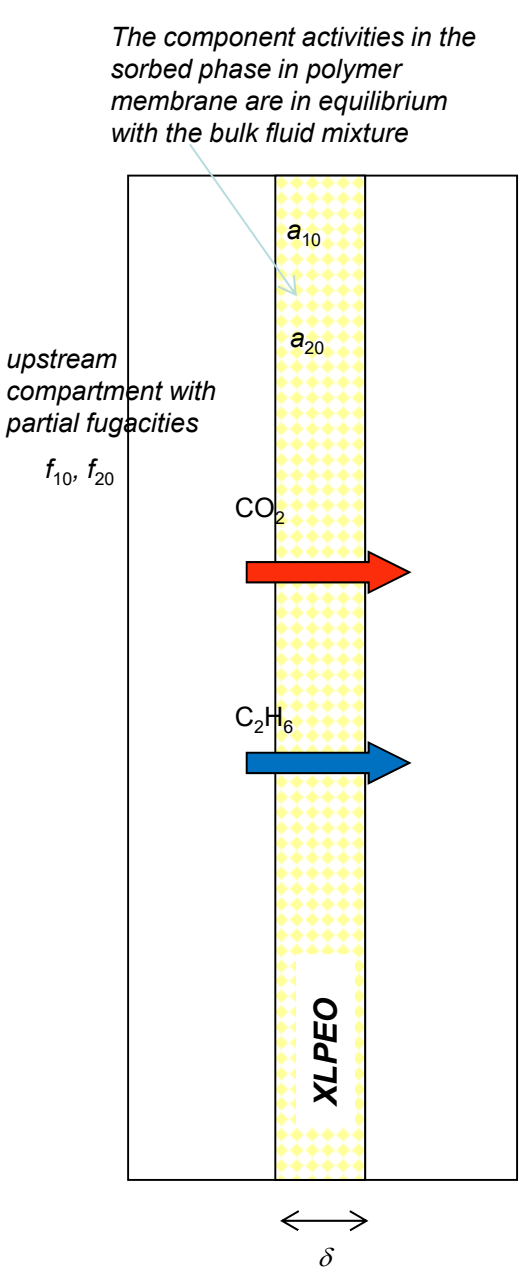

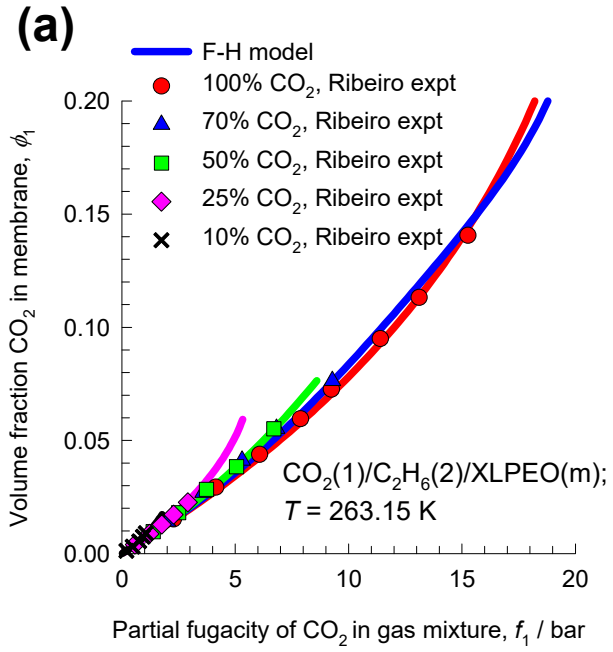

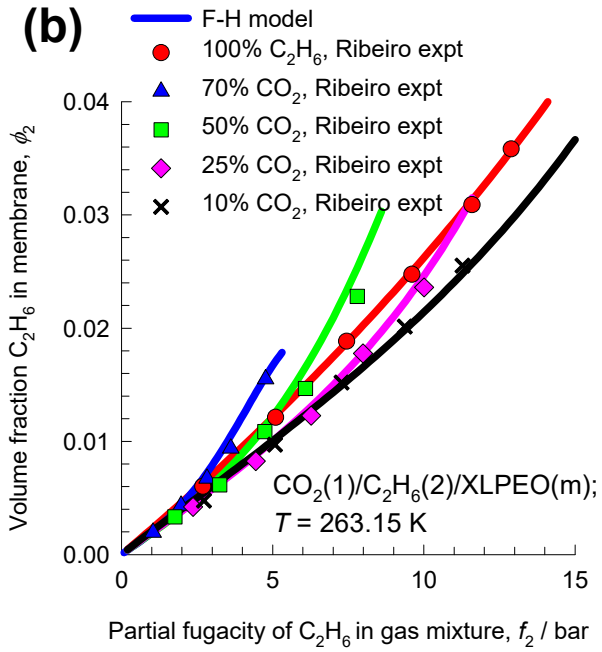

χ_{12} parameter determination

Fig. S6

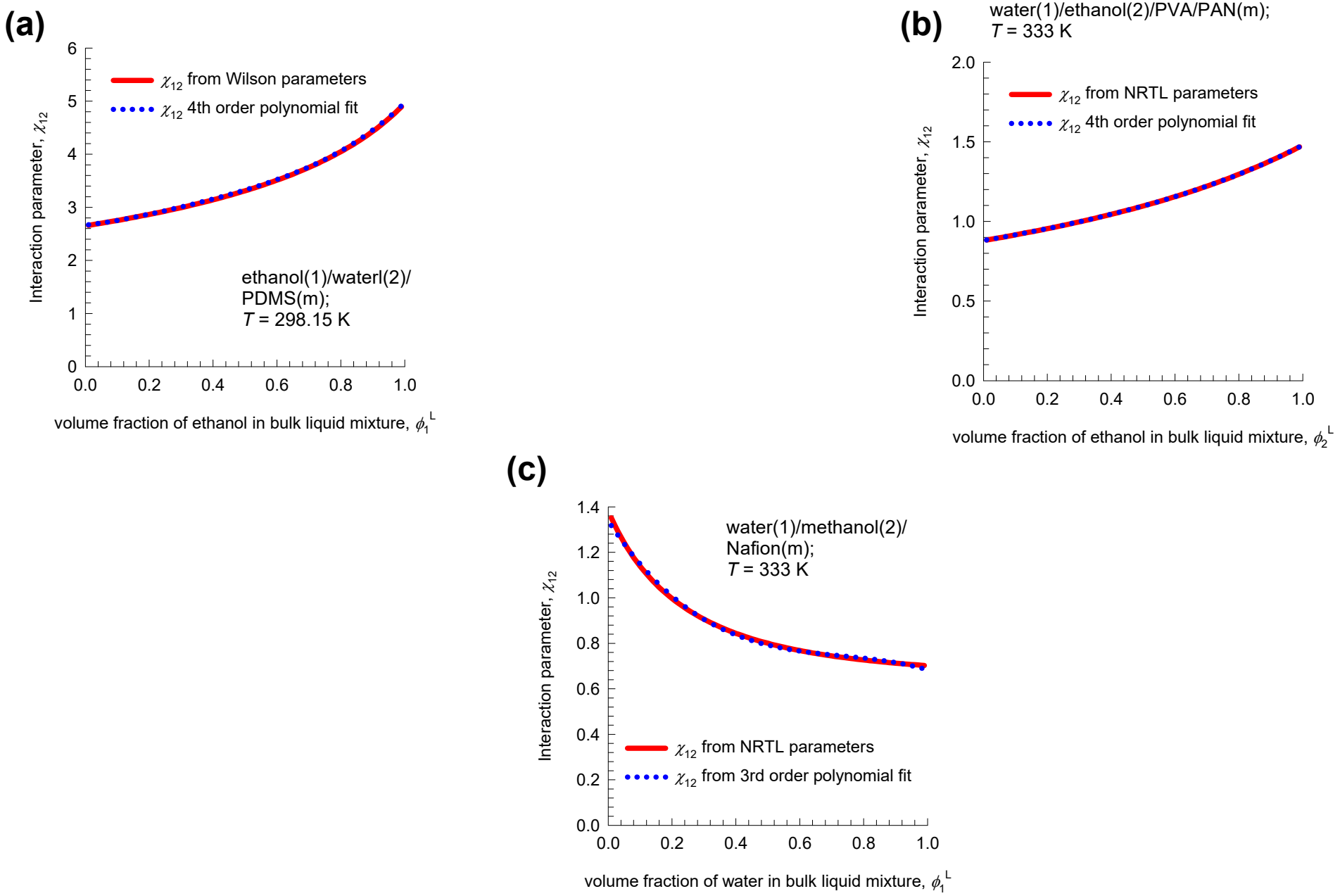

Water/ethanol/CA equilibrium

Fig. S7

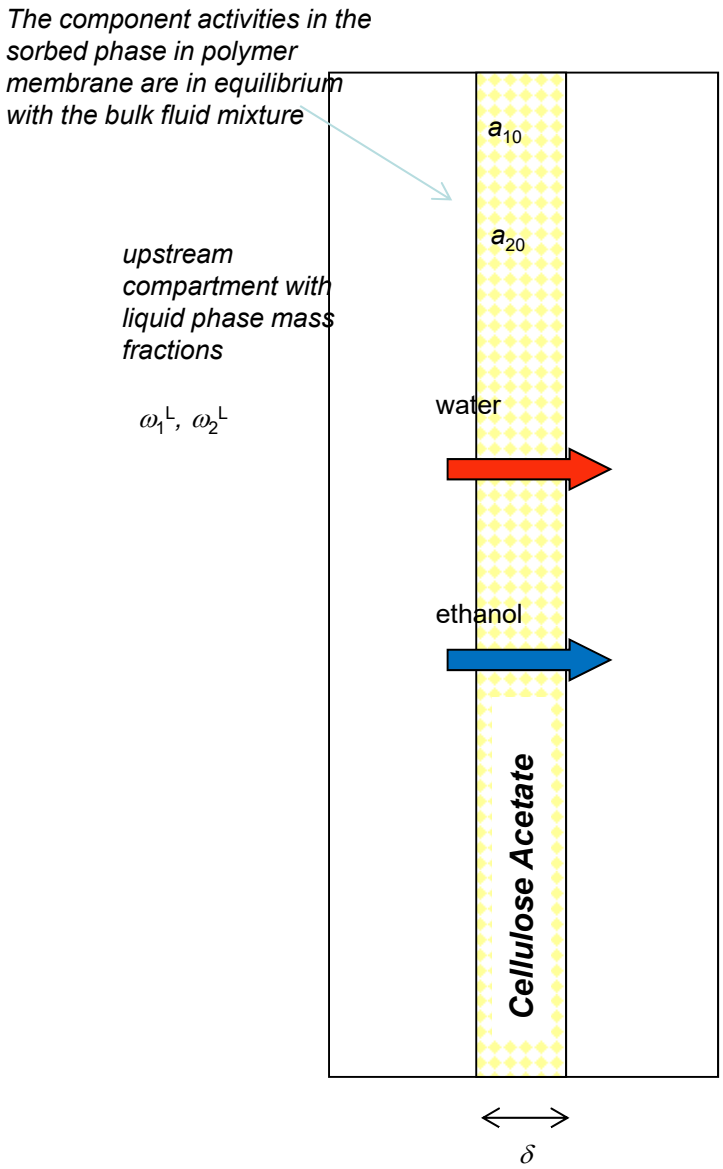

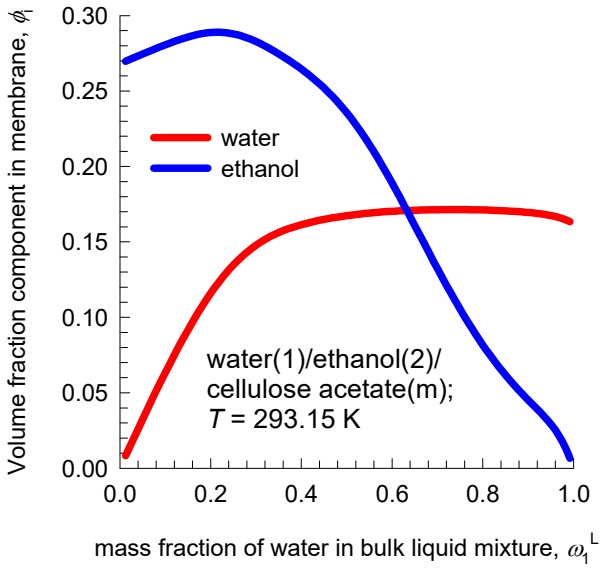

Water/ethanol/Polyimide equilibrium

Fig. S8

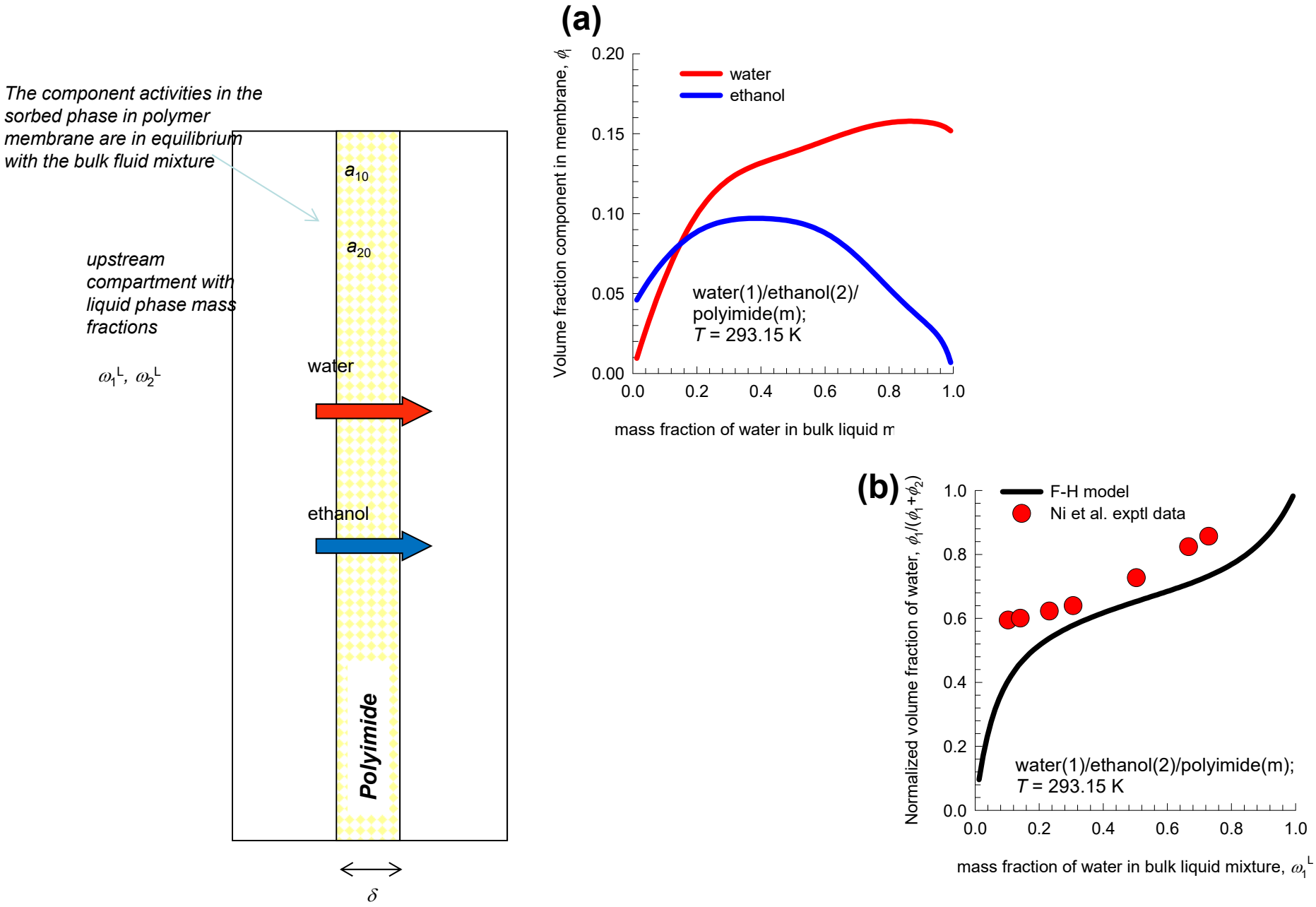

Ethanol/water/PDMS equilibrium

Fig. S9

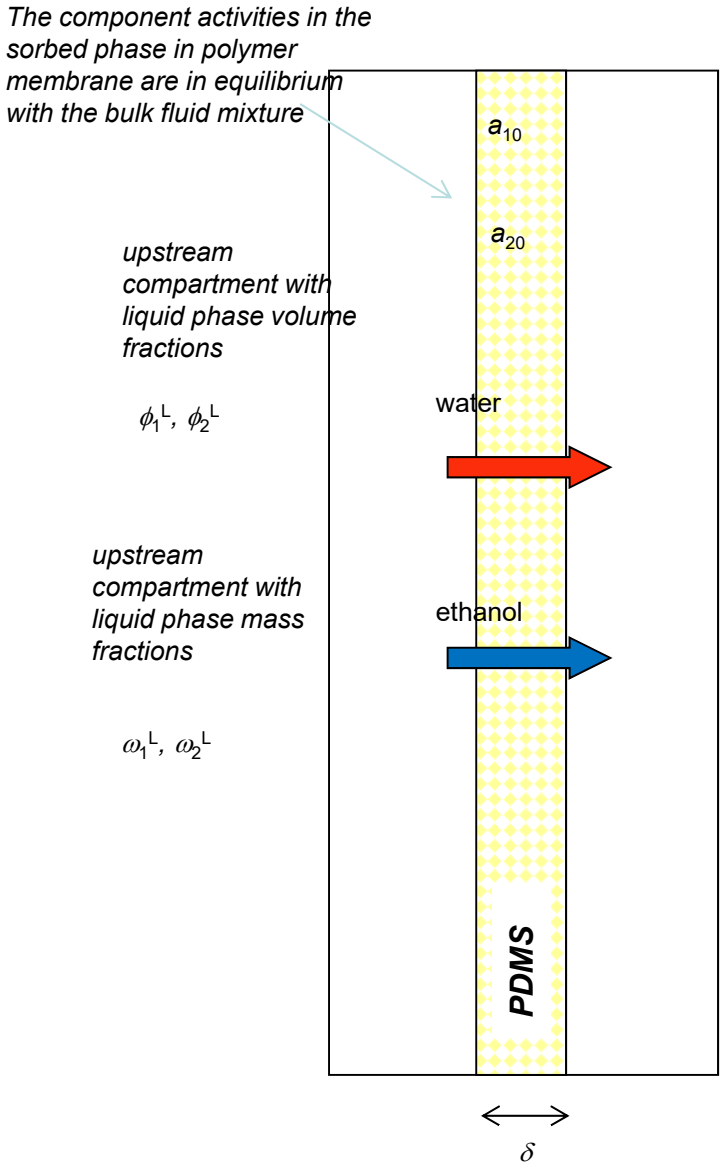

(a)

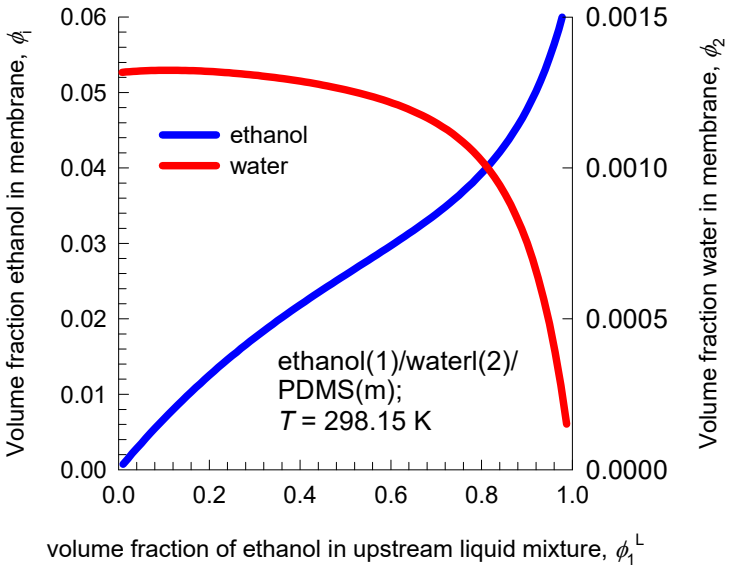

(b)

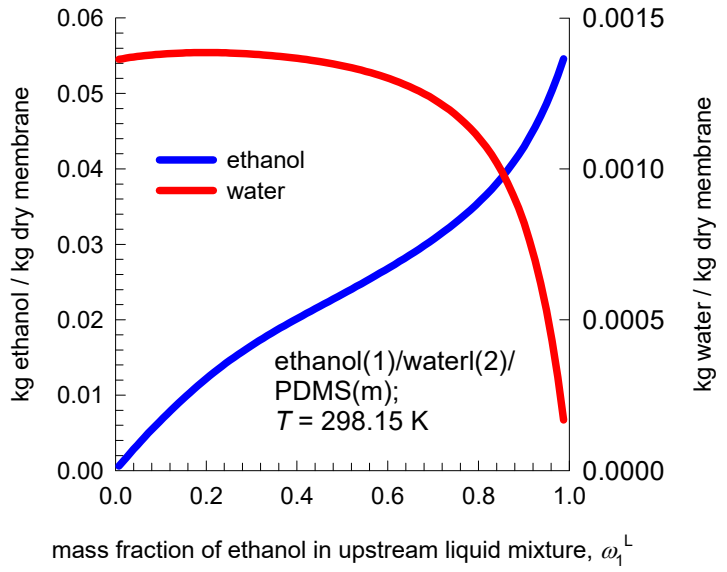

Ethanol/water/PDMS equilibrium

Fig. S10

The component activities in the sorbed phase in polymer membrane are in equilibrium with the bulk fluid mixture

upstream compartment with liquid phase volume fractions

ϕ_1^L, ϕ_2^L

upstream compartment with liquid phase mass fractions

ω_1^L, ω_2^L

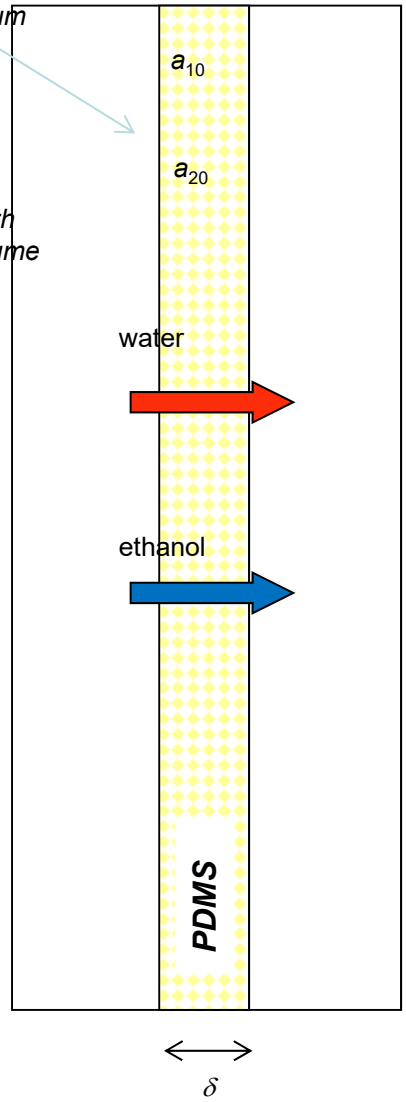

(a)

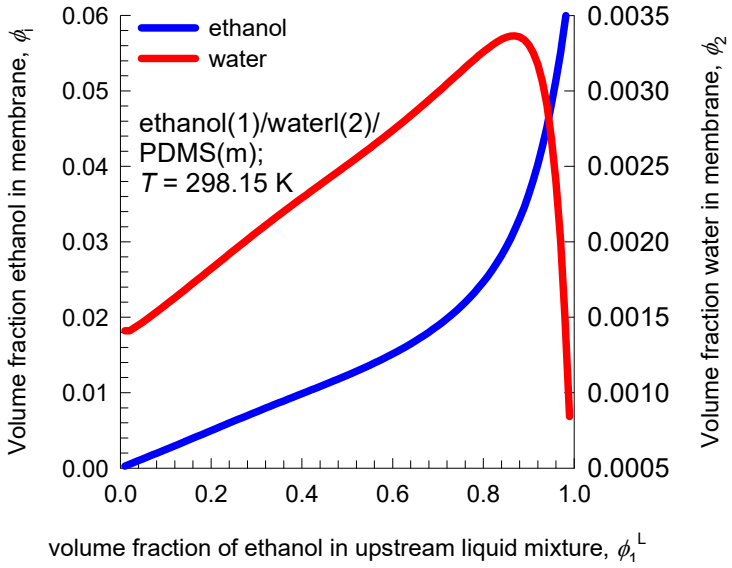

In these calculations all three interaction parameters

$\chi_{12}, \chi_{1m}, \chi_{2m}$

are composition dependent

(b)

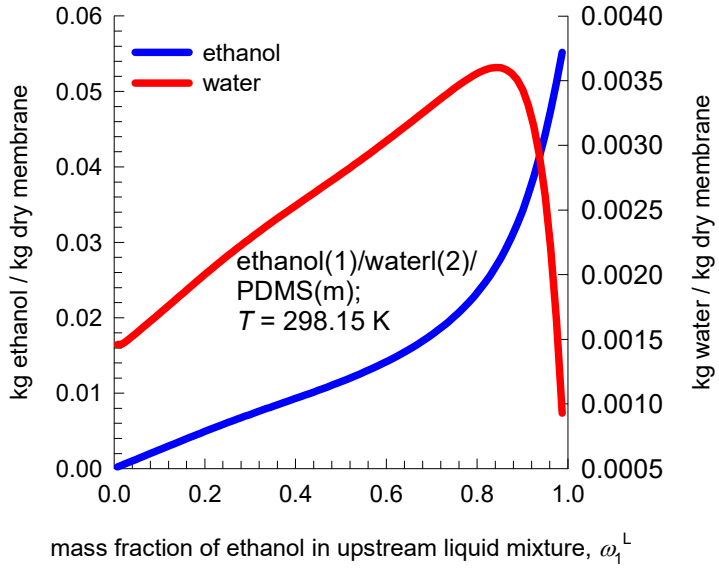

Water/ethanol/PVA/PAN equilibrium

Fig. S11

The component activities in the sorbed phase in polymer membrane are in equilibrium with the bulk fluid mixture

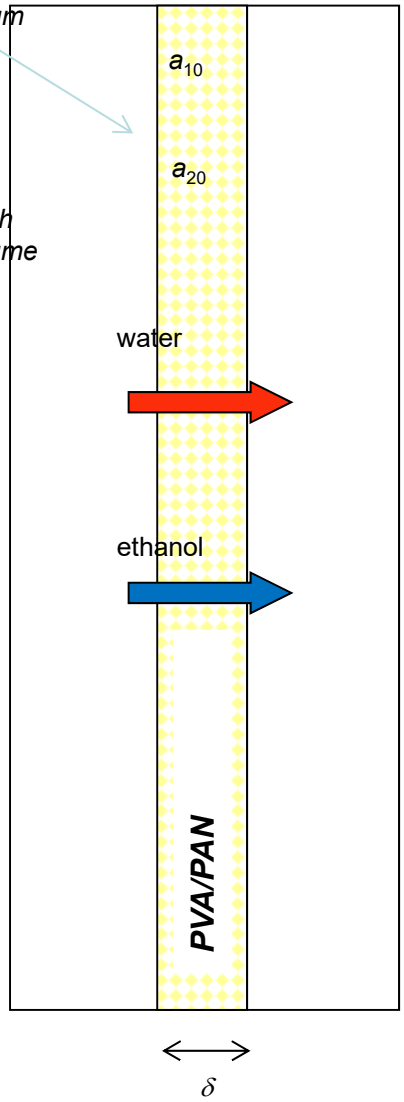

upstream compartment with liquid phase volume fractions

$\phi_1^L,\ \phi_2^L$

upstream compartment with liquid phase mass fractions

$\omega_1^L,\ \omega_2^L$

In these calculations all the interaction parameters

$\chi_{12}, \chi_{1m}, \chi_{2m}$

are composition dependent

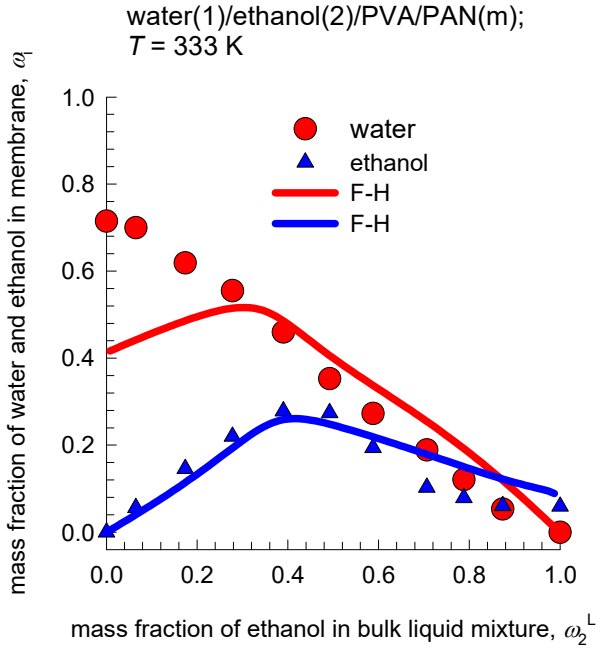

Water/methanol/Nafion equilibrium

Fig. S12

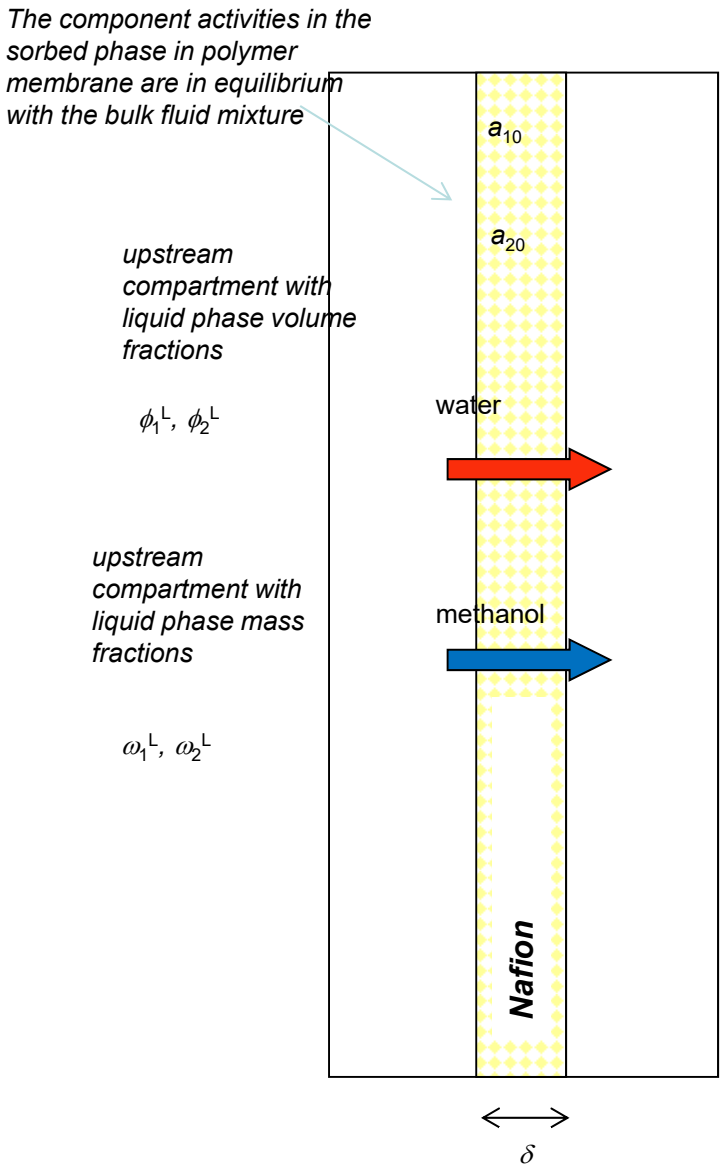

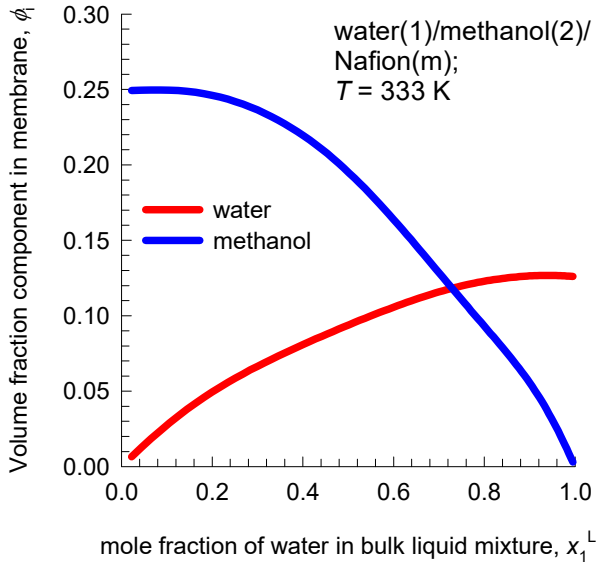

Fig. S13

Diffusivity vs Temperature

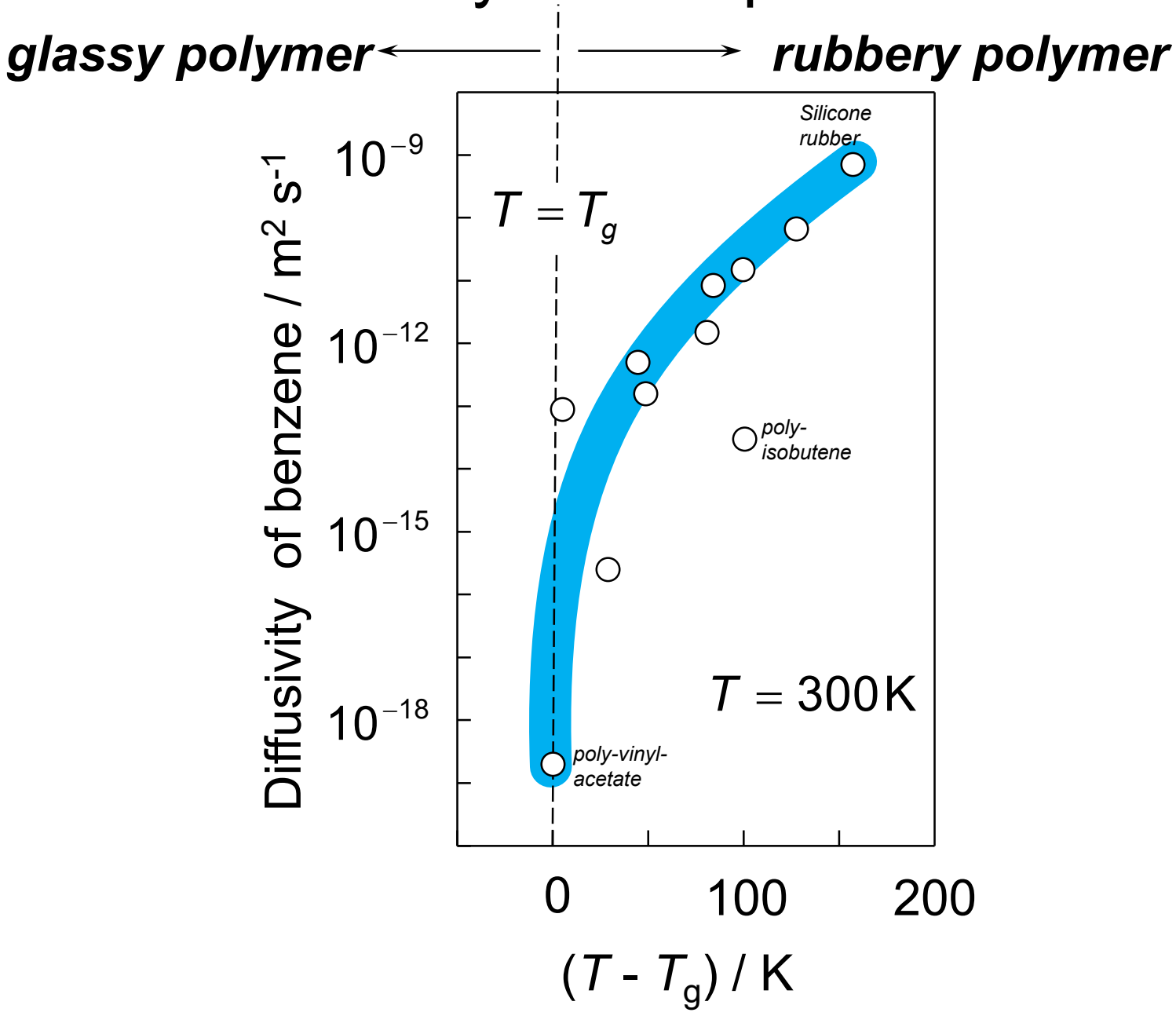

Fig. S14

Diffusivity vs Penetrant Molar Volume

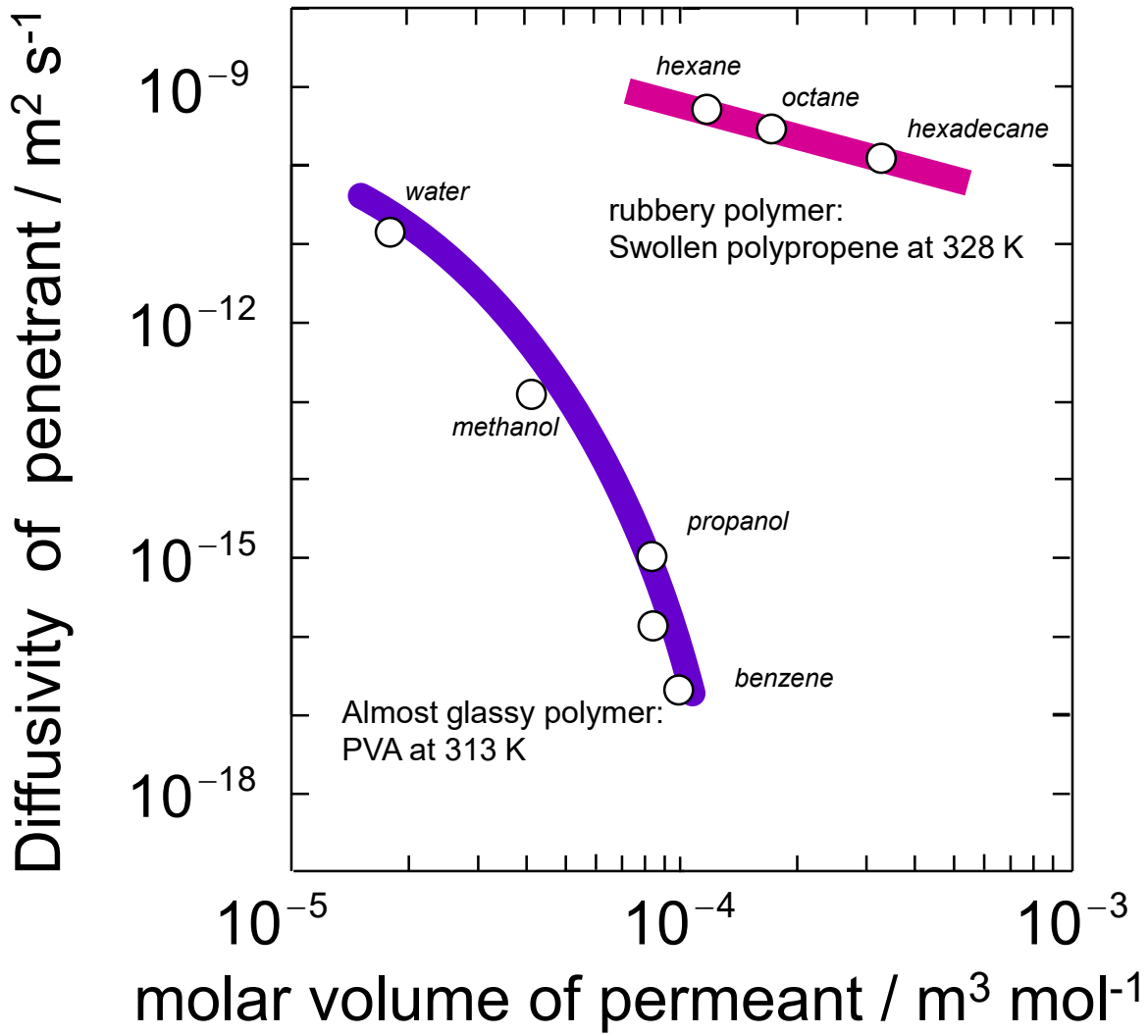

Fig. S15

Influence of Swelling on Diffusivity

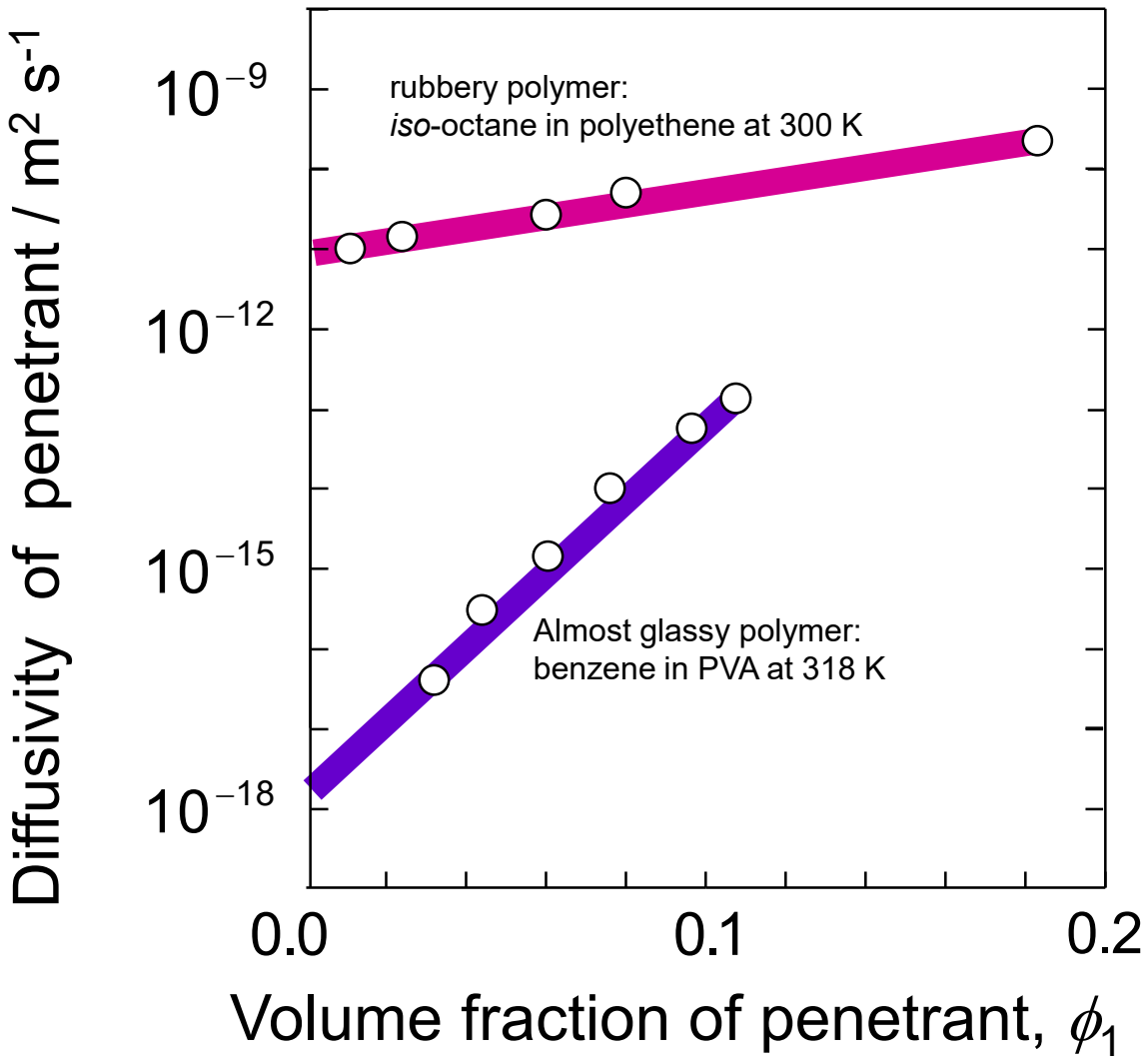

Diffusion of water in Soft contact lens material

(a)

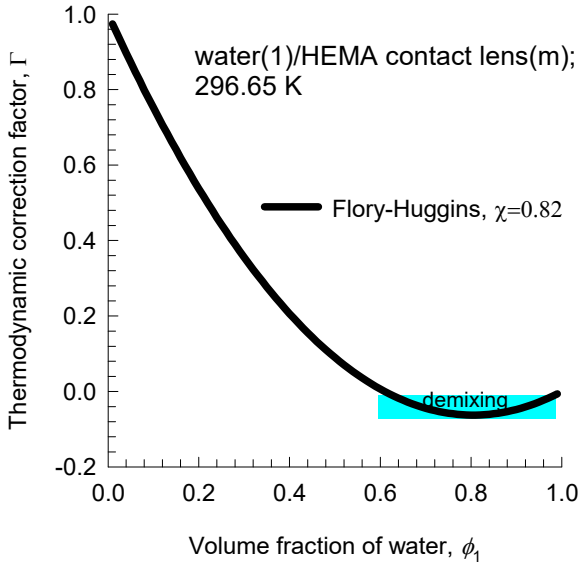

(b)

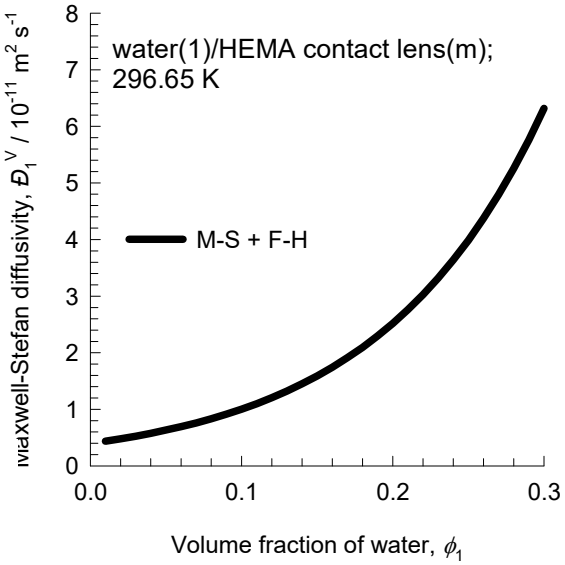

(c)

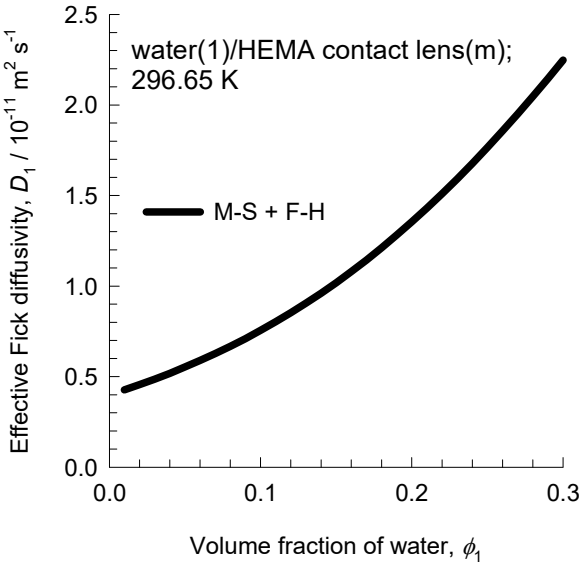

Unary CO_2 and C_2H_6 permeation across XLPEO

Fig. S17

(a)

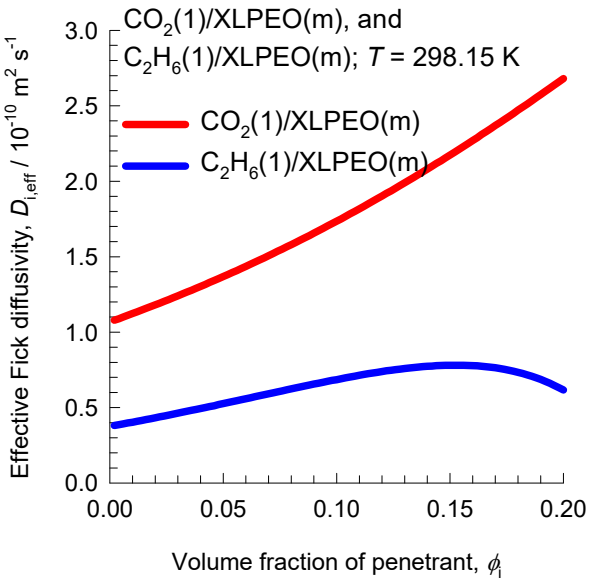

(b)

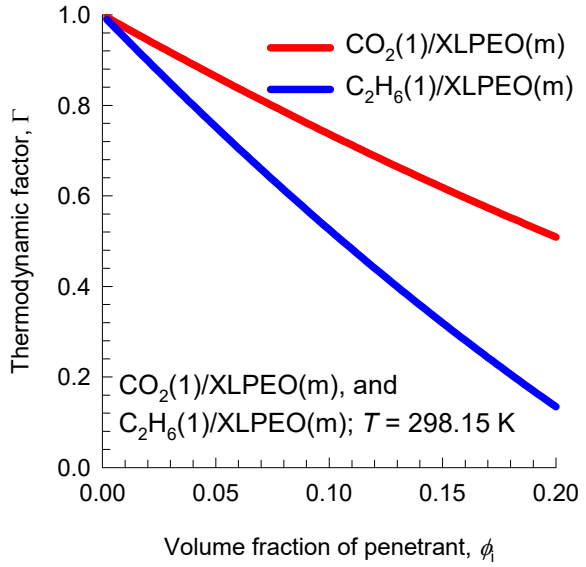

Unary CO_2 and C_2H_6 permeation across XLPEO

Fig. S18

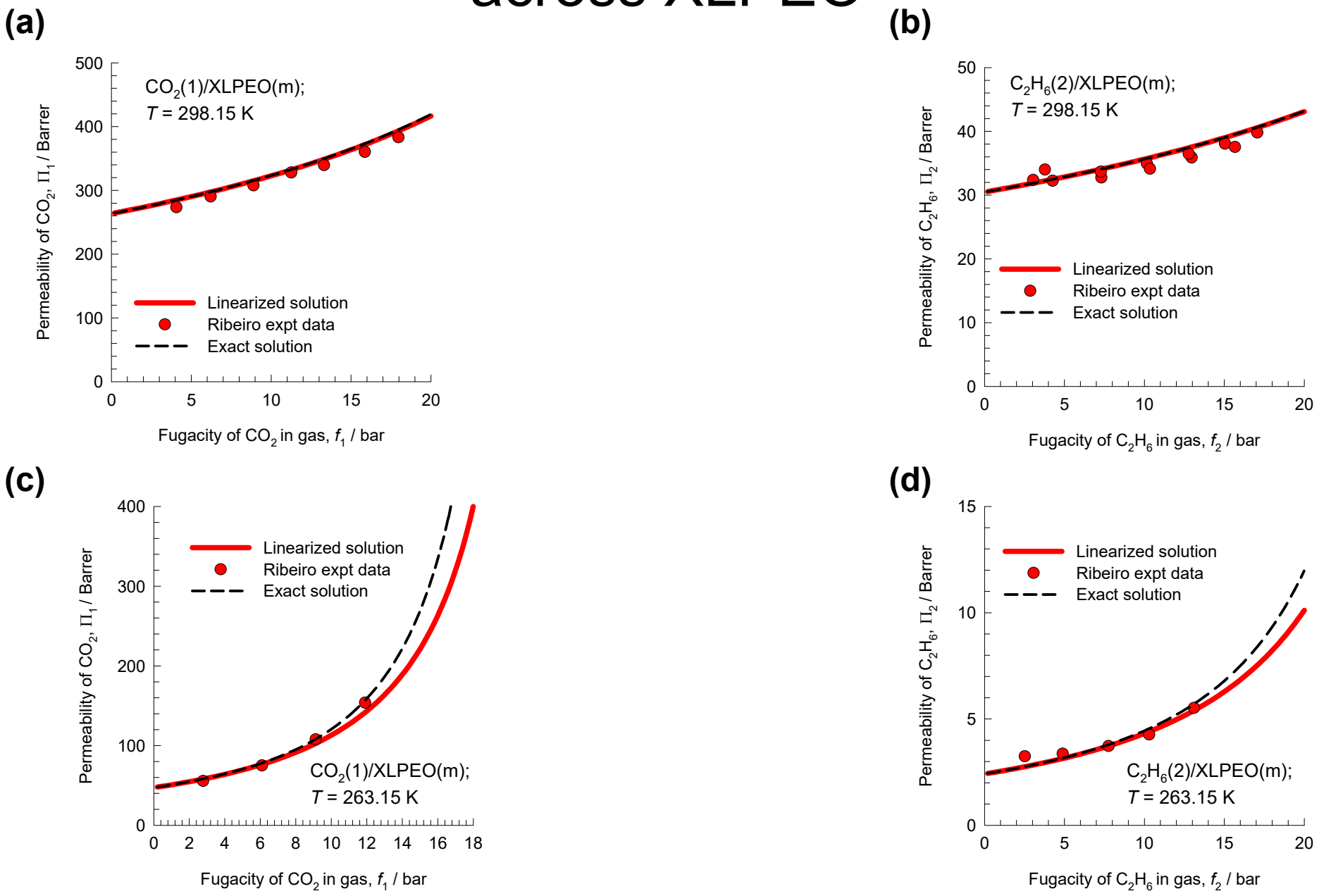

Significance of thermodynamic coupling

Fig. S19

(a)

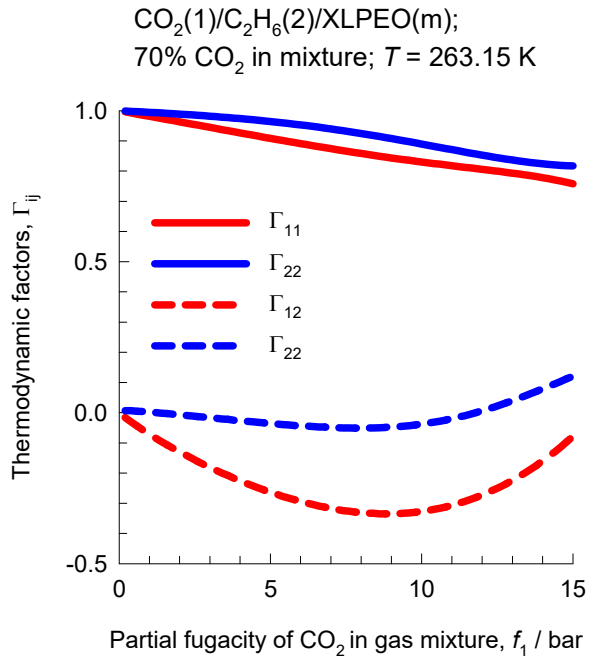

(b)

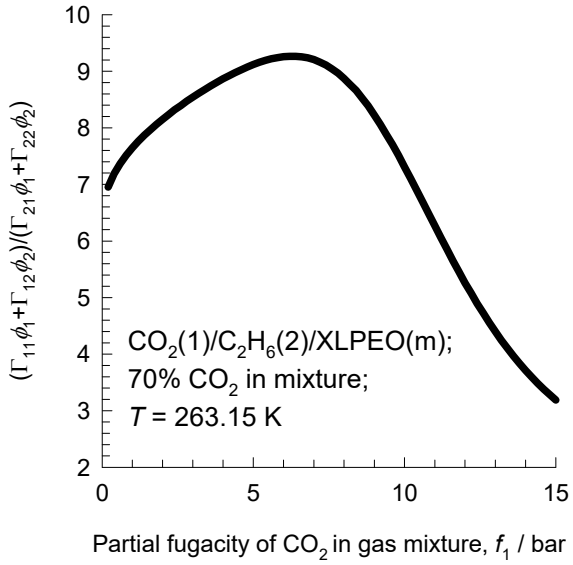

(c)

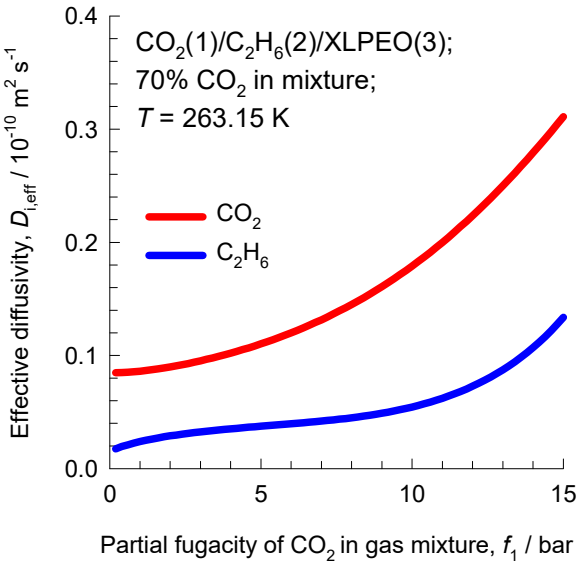

These are calculations using the linearized Maxwell-Stefan equations

CO_2/C_2H_6 permeation across XLPEO

Fig. S20

(a)

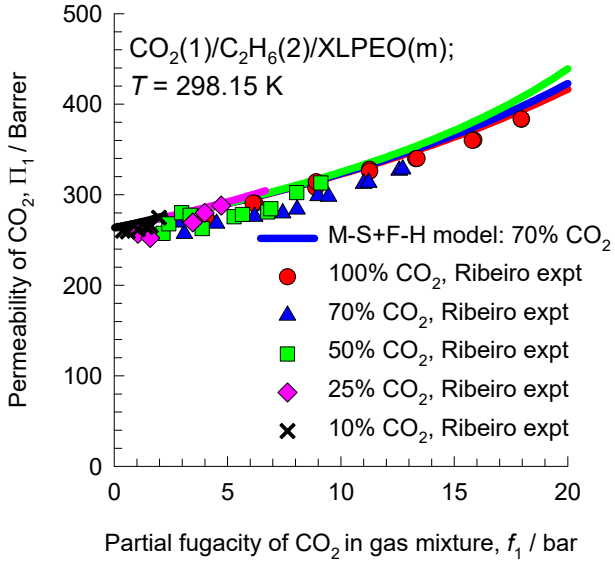

T = 298.15

(b)

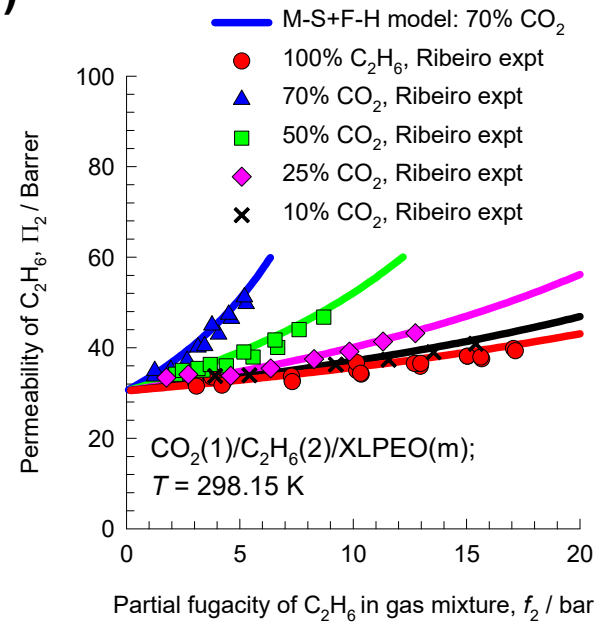

These are solutions using the linearized Maxwell-Stefan equations

Fig. S21

Binary Permeation across Polymer Membrane

(a)

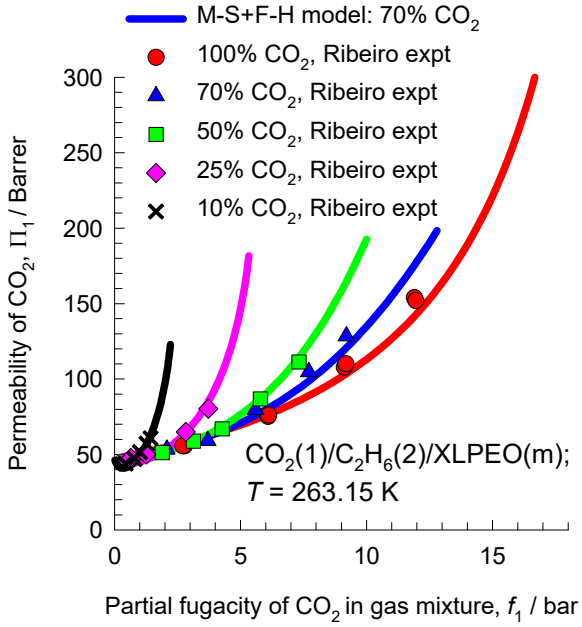

***T* = 263.15**

(b)

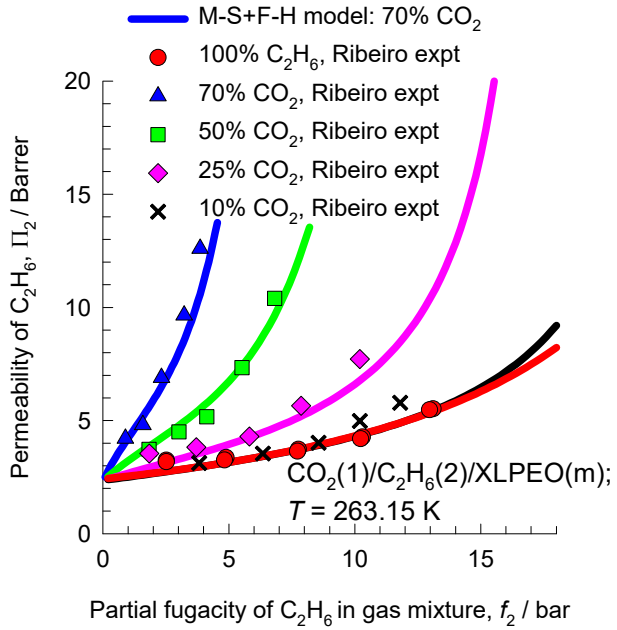

These are solutions using the linearized Maxwell-Stefan equations

Fig. S22

Binary Permeation across Polymer Membrane

(a)

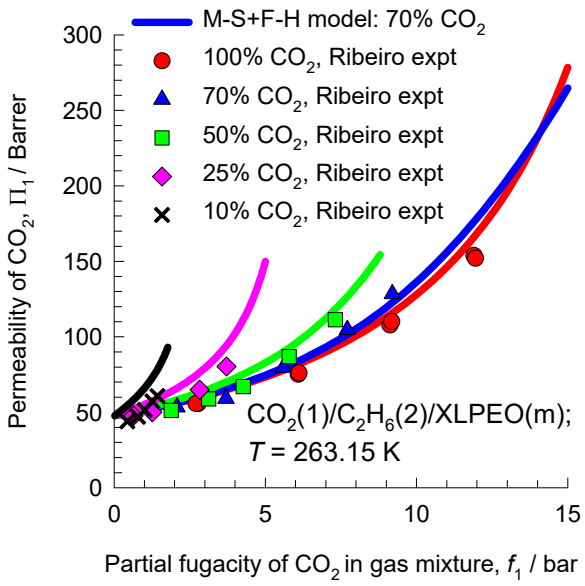

***T* = 263.15**

(b)

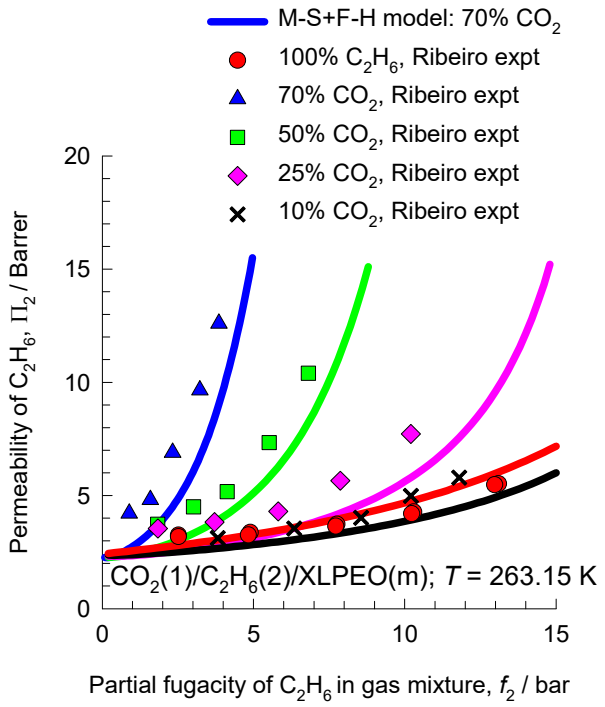

These are solutions using the linearized Maxwell-Stefan equations in which the 1-2 friction has been ignored

Water/ethanol/cellulose acetate

Fig. S23

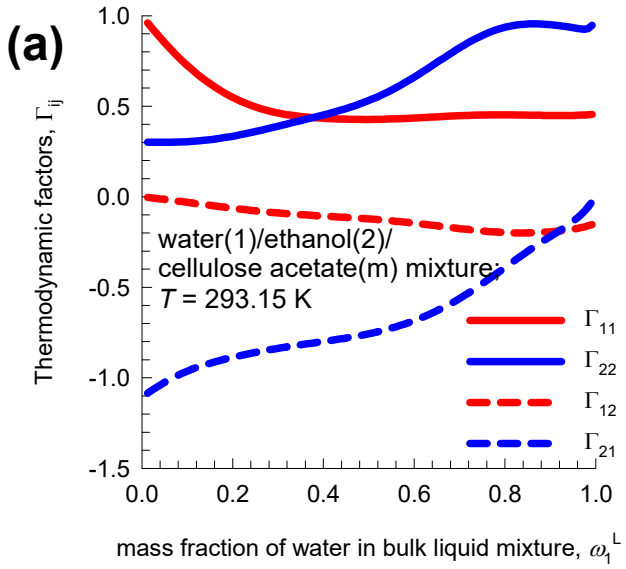

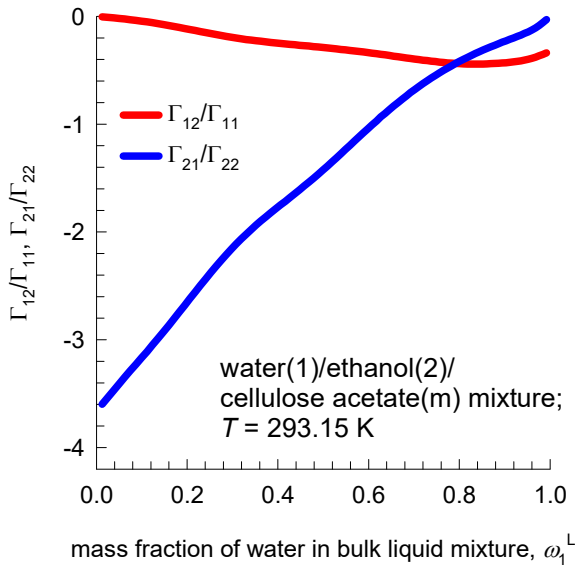

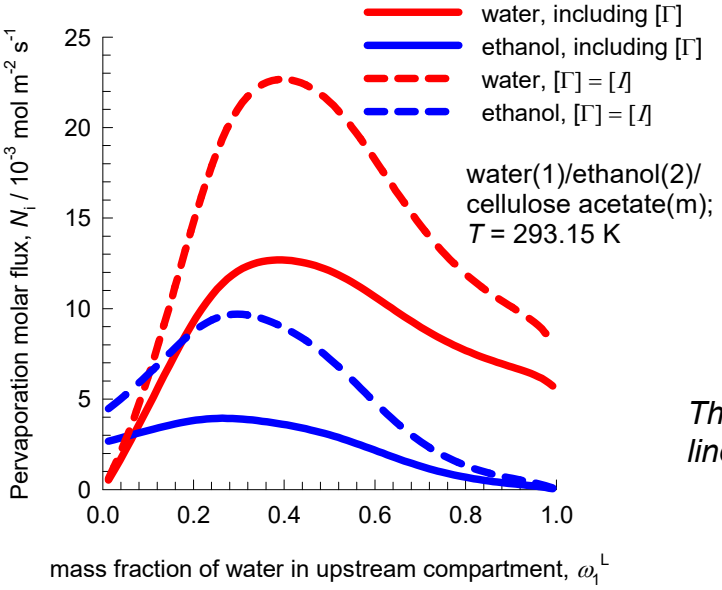

These are solutions using the linearized Maxwell-Stefan equations

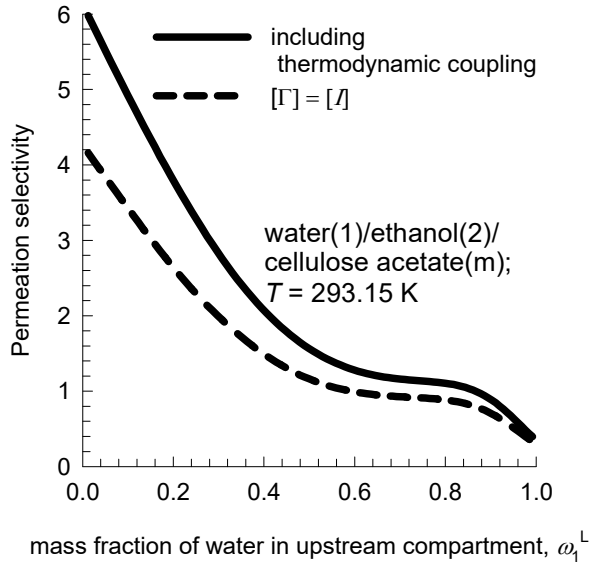

Water/ethanol/polyimide

Fig. S24

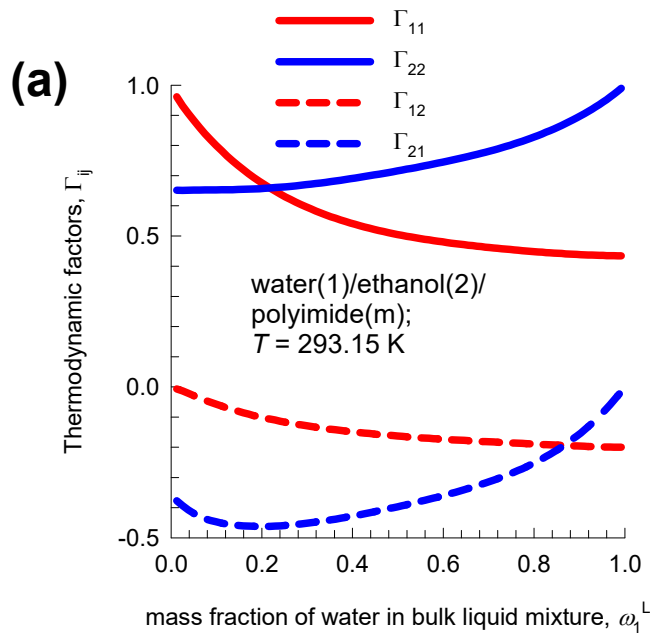

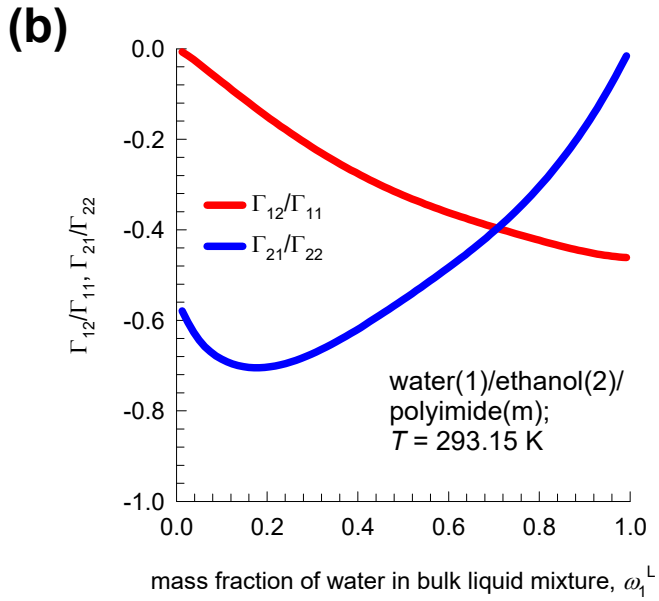

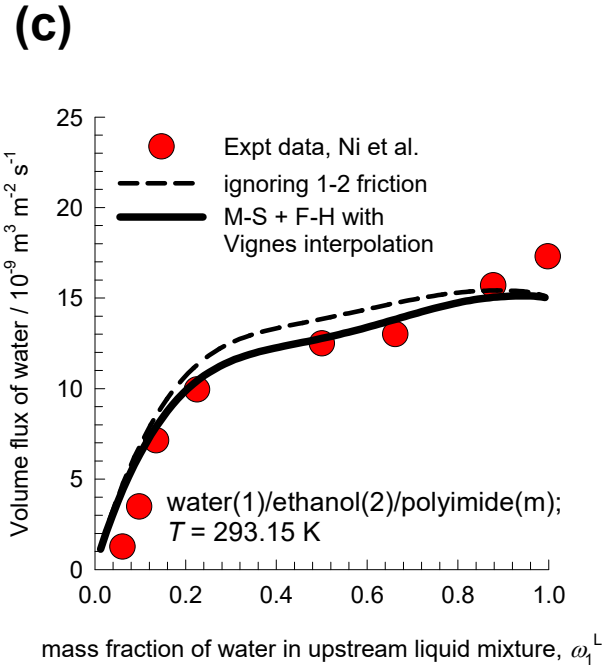

These are solutions using the linearized Maxwell-Stefan equations

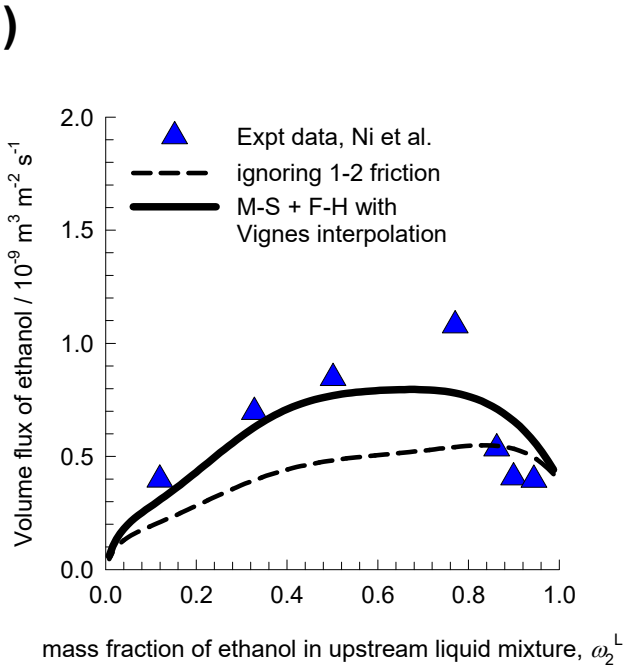

Water/ethanol/PVA/PAN pervaporation

Fig. S25

(a)

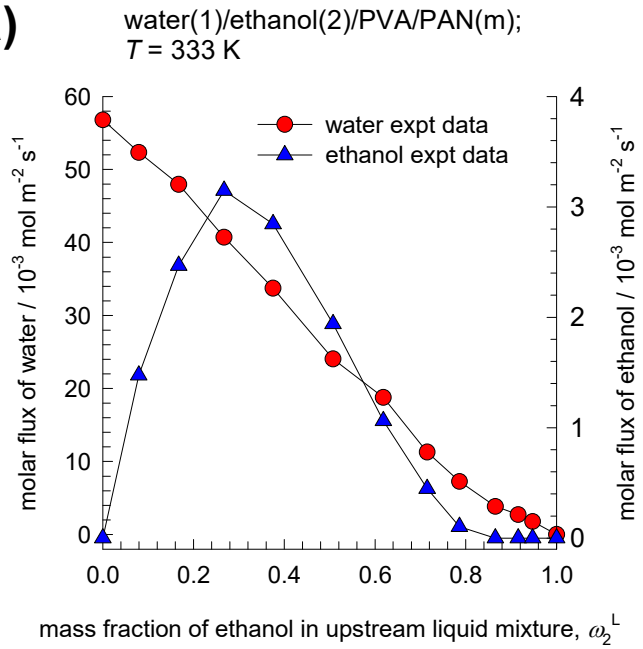

(b) Strong 1-2 friction

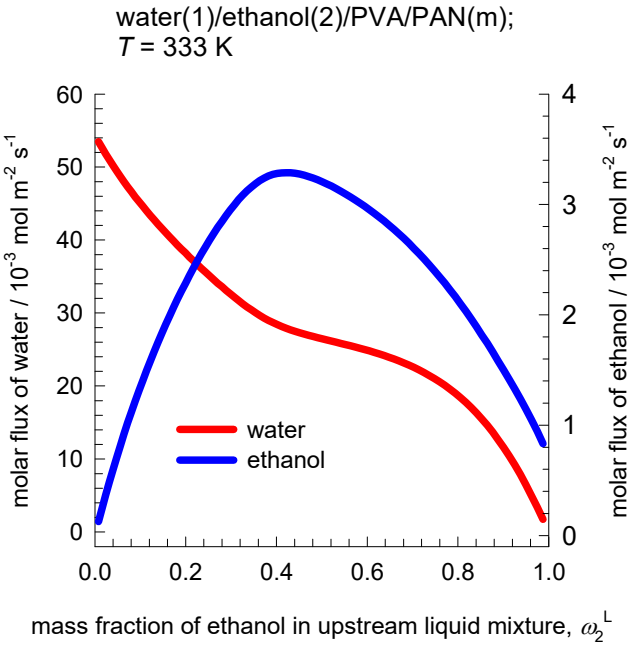

(c) Weak 1-2 friction

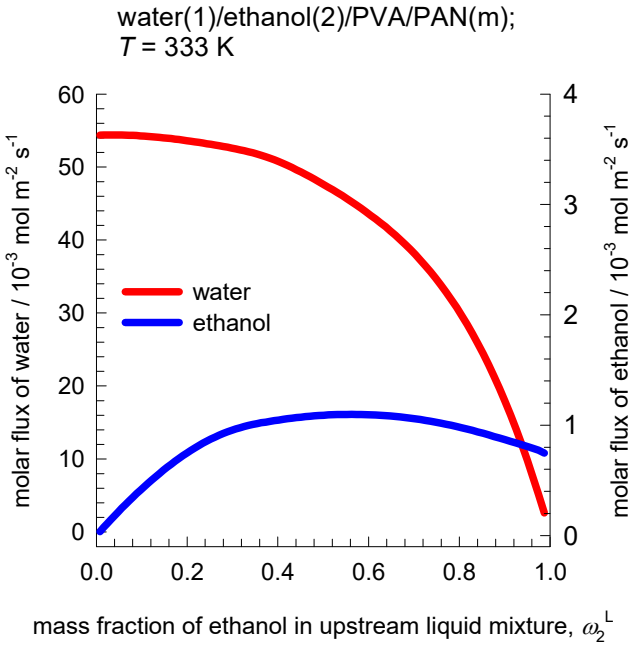

Diffusion of toluene in polystyrene

Fig. S26

(a)

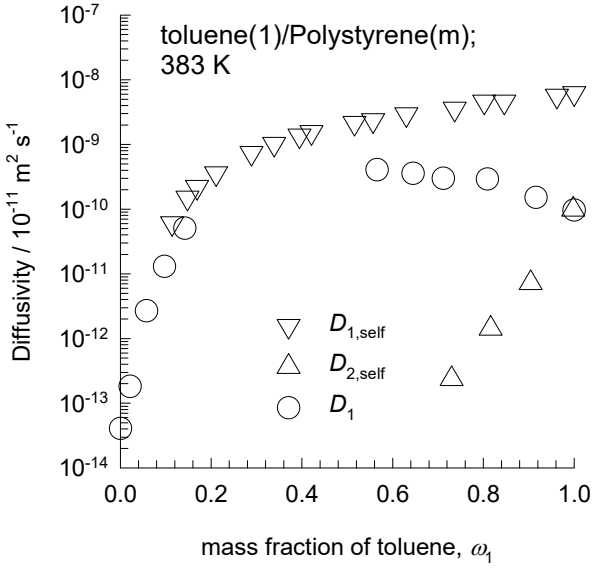

(b)

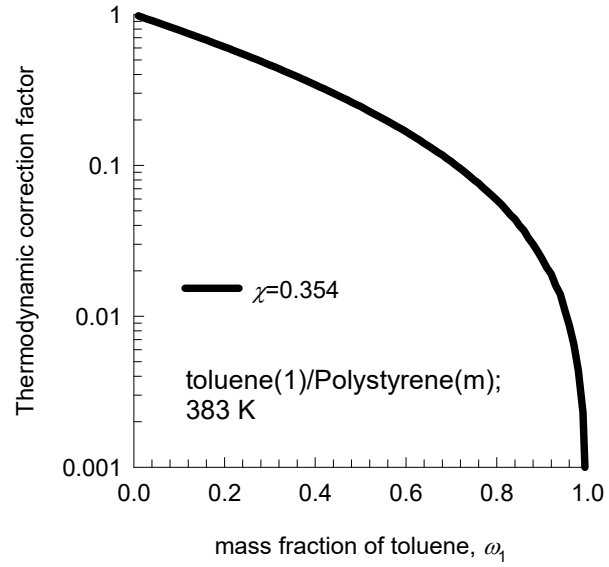

(c)

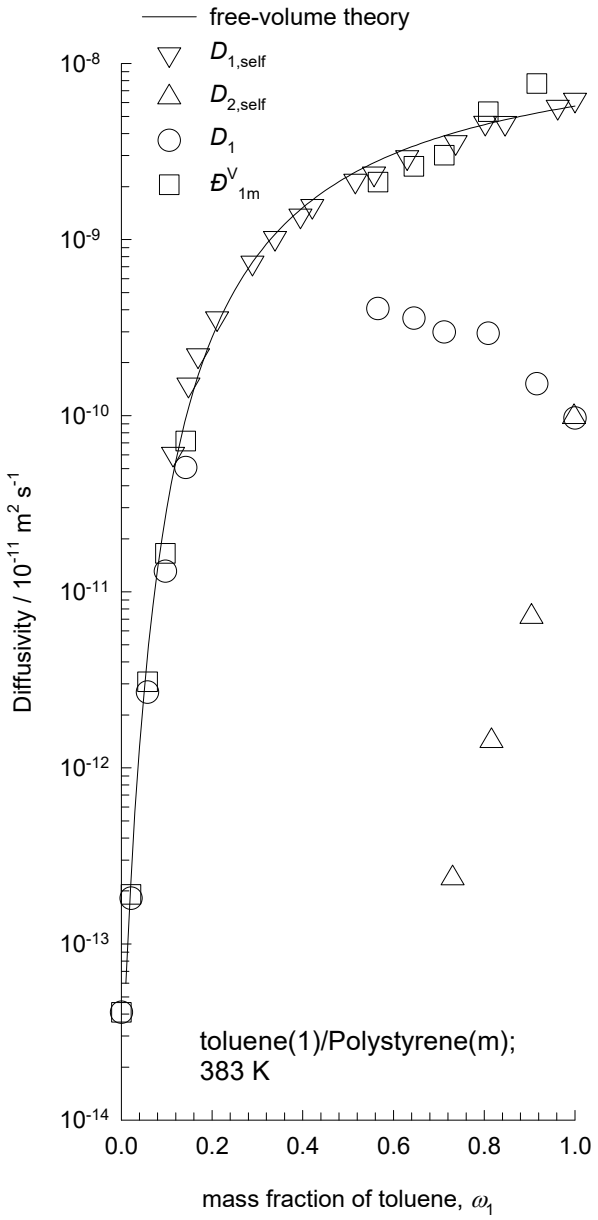

Diffusion of acetone in cellulose acetate

Fig. S27

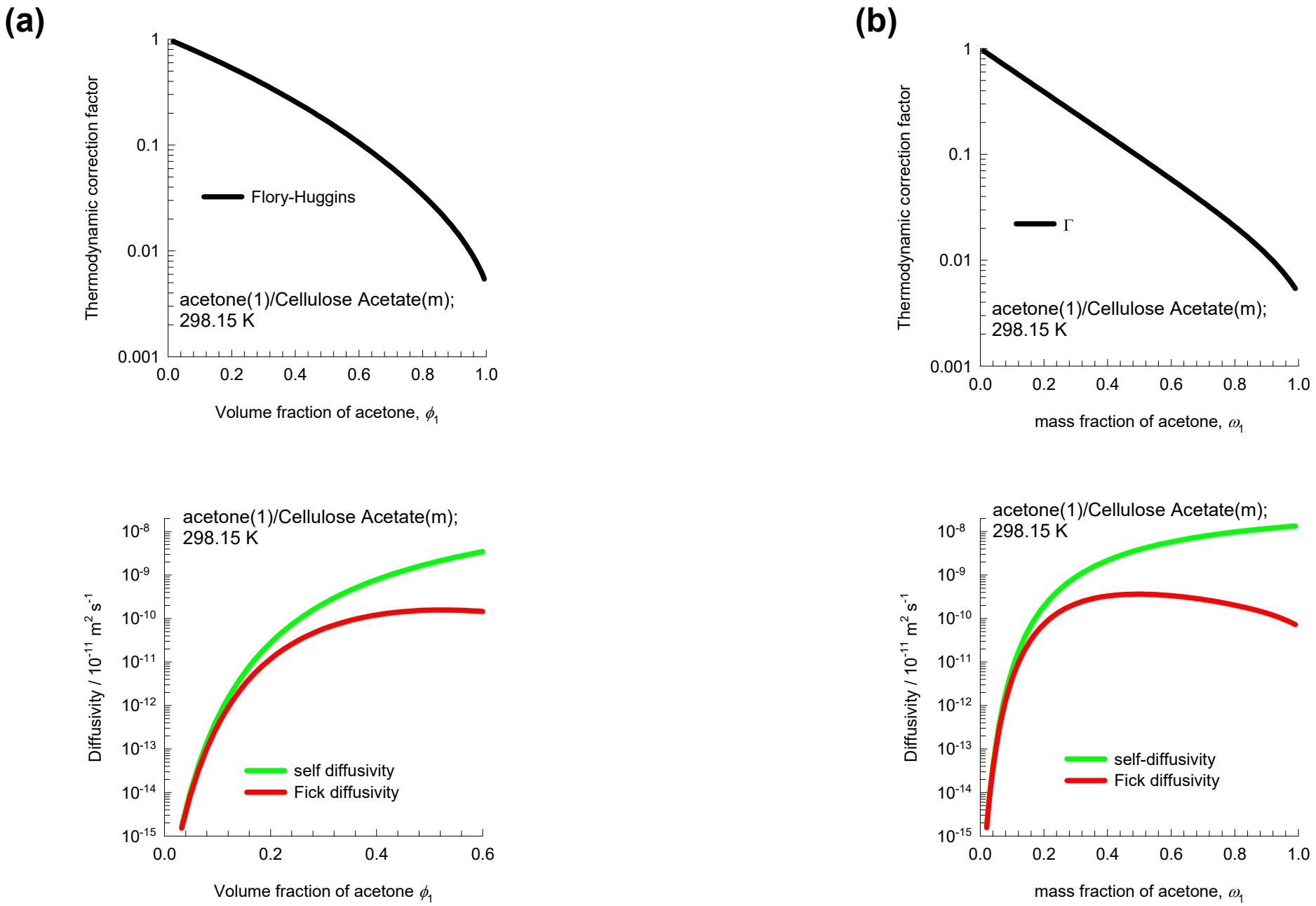

Methanol(1)/Toluene(2)/PVAc(m) system

Fig. S28

(a)

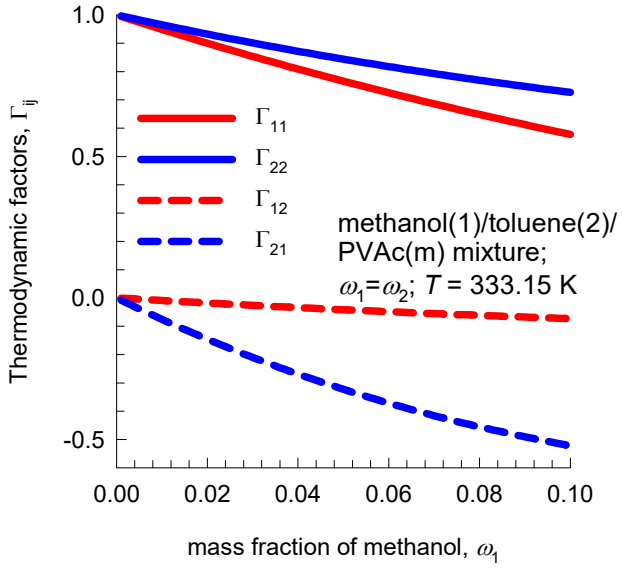

(b)

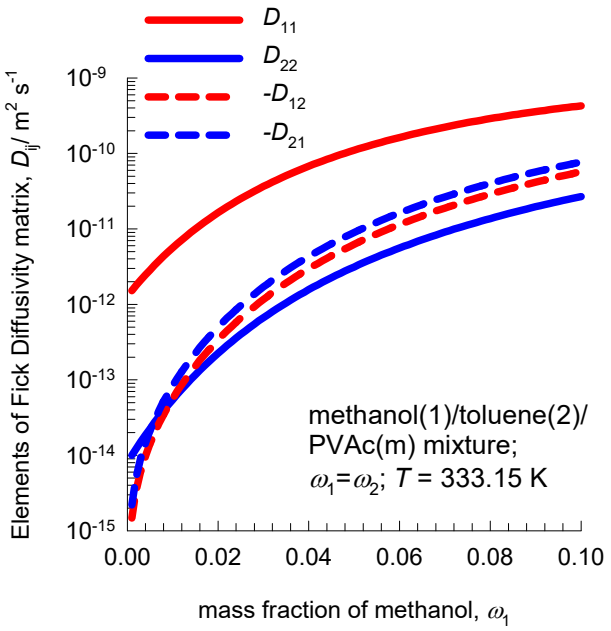

Equilibration trajectories in Water/acetone/cellulose acetate

Fig. S29

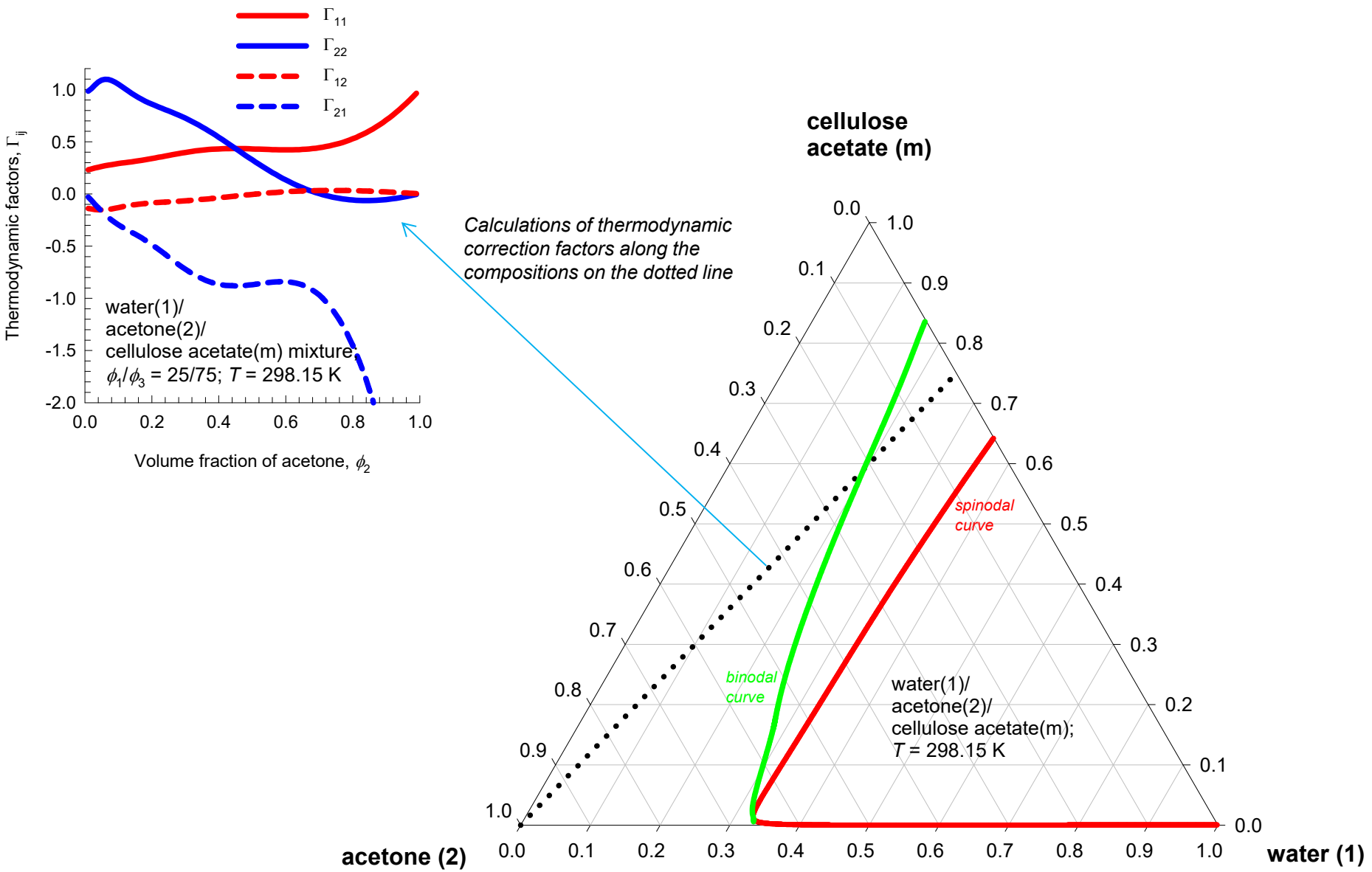

Transient equilibration: CA

Fig. S30

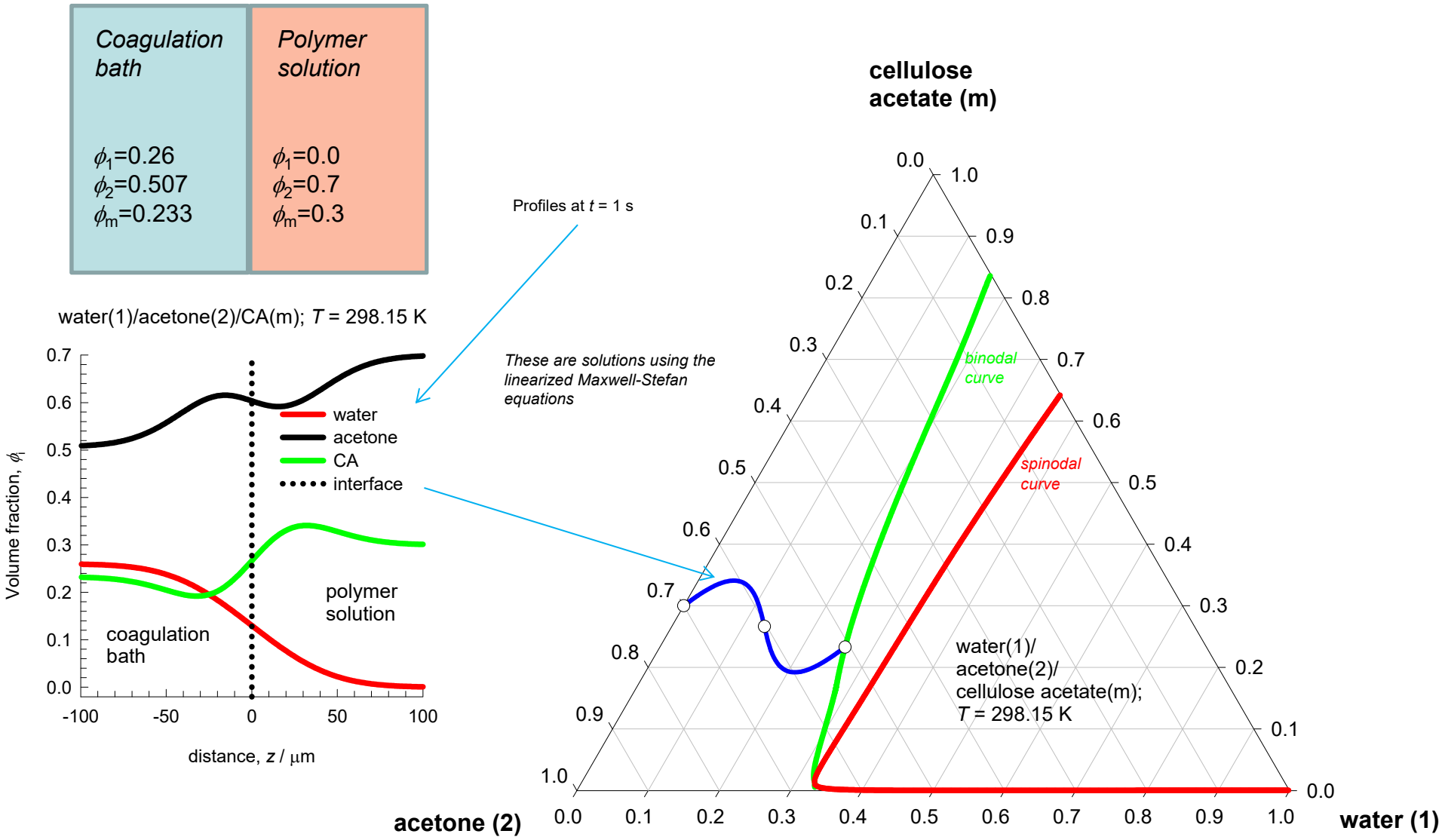

Fig. S31

Water/acetone/CA

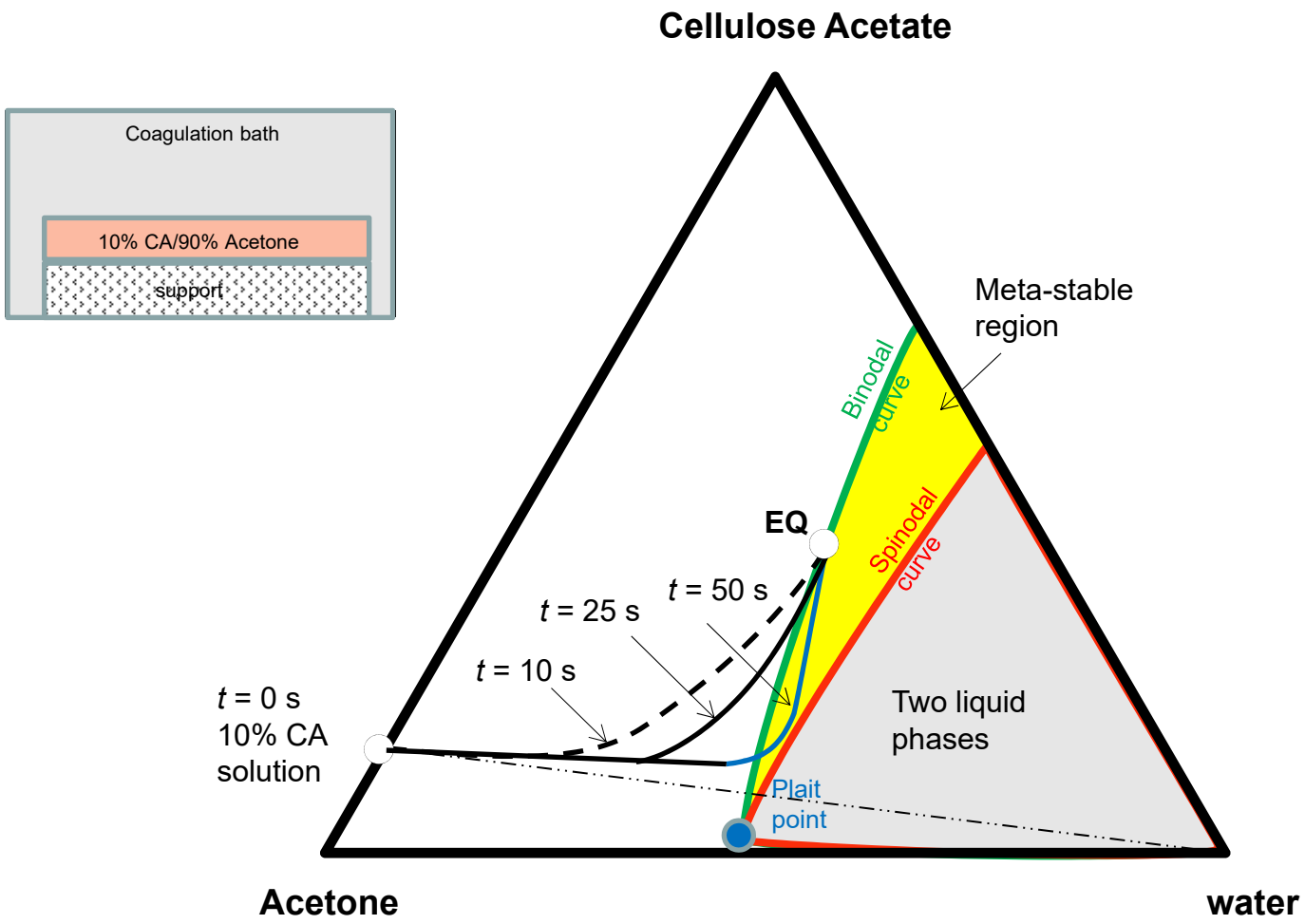

Foray into meta-stable region

Fig. S32

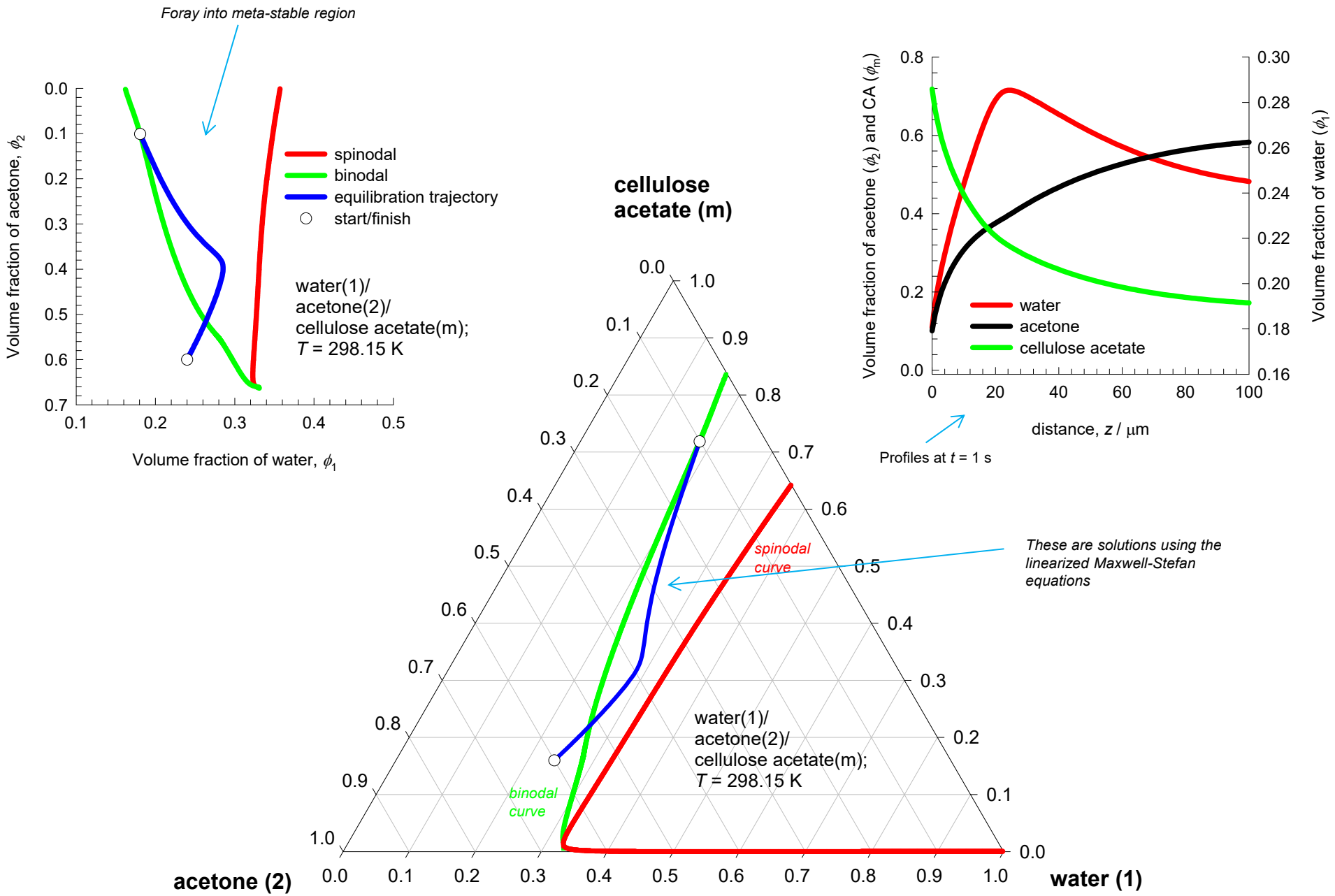

Foray into meta-stable region

Fig. S33

(a)

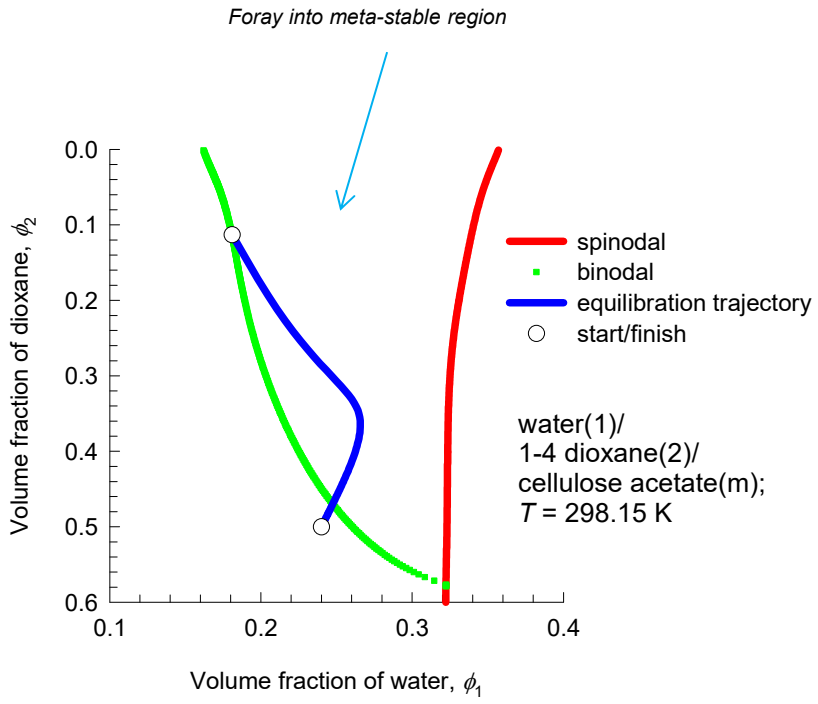

(b)

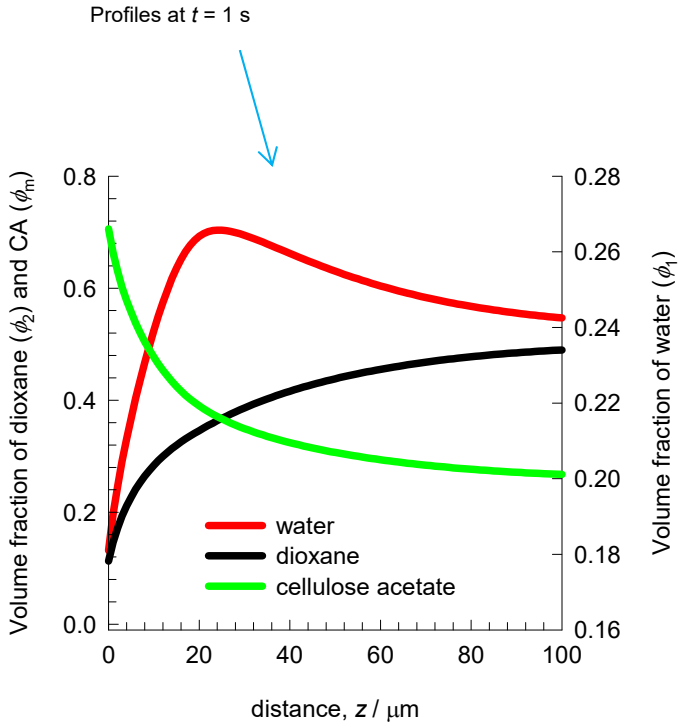

These are solutions using the linearized Maxwell-Stefan equations

Transient equilibration trajectory

Fig. S34

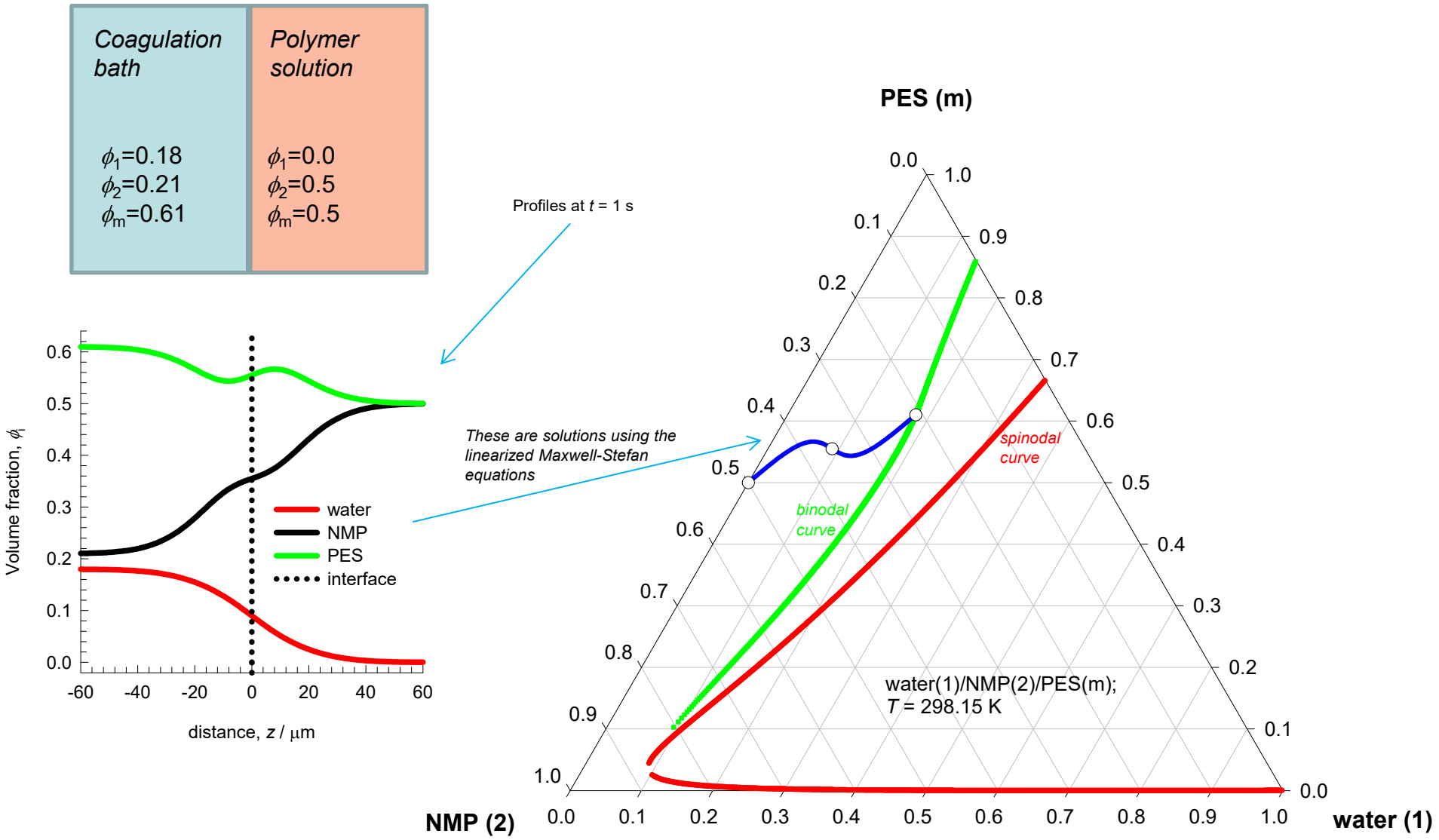

Foray into meta-stable region

Fig. S35

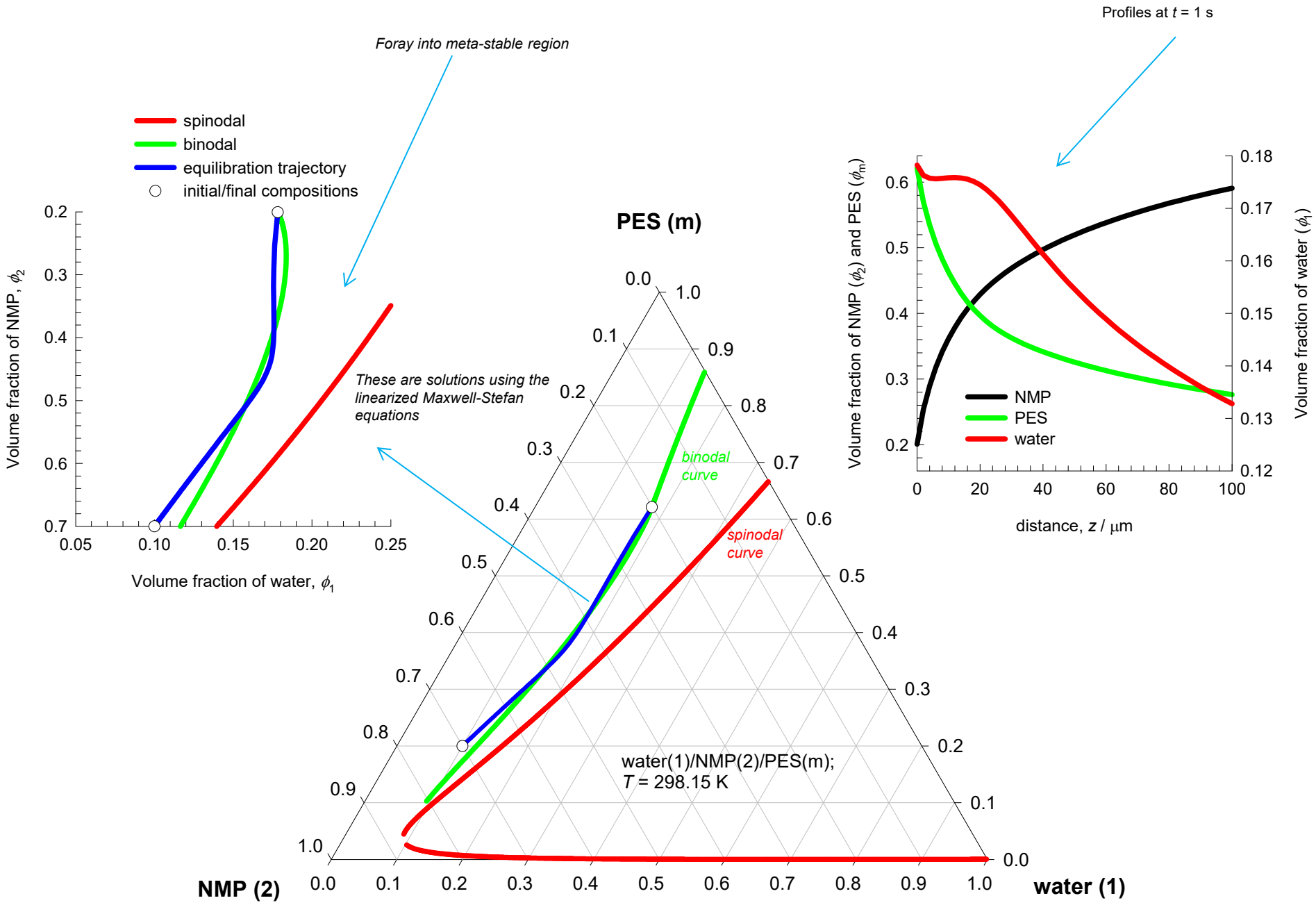

Foray into meta-stable region

Fig. S36

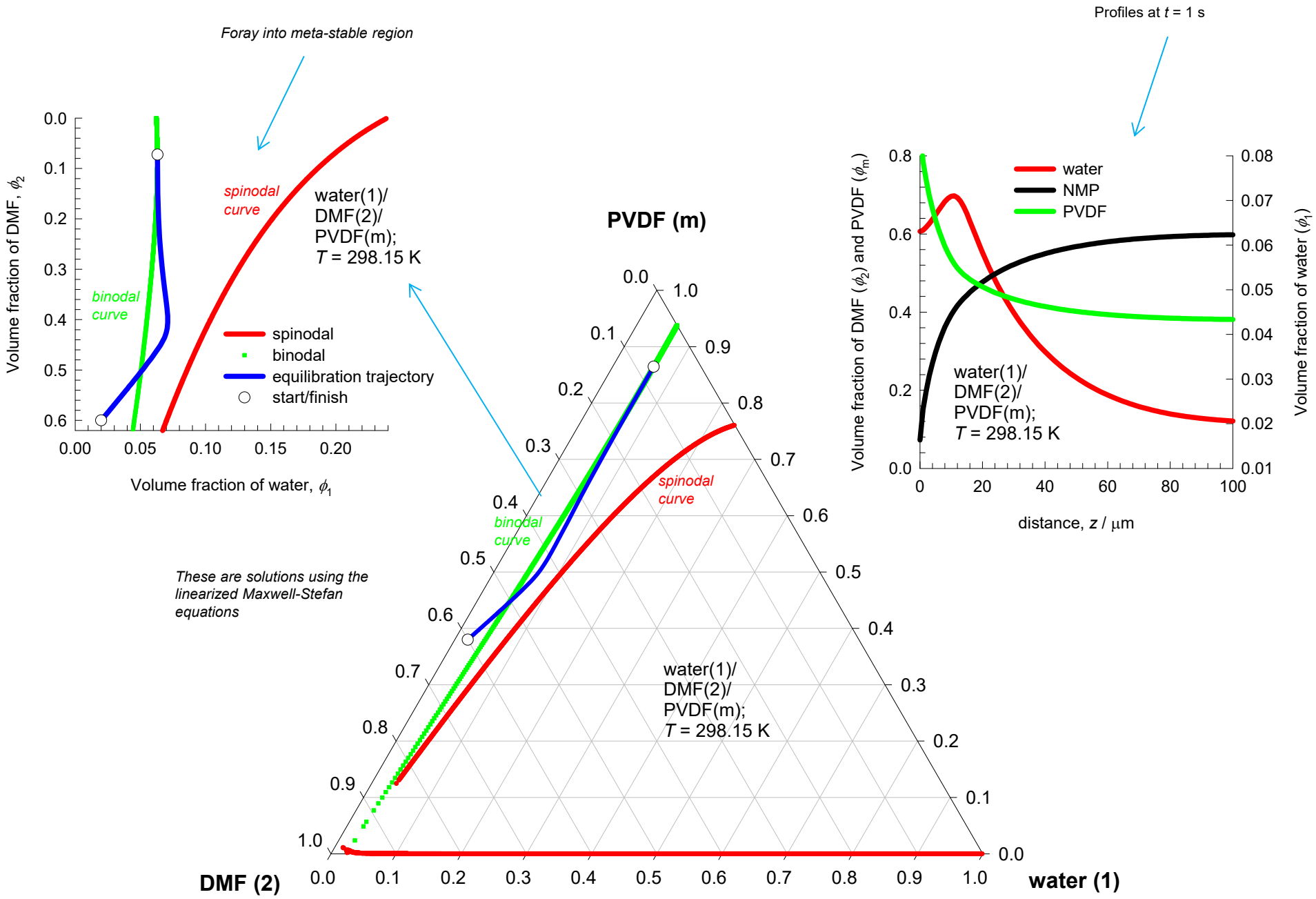

Foray into meta-stable region

Fig. S37

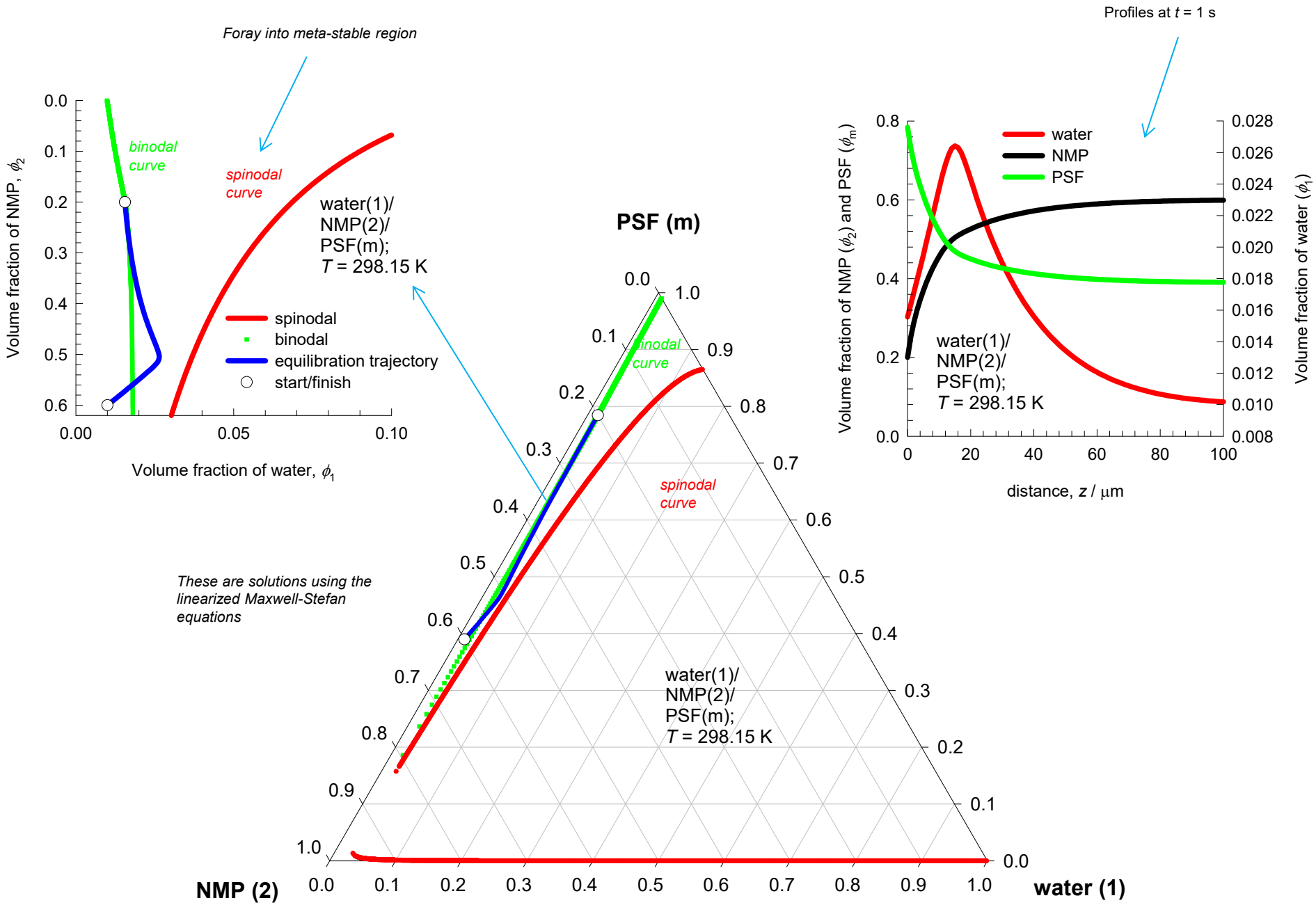

Foray into meta-stable region

Fig. S38

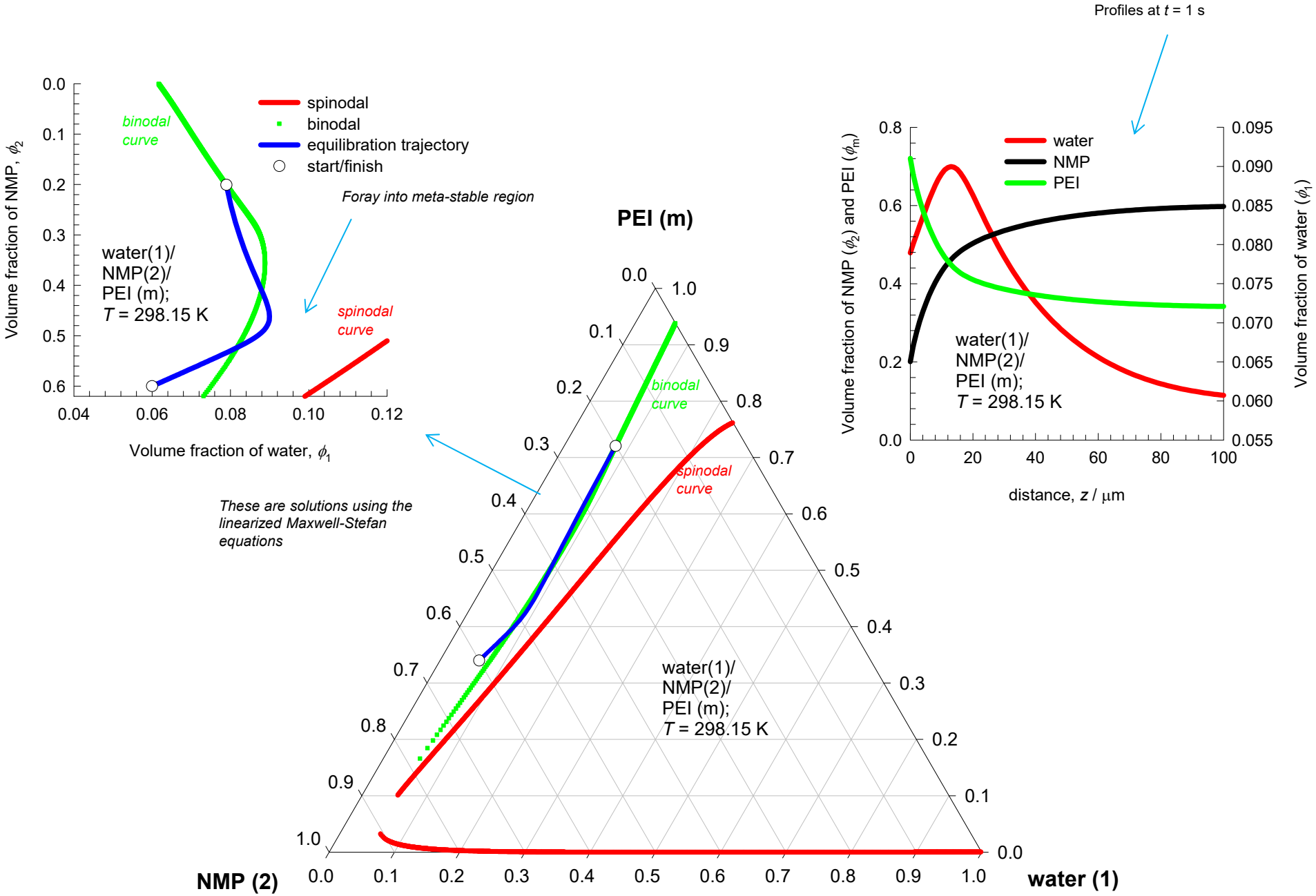

Foray into meta-stable region

Fig. S39

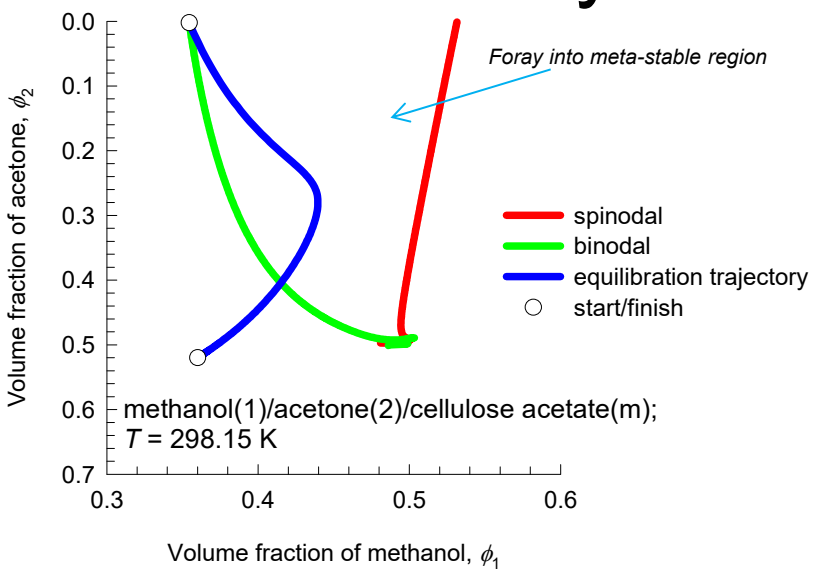

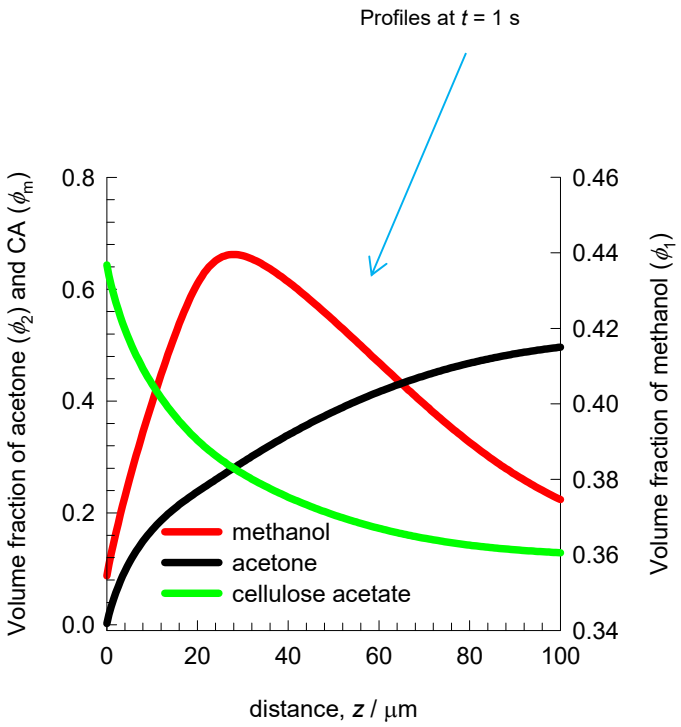

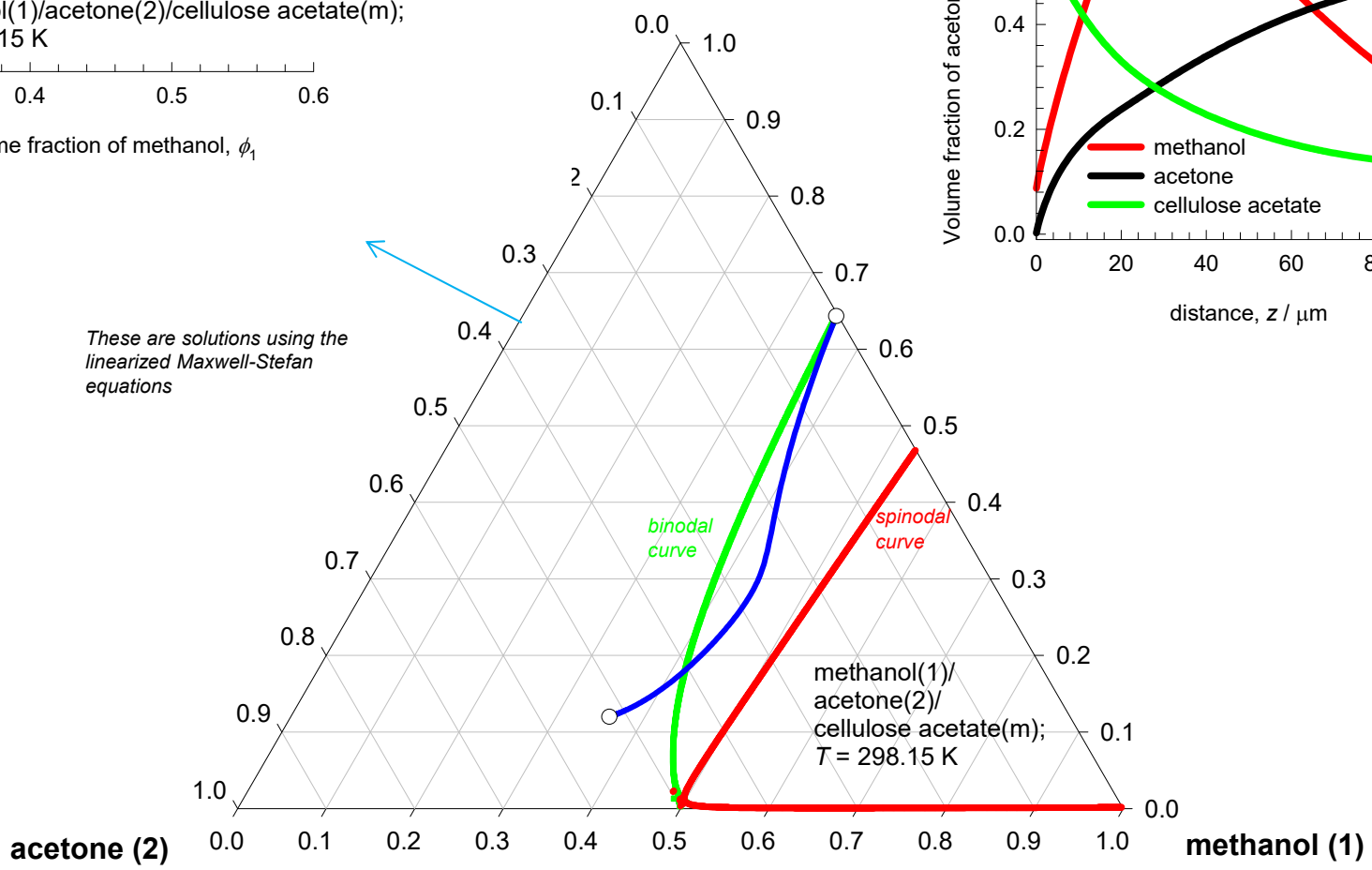

Foray into meta-stable region

Fig. S40